FINAL REPORT

Coupling Between Overlying Hydrodynamics, Bioturbation, and Biogeochemical Processes Controls Metal Mobility, Bioavailability, and Toxicity in Sediments

SERDP Project ER-1745

MAY 2016

Aaron I. Packman
Jean-François Gaillard
Northwestern University

G. Allen Burton, Jr
University of Michigan

SERDP
DOD ▪ EPA ▪ DOE

Page Intentionally Left Blank

Page Intentionally Left Blank

		Form Approved
REPORT DOCUMENTATION PAGE		OMB No. 0704-0188

Public reporting burden for this collection of information is estimated to average 1 hour per response, including the time for reviewing instructions, searching existing data sources, gathering and maintaining the data needed, and completing and reviewing this collection of information. Send comments regarding this burden estimate or any other aspect of this collection of information, including suggestions for reducing this burden to Department of Defense, Washington Headquarters Services, Directorate for Information Operations and Reports (0704-0188), 1215 Jefferson Davis Highway, Suite 1204, Arlington, VA 22202-4302. Respondents should be aware that notwithstanding any other provision of law, no person shall be subject to any penalty for failing to comply with a collection of information if it does not display a currently valid OMB control number. **PLEASE DO NOT RETURN YOUR FORM TO THE ABOVE ADDRESS.**

1. REPORT DATE (DD-MM-YYYY) 05-24-2016	**2. REPORT TYPE** Final	**3. DATES COVERED** (From - To) 05 May 2010 – 29 May 2015

4. TITLE AND SUBTITLE

Coupling between Pore Water Fluxes, Structural Heterogeneity, and Biogeochemical Processes Controls Contaminant Mobility, Bioavailability, and Toxicity in Sediments

5a. CONTRACT NUMBER
W912HQ-10-C-0024

5b. GRANT NUMBER

5c. PROGRAM ELEMENT NUMBER

6. AUTHOR(S)

Packman, Aaron I. Xie, Minwei. Gaillard, Jean-François. Burton, G. Allen, Jr.

5d. PROJECT NUMBER
ER-1745

5e. TASK NUMBER

5f. WORK UNIT NUMBER

7. PERFORMING ORGANIZATION NAME(S) AND ADDRESS(ES)

Northwestern University   University of Michigan
2145 Sheridan Road,   440 Church Street,
Evanston, IL 60208   Ann Arbor, MI 48109

8. PERFORMING ORGANIZATION REPORT NUMBER

9. SPONSORING / MONITORING AGENCY NAME(S) AND ADDRESS(ES)

Strategic Environmental Research and Development Program
901 North Stuart Street, Suite 303 Arlington, VA 22203

10. SPONSOR/MONITOR'S ACRONYM(S)
SERDP

11. SPONSOR/MONITOR'S REPORT NUMBER(S)

12. DISTRIBUTION / AVAILABILITY STATEMENT

Approved for public release; distribution is unlimited

13. SUPPLEMENTARY NOTES

14. ABSTRACT

The complex behavior of metals in contaminated sediments often confounds risk assessments and hinders development of effective remediation schemes. We performed laboratory experiments to determine the coupled effects of hydrodynamics, bioturbation, and biogeochemical processes on the transformation, mobility, bioavailability and toxicity of metals in contaminated sediments. Oxidation of surficial sediments liberated metal species that were then mobilized to both porewater and overlying water. Liberation of metals generally increased with hydrodynamic shear on the sediment-water interface, even in some low-permeability sediments. Sediment resuspension transitorily mobilized particulate metals, but did not significantly mobilize dissolved metals or increase contaminant bioavailability or toxicity. Bioturbation and bioirrigation by burrowing worms greatly increased sediment heterogeneity, oxygen delivery into sediments, and efflux of metals to both porewater and overlying water. Bioturbation also destabilized sediments, resulting in greater particle resuspension and metals efflux following flow perturbations. Based on these findings, assessments of metals bioavailability and toxicity in contaminated sediments should include measurements of the effects of flow forcing and sediment resuspension in concert with biological perturbations (bioturbation, bioirrigation).

15. SUBJECT TERMS

metal contaminated sediments, mobility, bioavailability, flow hydrodynamics, biogeochemistry, sediment resuspension, bioturbation

16. SECURITY CLASSIFICATION OF:			**17. LIMITATION OF ABSTRACT**	**18. NUMBER OF PAGES**	**19a. NAME OF RESPONSIBLE PERSON**
a. REPORT U	**b. ABSTRACT** U	**c. THIS PAGE** U	UU (SAR)	116	**19b. TELEPHONE NUMBER** (include area code)

Page Intentionally Left Blank

<h1 align="center">FRONT MATTER</h1>

Table of Contents

List of Figures

Figure 5-4. EXAFS spectra (full lines) and LCF reconstructed curves (dotted lines) for sediment samples in experiment G2 and G3. (a) Sediment core from experiment G2; (b) Sediment core obtained from experiment G3; (c) Resuspended sediments from experiment G3.

Figure 5-5. The first five components identified by PCA analysis. Amplitudes of C2, C3, C4 and C5 were multiplied by 2, 4, 8, and 8 respectively for clarity.

Figure 5-6. Zn K-edge EXAFS spectra (full lines), target transformations (dotted lines), and NSS values of 13 reference compounds.

Figure 5-7. XANES spectra (full lines) and reconstructed curves (dotted lines) of sediment samples.

Figure 5-8. Correlation between percentages of Zn species determined by LCF from EXAFS and XANES spectra.

Figure 5-9. (a) Zn speciation in sediment core from experiment G2, obtained immediately after a resuspension event; (b) Zn speciation in sediment core of experiment G3, obtained two days after a resuspension event. (c) Temporal evolution of Zn speciation in resuspended sediments in the water column from experiment G3. t = 0 corresponds to the initiation of resuspension.

Figure 5-10. Mean ($\pm$ 1 SD, $n = 8$) pH (A) and dissolved O_2 (B) in overlying water during 4-h resuspension experiments of Lake DePue and Portsmouth Naval Shipyard (MS03 and MS04) sediments. pH and DO remained stable through time for all bedded experiments (data not shown).

Figure 5-11. Mean ($\pm$ 1 SD, $n = 4$ to 8) dissolved Zn (A) and particulate Zn, Cu and Ni (B) during 4-h resuspension and bedded experiments with Lake DePue sediment. Equation in panel A represents nonlinear least squares regression fit model for dissolved metal release during sediment resuspension. Dissolved Cu, Ni, Cr, and Pb were not detected for the duration of experiments.

Figure 5-12. Mean ($\pm$ 1 SD, $n = 4$–8) calculated enrichment factors (e.g., Zn_{SPM}/Zn_{BEDDED}) after 4-h resuspension experiments of Lake DePue and Portsmouth Naval Shipyard (MS03 and MS04) sediments (POC = particulate organic carbon)

Figure 5-13. Mean ($\pm$ SD, n = 4-8) organism survival following resuspension and bedded experiments, and subsequent post-exposure hold. Note: *Hyalella azteca* held for 7 d, *Daphnia magna* 4 d and *Neanthes arenaceodentata* 10 d.

Figure 5-14. Mean ($\pm$ 1 SD, $n = 4$) bioluminescence response of Pyrocystis *lunula* following 4-h exposure to unfiltered and filtered overlying water in resuspension and bedded experiments with Portsmouth Naval Shipyard MS03 and MS04 sediments, expressed as % of control.

Figure 5-15. Mean ($\pm$ 1 SD, $n = 4$ for bedded and resuspension, $n = 8$ for controls) relative growth rates of *Neanthes arenaceodentata* following 4-h exposure to overlying water from control, bedded and resuspension experiments and after 10-d post-exposure recovery period.

Figure 5-16. MS03 surficial sediment oxidation and color change following resuspension and redeposition.

List of Acronyms

ADV	Acoustic Doppler Velocimetry
ARFW	Artificially Reconstituted Freshwater
ASW	Artificially Seawater
AVS	Acid Volatile Sulfide
AWQC	Acute ambient Water Quality Criteria
C.S.	Critical Shear
CSM	Conceptual Site Model
DBL	Diffusive Boundary Layer
DL	Detection Limit
DND-CAT	DuPont-Northwestern-Dow Collaborative Access Team
DO	Dissolved Oxygen
DOC	Dissolved Organic Carbon
EXAFS	Extended X-ray Absorption Fine Structure
EF	Enrichment Factors
ICP-OES	Inductively Coupled Plasma Optical Emission Spectroscopy
IDL	Instrument Detection Limit
IND	Indicator Parameter
K_D	Distribution Coefficient
LCF	Linear Combination Fitting
LDP	Lake DePue
LED	Light-inducing Diode
LIF	LED Induced Fluorescence
MDL	Method Detection Limit
NSS	Normalized Sum-square Residual

OC	Organic carbon
PCA	Principal Component Analysis
PNS	Portsmouth Naval Shipyard
POC	Particulate Organic Carbon
PQL	Practical Quantification Limits
PSD	Particle Size Distribution
RISS	Rhizon *in situ* Sampler
SeFEC	Sediment Flux Exposure Chambers
SEM	Simultaneously Extracted Metals
SPM	Suspended Particulate Matter
SWI	Sediment Water Interface
TC	Total Carbon
TOC	Total Organic Carbon
TRIS	Total Reducible Inorganic Sulfur
TT	Target Transformation
XANES	X-ray Absorption Near Edge Structure
XAS	X-ray Absorption Spectroscopy
Z-GFAAS	Zeeman Graphite Furnace Atomic Absorption Spectroscopy

Key Words

   Overlying Hydrodynamics, Bioturbation, Biogeochemical processes, Metals, Mobility, Bioavailability, Toxicity, Metal Speciation, Resuspension

1. ABSTRACT

Objectives: Sediments, with their resident organisms, represent a highly complex system. Contaminant behavior and effects are highly dependent on an interrelated suite of sedimentary processes, including sediment precipitation/dissolution, sorption/desorption of metals, aquatic and surface-chemical transformations leading to changes in metals speciation, pore water flow that both transports metals within sediments and controls delivery of oxygen from the overlying water column, and diverse biological processes including bioturbation and bioirrigation that affect sediment dynamics and biological uptake and transformation of metals. This complexity often confounds assessment of the potential adverse effects of metals in contaminated sediments, and hinders development of effective remediation schemes. To support management and remediation of contaminated sites, the objectives of project ER-1745 were to improve understanding of key processes that regulate the behavior and effects of metals in contaminated sediments, and to develop approaches for improved characterization of sediments obtained from contaminated sites to foster the development of better site conceptual models. The project specifically sought to determine how the interplay of physical, chemical and biological processes controls the transformation, mobility, bioavailability and toxicity of metals in contaminated sediments.

Technical Approach: A series of laboratory experiments were executed to study the coupled effects of overlying hydrodynamics, bioturbation, and biogeochemical processes on mobility, bioavailability, and toxicity of metals in contaminated sediments. Gust chamber and laboratory flume experiments with the capability to provide precisely controlled hydrodynamic conditions were performed with contaminated sediments collected from two sites: Lake DePue (LDP), IL and Portsmouth Naval Shipyard (PNS), ME. Experiments were performed both with and without bioturbating organisms (burrowing worms). Metals concentrations were characterized in overlying water, porewaters and sediments over the course of experiments to assess the effects of hydrodynamic and biological processes on metals distribution, speciation, mobility, and efflux. Resulting metals bioavailability and toxicity were also evaluated using multiple test organisms in targeted experiments.

Results: Oxidation of surficial sediments promoted the formation of more mobile metal species that represented a source of metals to both the porewater and overlying water. Hydrodynamics of the overlying water column clearly influenced the efflux of metals from the sediments. In coarser-grained PNS sediments, hydrodynamic forcing substantially promoted the release of Cu to the overlying water. These effects were damped in finer-grained sediments. Sediment resuspension also transitorily mobilized particulate metals. Metals concentrations in the water column increased substantially during resuspension and decreased back to the pre-resuspension levels following cessation of sediment transport. However, little mobilization of dissolved metals was observed from the resuspended sediments, and resuspension did not substantially increase metals bioavailability or acute toxicity to multiple test organisms (based on observed survival of *Hyalella azteca* and *Daphnia magna*; bioluminescence of *Pyrocystis lunula*; and survival, growth, and tissue metal concentration of *Neanthes arenaceodentata* during and following resuspension events). Redeposited sediments exhibited increased metal bioavailability and acute toxicity to *H. azteca*, indicating potential for adverse ecological impacts due to changes in metal speciation associated with flow perturbations and sediment resuspension. Bioturbation greatly altered sediment structure, mixed sediments leading to enhanced exposure of buried sediments to oxic conditions, and increased oxygen delivery into the sediments by pumping oxygenated water into

1

burrow structures. As a result, bioturbation substantially increased the flux of metals from the sediments to both the overlying water and porewater.

Benefits: The project improves assessment of risks at DOD's contaminated sediment sites by enhancing the knowledge base of fundamental processes that govern the behavior and effects of metal contaminants in sediments and providing strategies for measuring key effects including metals efflux, bioavailability, and toxicity under complex site conditions. The project results indicate that metal concentrations in pore waters are strongly regulated by the metal speciation in the sediments. Oxidation reactions near the sediment water interface change the speciation by dissolving insoluble metal sulfides, form weakly bound metal species, and release aqueous metals to the pore water and overlying water. Oxygen penetration into sediments is a dynamic balance between the delivery of dissolved oxygen from overlying water and consumption of oxygen by chemical reactions and biological metabolisms. As the most thermodynamically favorable terminal electron acceptors in the sediment, oxygen distribution substantially influences the biogeochemical zonation, organic matter mineralization and fate of metals. While the effect of hydrodynamics on solute transport and metal dynamics have been extensively studied in permeable sediments, hydrodynamic effects in low permeability sediments have rarely been studied. The project results clearly demonstrate that hydrodynamic forces promote the mobility and efflux of metals in low permeability sediments. Oxidation of surficial sediments liberated metal species that were then mobilized to both porewater and overlying water. Liberation of metals generally increased with hydrodynamic shear on the sediment-water interface. Further, sediment resuspension transitorily mobilized particulate metals, but did not significantly mobilize dissolved metals or increase contaminant bioavailability or toxicity. These effects become more complicated when co-occurring with biological processes that disrupt sediments. Bioturbation and bioirrigation produced a high degree of heterogeneity within the sediments, and also destabilized the sediments, resulting in greater particle resuspension and metals efflux following flow perturbations. Based on these findings, time-variable flow and sediment resuspension should be considered in conceptual site models, and assessments of contaminated sediment bioavailability and toxicity should also include measurements of the effects of flow forcing and sediment resuspension in concert with bioturbation and bioirrigation. The experimental approaches developed in this project to measure the effects of flow forcing, sediment resuspension, bioturbation, and bioirrigation can be directly employed in site assessments using sediment cores or homogenized sediments obtained from DOD sites.

2. OBJECTIVES

The overarching objective of project ER-1745 was to substantially improve understanding of how the interplay of physical, chemical and biological processes controls the transformation, mobility, bioavailability and toxicity of metals in sediments. The project was intended to both advance fundamental understanding of the processes that regulate the behavior and effects of metals in contaminated sediments, and to develop a set of practical tools that can be used to effectively characterize and assess contaminated sites. Specific objectives were 1) to develop an *ex situ* experimental methods that could provide the capability to study the effects of coupling between overlying hydrodynamics, biogeochemical reactions, and bioturbation on mobility, bioavailability and toxicity of metals, 2) to characterize the effects of biogeochemical reactions on metal speciation in sediments and the resulting mobility and efflux of metals, 3) to assess the effects of flow hydrodynamics on mobility and efflux of metals and the associated bioavailability and toxicity effects, 4) to characterize the physical and chemical heterogeneity caused by biological activities using innovative 2D imaging methods, 5) to study the interplay between overlying hydrodynamics and bioturbation on mobility and efflux of metals.

3. BACKGROUND

3.1 Current state of contaminated sediment management

Sediments are essential components of aquatic ecosystems and play critical roles in a number of important ecosystem functions and services, such as providing habitat and substrates for a wide range of organisms.[1] Contaminated sediments have been recognized as long-term diffuse sources of pollution to aquatic ecosystems, thereby impairing the beneficial use of water bodies, impacting benthic communities, and posing ongoing threats to larger pelagic organisms by food web contamination.[2] Sediment contamination is a major concern worldwide and has been found in every type of aquatic environment within United States, from mountain streams to large rivers, from small lakes to the Great Lakes, and in estuaries and bays.[3] Cleanup of contaminated sediments often costs millions of dollars and requires confined disposal facilities for large quantities (thousands of cubic meters) of sediments. Dredging and disposing of contaminated sediments in US (1.2 billion cubic yards estimated by USEPA in 1998) has been estimated to require a total cost of trillions of dollars.[4] Such high costs indicate that the extent of sediment contamination and its associated adverse effects need to be carefully assessed before remedial actions are selected.

Traditionally, assessment of the potential effect of sediment contamination has been primarily based on comparing bulk chemical concentrations of individual compounds with background or reference values. However, these approaches provide little direct insight into ecological impacts, and it has been recognized that the relationship between contaminant concentration in sediments and risk from exposure can be highly non-linear.[4] Current approaches for assessing bioavailability and toxicity of metals in sediments employ bulk sediment characterizations, often relying on batch organism exposure in a laboratory setting in combination with equilibrium partitioning models that attribute toxicity to the presence of dissolved metals in pore water.[5] However, sediments are highly complex systems (Figure 3-1), in which the contaminant behavior and effects are highly dependent on an interrelated suite of sedimentary processes, e.g. surface water and pore water interactions, bioturbation and bioirrigation. Failure to consider interactions driven by time-variable physical and biological processes could easily result in misestimate of the ecological and human health risks of contaminated sediments.
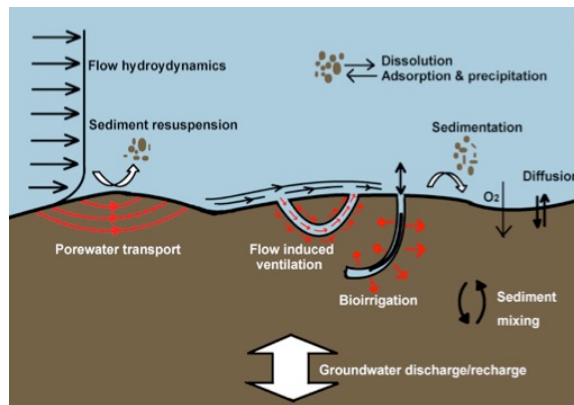
Figure 3-1. Processes affecting mobility and efflux of metals in contaminated sediments.

3.2 Metal cycling in sediments

Most metals have a high affinity for solid phases,[6] and thus metals discharged to surface waters often end up accumulating in sediments. Once in sediments, the chemical evolution and transformation of metals are controlled by a wide range of biogeochemical processes fueled by the degradation of organic matter.[7, 8] Mineralization of organic matter is mediated by microorganisms using different electron acceptors (e.g. O_2, NO_3^-, Mn and Fe oxides and hydroxides, and SO_4^{2-}) as part of their metabolism (Figure 3-2). The sequences of redox reactions tend to be distributed vertically in the order of decreasing free energy yield, thus forming sediment stratifications with unique chemical composition and redox properties.[9] These reactions also release a series of metabolic byproducts into the pore water, including CO_2, Fe^{2+}, Mn^{2+}, HS^-. The reactions induced by these metabolites strongly regulate the fate of metals in sediments (Figure 3-2). For example, the increased carbonate in pore water from aerobic respiration facilitates the precipitation of metal carbonate species.[10, 11] Reductive dissolution of oxide of manganese and iron releases adsorbed metals to the pore water while freshly precipitated Fe and Mn oxides are efficient scavengers of metals due to their high surface reactivities.[6] Sulfate reduction reactions produce sulfide species, leading to sequestration of metals in the form of metal sulfides. This has been shown to be a major sink for trace metals in anoxic sediments.[12, 13]
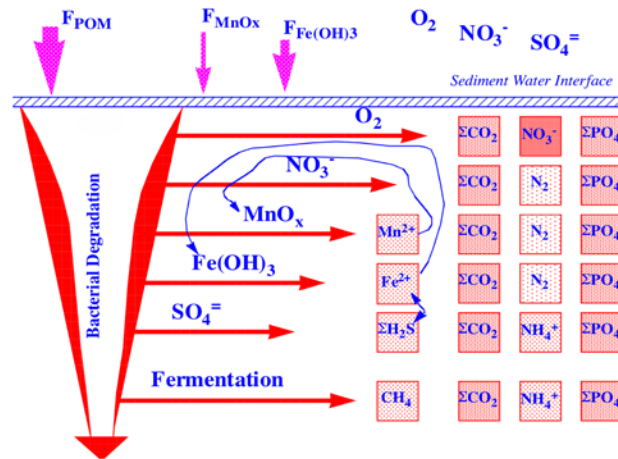
Figure 3-2. Schematic representation of biogeochemical transformations occurring within surficial sediments. (Credit: J.-F., Gaillard)

3.3 Processes influencing the mobility, bioavailability, and toxicity of metals

A wide variety of physical, chemical and biological processes produce heterogeneity in contaminant form and flux, which dictate both exposure of benthic organisms to contaminants and the toxicity of the contaminant phases (Figure 3-1). Metals are often bound to a variety of sediment fractions and a wide range of factors, including redox distribution and pH, influence the mobility, bioavailability and toxicity of metals in the sediment.[14, 15] These factors are known to vary with many transport and mixing processes, such as hyporheic exchange, groundwater water discharge and recharge, bioturbation and bioirrigation.[16-21] For example, the penetration of oxygen is directly controlled by the interplay between transport and consumption within the sediments, and plays an important role in the precipitation and stability of oxidized mineral phases that are excellent scavengers of metals, notably Fe and Mn oxides and hydroxides. Hyporheic exchange – advective

exchange of pore water with the overlying water column – directly influences mass transfer of both solutes and particulate matter across the sediment-water interface (SWI).[22-26] Pore water advection and molecular diffusion in sediments generate complex pore-fluid flow fields, modifying redox gradients and the redistribution of metals between sediment and pore water.[22, 27-32] Biological activities, such as construction of sediment burrows, turnover of sediments during burrowing, and biologically-induced irrigation of oxygen- rich water into anoxic burrows further reworks and reorganizes the sediments (Figure 3-3). Burrow structures penetrate the sediments, increasing porosity and extending area of the SWI.[33, 34] Irrigation of oxygenated water into burrows enhances oxidation of sediments and also modifies pH, both of which are expected to strongly influence the fate of metal contaminants. [18, 35] Mixing of surface water and porewater also creates strong chemical and hydrodynamic gradients that are readily influenced by the sediment permeability, groundwater discharge, and sediment structural heterogeneity.[22, 36]
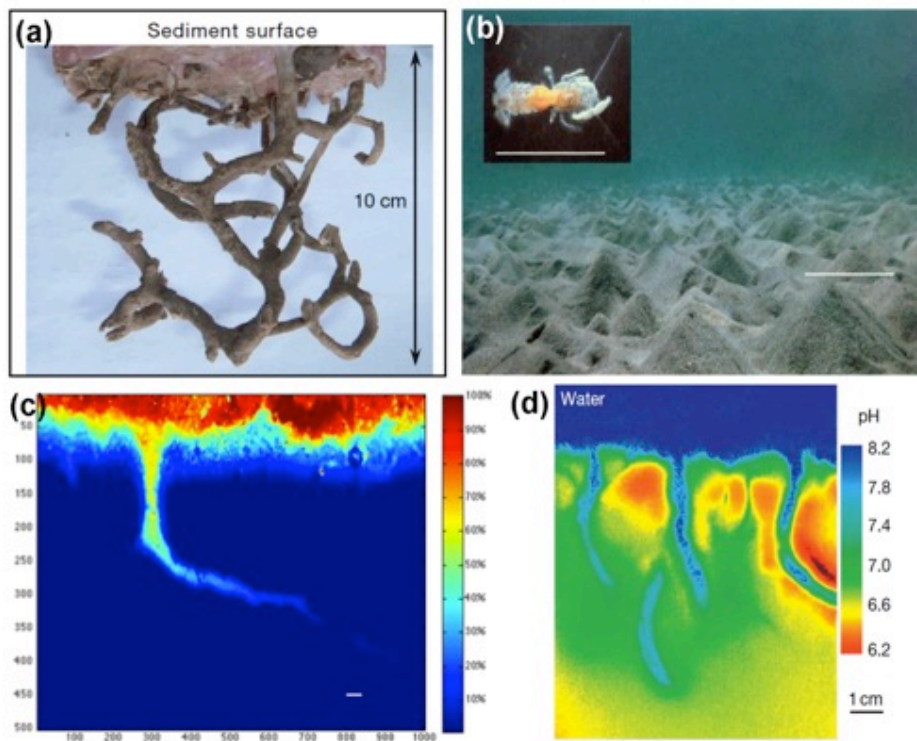
Figure 3-3. Bioturbation activities strongly influence the physical, chemical and biological properties of sediment. (a) Typical burrow structure for *Nereis virens* in sediment.[33] (b) Sediment surface topography created by the burrowing shrimp, *Calianassa truncata*. Conical mounds with an average height of 4 cm, maximum 6 cm cover the seabed between 2 and 15 m water depth in the entire bay.[34] (c) *Lumbriculus variegatus* bioturbation causes advection of oxygen into anoxic sediment. (d) Bioturbation modifies pH distribution in the sediment.[37]

4. Materials and Methods

4.1 Coupled Effects of Hydrodynamics and Biogeochemistry on Zn Mobility and Speciation in Highly Contaminated Sediments

4.1.1 Sediment Source.

Laboratory experiments were performed with Zn-contaminated sediments from Lake DePue, a shallow backwater lake of the Illinois River located in north-central Illinois (Figure 4-1), Lake DePue has an average surface area of 212 ha with 18.2 km of shoreline. Lake DePue has received substantial metal contamination from industries, particularly Zn smelting, since the early 1900s. Zn has been found in Lake DePue sediments at concentrations ranging from 304 to 42,300 mg/kg. These extremely high concentrations make Zn the primary chemical of concern in LDP sediments.[24] Zn in lake sediments has been shown to be associated with P close to the contamination source, and becomes more predominately associated with S farther from the source.[25, 26]

Figure 4-1. Left: Location of Lake DePue. Right: Aerial photograph of Lake DePue indicating the sampling site (Google Earth, Retrieved on March 4, 2013)

4.1.2 Sediment collection.

Experiments were performed on both intact sediment cores and homogenized sediments. Sediments were collected from Lake DePue in September 2011 at the location shown in Figure 4-1. Three cores (diameter = 10 cm and length = 45 cm, polycarbonate) were hand driven into sediment to a depth of 35 cm carefully to minimize the disturbance of the sediment-water interface, leaving 10 cm headspace of overlying water. Following insertion into the sediment, the upper part of each core was sealed with a piston, carefully retrieved, and closed from below with another piston. Sediments for homogenized experiments were collected from the same location to a depth of 15 cm. Sediment samples were immediately transported to the laboratory and refrigerated at 4°C until used in laboratory experiments.

4.1.3 Sediment characterization.

Bulk sediment properties (porosity, particle size distribution (PSD), permeability, total metals) were measured on homogenized sediment samples. Porosity was determined by drying 3 cm3 sediment samples at 70 °C for 48 h and converting the weight loss to water volume fraction. The sediment grain size distribution was determined by wet-sieving at 45 μm and 106 μm and measuring the dry weight. In addition, smaller particles were sized using a Beckman Coulter Multisizer 3 (Fullerton, CA). Permeability was measured in a constant-head permeameter with a test section of 2.5 cm diameter and 5 cm length (Chromatography column, Omnifit Ltd). Total bulk sediment metal concentrations were measured by Inductively Coupled Plasma Optical Emission Spectrometry (ICP-OES, Vista-MPX, Varian) after microwave-assisted acid digestion following USEPA method 3051A. Total organic carbon was measured with a Costech ECS 4010 elemental analyzer (Costech Analytical Technologies Inc., Valencia, CA) after acidifying 80 mg of dried and powdered sediment with 1.5 mL of 4M HCl to remove inorganic carbon.

4.1.4 Experimental setup.

The Gust chambers (Green Eyes LLC, Cambridge, MD, USA) (Figure 4-2) use a combination of a spinning disk and central suction to generate nearly uniform shear stress across the sediment-water interface. All parts of the Gust chamber in contact with sediments and water were made of polycarbonate to minimize metal contamination. Overlying water was recirculated by means of a peristaltic pump to a 500 mL HDPE water reservoir (Nalgene). Shear stresses from 0.01 to 0.45 Pa were achieved by varying the rotation rate of the spinning disk, and the recirculation flow rate. Oxygenated artificially reconstituted fresh water (ARFW), composed of 5 g $CaSO_4$, 5 g $CaCl_2$, 3 g $MgSO_4$, 9.6 g $NaHCO_3$ and 0.4 g KCl to 100 L milli-Q water (Millipore),[38] was recirculated throughout the experiment.
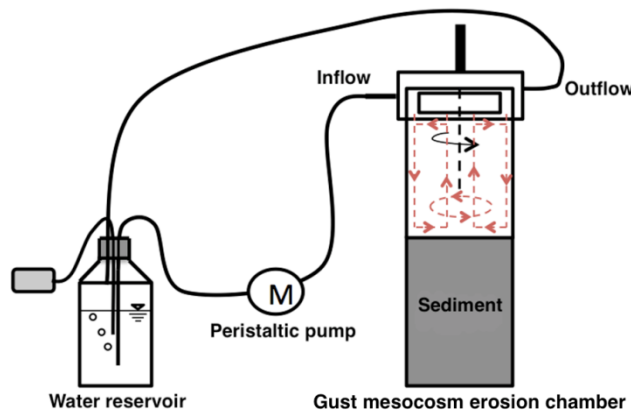
Figure 4-2. Gust chamber setup. Dashed lines inside the chamber indicate the flow pattern within the chamber.

4.1.5 Hydrodynamic conditions and sediment resuspension.

The Gust chambers support controlled investigations of sediment resuspension.[39, 40] The critical shear for resuspension of Lake DePue sediment was measured by increasing the shear imposed on the sediments in a stepwise fashion while recording the turbidity of the overlying water. The critical shear stress was determined as the shear stress that caused general sediment resuspension, leading to a large increase in turbidity. Based on these Gust chamber experiments, the critical shear stress for LDP sediment was determined to be 0.36 Pa. Metals efflux and speciation were then observed in Gust chambers with intact cores and homogenized sediments, and with and without periods of episodic resuspension, as detailed in Table 4-1.

Table 4-1. Conditions for Gust chamber experiments. All experiments were conducted under a baseline hydrodynamic shear of 0.19 Pa (50% of the shear required for resuspension). Experiments G2 and G3 were also subject to episodic resuspension. Experiment G2 was disassembled immediately after resuspension on day 9, while experiment G3 was disassembled on day 14, two days after the sediment resuspension event on day 12.

	Duration (days)	Periods of Sediment Resuspension		Sediment structure
G1	14.2	-		Intact core
G2	9.0	4 h on day 9	-	Intact core
G3	14.2	0.3 h on day 6	4 h on day 12	Intact core
G4	14.7	-		Homogenized

4.1.6 Experimental procedure.

Before each experiment, all parts of the Gust chamber, including tubing and reservoir container, were cleaned by soaking in 10% HNO$_3$ (v/v) for 24 h followed by soaking and rinsing twice with Milli-Q water. For experiments with homogenized sediment structure, 800 mL of sediments were homogenized with a plastic utensil and then packed into the Gust chamber to form a 10 cm sediment bed with a flat surface, leaving 10 cm of headspace for overlying water. ARFW was then introduced slowly to avoid disturbing the sediment-water interface (SWI). The Gust chamber erosion head was placed on the core, with the inlet and outlet ports connected to the recirculation system using Tygon tubing (VWR International, USA) and a peristaltic pump (Masterflex, Cole Parmer). Sediments were allowed to consolidate overnight, and then the experiments were initiated by rotating the stirring disk at a constant speed and recirculating the water at a constant rate. For experiments performed on intact sediment cores, the overlying water brought with the core from the field was slowly replaced with ARFW and then the Gust chamber erosion head was fit directly onto the cores. Experiments were run continuously for 9-15 days, as noted in Table 4-1. In experiments G2 and G3, episodic periods of resuspension were imposed by increasing the shear above the critical value for the defined period noted in Table 4-1, and then returning to the baseline condition. In experiment G2, the Gust chamber was disassembled on day 9, immediately after the resuspension event, to observe transient changes in metals speciation caused by resuspension. In experiment G3, two periods of resuspension were imposed, and then the shear was returned to the baseline level for the remainder of the two-week experiment.

4.1.7 Sampling and analysis.

At the end of each experiment, sediment subcores were obtained using 60 mL modified plastic syringes. Four subcores of each experiment were transferred to an anaerobic chamber (3%

H$_2$ and 97% N$_2$) (Coy laboratory products Inc., USA). Two subcores were then sectioned at 1 cm intervals and centrifuged at 3414×g for 20 min to extract porewater (Legend RT plus, Thermo Scientific). The supernatant was then filtered through 0.2 μm nylon filter (VWR International, USA), acidified with concentrated, trace-metal grade HNO3 (Sigma Aldrich, USA) to pH<2 and stored at 4°C until analyzed by ICP-OES. Another subcore was sectioned at 1 cm intervals and stored at -20°C for analysis of acid volatile sulfides (AVS) and simultaneously extracted metals (SEM). The last core was sectioned at 1 mm intervals over the first centimeter of sediment, and then at 1-2 cm intervals over the remainder of the core for analysis of metals speciation by XAS. These samples were smeared on filter paper, sandwiched between two layers of Kapton tape and stored under N2 atmosphere frozen at -80°C until analysis. Resuspended particles from experiment G3 were also analyzed by XAS. 8 mL of overlying water was filtered using a 0.2 μm isopore polycarbonate membrane filter (Millipore, MA, USA). The filters were then sandwiched between two layers of Kapton tape, and then handled as described above.

AVS and SEM were determined by the 1M cold HCl extraction and 0.5M NaOH trap technique.[41] S^{2-} was measured by colorimetry with a UV-visible spectrophotometer (Spectronic 20, Spectronic Instrument) after the addition of a mixed di-amine reagent. Metal concentrations in the extractant were measured using ICP-OES.

The ICP-OES was calibrated performed using single-element standards (Zn, Cu, 1000 mg L^{-1}) (Sigma Aldrich, USA) added to Milli-Q water to span the concentration range of each metal in the experimental samples. Standards were reanalyzed after every ten experimental samples to correct for drift.

XAS was performed at the Zn K-edge on sediment samples and reference phases using the bending magnet beamline of the DuPont-Northwestern-Dow Collaborative Access Team (DND-CAT), Sector 5 of the Advanced Photon Source, Argonne National Lab. A Si (111) double crystal monochromator was used to vary the x-ray energy from -100 eV to +600 eV above the Zn K-edge (9658.6 eV). Sample spectra were collected in fluorescence mode using either a silicon drift detector (Vortex-ME4) or a 13 element HP-Ge solid state detector (Canberra) while reference spectra were collected in transmission mode. The intensity of the incoming beam (I0) and the transmitted beams (IT1 and IT2) were measured using Oxford ionization chambers with path lengths of 29.6 cm. The energy scale of the monochromator was calibrated to 9658.6 eV using the first derivative of the absorption threshold of a Zn foil that was simultaneously measured during data acquisition.

The chemical speciation of Zn in bed and re-suspended sediments was assessed directly using XAS based on the decomposition of observed spectra as the sum of its components. Mathematically:

$$FIT = \sum_i f_i \times REF_i$$

where FIT is the reconstructed sample spectrum for a mixture of compounds, and f_i is the fraction corresponding to the reference compound spectrum REF_i.

Extended X-ray absorption fine structure (EXAFS) data were processed and analyzed with the Athena software[42] to determine the distribution of Zn major chemical species in bulk sediment samples.[43-45] Briefly, EXAFS spectra were first normalized to an edge step of 1 and the EXAFS were extracted using a smooth background function ($\mu_0(E)$) as calculated by the AUTOBK algorithm, integrated into Athena, imputing the same set of parameters for the entire observed spectra.[46] Principal component analysis (PCA) was performed on k^2-weighted EXAFS spectra (k ranging from 3 to 10 Å^{-1}) of the 20 sediment samples analyzed to determine the minimum number of statistically relevant components necessary to reproduce the observed spectra. Target transformation (TT) analysis was then carried out on a library of 13 reference spectra (with 3<k<10 Å^{-1}) with the identified principal components to select reference compound EXAFS for spectral decomposition. Finally, Zn speciation in the sediment samples was determined by least-squares linear combination fitting (LCF) of the EXAFS using the basis set defined by the selected reference compounds. X-ray absorption near edge structure (XANES) data were also processed following the same procedures.

4.2 Toxicological Effects of Short-term Resuspension of Metal-contaminated Freshwater and Marine Sediments

4.2.1 Site descriptions

Sediments were obtained from Lake DePue, IL (41° 19' N, 89° 18' W) and Portsmouth Naval Shipyard (PNS, 43° 5' N, 70° 44' W) in Kittery, ME. Lake DePue sediments are contaminated from historic industrial activities, particularly 80 years of Zn smelting and production of sulfuric acid and diammonium phosphate fertilizer in its watershed.[47] Marine sediments from Portsmouth Naval Shipyard (PNS) were collected from two sites, MS04 and MS03, and are contaminated with a mixture of metals and PAHs from foundry slag, historic industrial point sources, and groundwater/surface water runoff.[48] Sediments were collected in September of either 2011(DePue) or 2012 (PNS) and stored (< 1 year before use) under anoxic conditions at 4 °C in the laboratory.

4.2.2 Resuspension and exposure chambers

Sediment flux exposure chambers (SeFEC; Figure 4-3) were modified from chamber designs of others.[49] SeFEC were constructed from polycarbonate core tubes (7.1 cm ID, 16.5 cm height) with polycarbonate end caps. Pairs of chambers were connected by a recirculating-system, with one chamber as a resuspension chamber and the other as an organism exposure chamber (Figure 4-3). Each pair of chambers was one experimental unit and treated as a replicate. Sediment was resuspended by an inverted stir plate and Teflon coated stir bar. A sampling port at 1.5 cm from the bottom allowed pore water sampling via Rhizon CSS soil samplers.

Resuspension events were simulated by adding homogenized sediment to the resuspension chamber to create a 2.5 to 3.5 cm thick layer, depending on sediment type, and then stirring at 370–400 rpm to achieve 0.2–1.0 g/L of suspended particulate matter (SPM). Bedded sediment experiments were run without induced shear stress but were otherwise identical. Water and suspended particles were recirculated between the resuspension and exposure chambers by a peristaltic pump at 12.5 mL/min through polyvinyl chloride tubing (one-eighth inch ID). Complete mixing of the water column between the two chambers was achieved within 1–1.25 h. Particulate matter in the exposure chamber was kept in suspension by use of an identical stir plate and stir bar

11

at the bottom of the exposure chamber. The exposure chamber contained an inner chamber (9 cm height × 2 cm ID) made of polycarbonate in which test organisms were held during resuspension and bedded experiments. This inner chamber had a window (26 cm^2) covered with 243 μm Nitex bolting cloth to allow for the mixing of suspended particles between exposure and inner chambers. All resuspension and bedded sediment experiments were 4 h in duration with 4 replicates each and with 5–10 organisms per replicate.
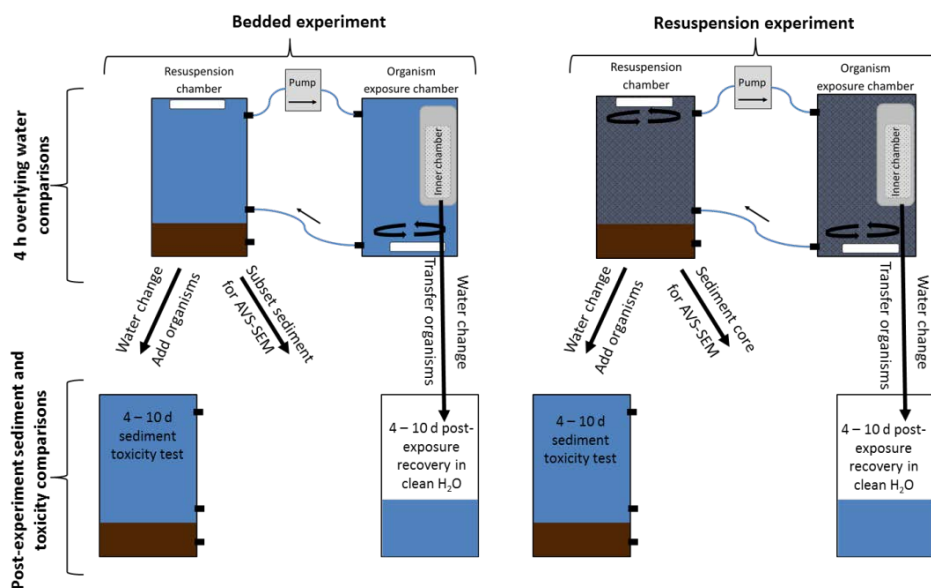
Figure 4-3. Experimental design and work flow depicting chemical and toxicological comparisons (e.g., overlying water comparison between 4-h bedded and resuspension exposures) between experimental units.

4.2.3 Study design

4.2.3.1 Overview

For each sediment, the geochemistry was characterized and the acute toxicity was determined for three sediment integrity conditions: bedded, resuspended, and redeposited (Figure 4-3 and 4-4). Direct comparisons of geochemistry and acute toxicity were made between: 1) overlying water during 4-h bedded and resuspension experiments and 2) sediments following bedded and resuspended sediment experiments (Figure 4-3). Overlying water acute toxicity was assessed with pelagic organisms (either the freshwater cladocera, *Daphnia magna*, or the marine dinoflagellate, *Pyrocystis lunula*), and sediment acute toxicity was assessed with epibenthic/benthic organisms (either the freshwater amphipod, *Hyalella azteca*, or the marine polychaete, *Neanthes arenaceodentata,* respectively). Organisms were exposed for 4 h followed by either: 1) 24 h depuration and metal analysis of tissue, or 2) holding for an additional 4 to 10 d in uncontaminated water, depending on organism, to monitor post-exposure survival and growth. Tests with Lake DePue sediment were conducted with moderately hard reconstituted water (101 mg/L CaCO$_3$) and those with PNS sediments were conducted with artificial seawater (salinity = 31) prepared from commercial sea salt (Tropic Marin: Wartenberg, Germany). Initial pH, DO and

conductivity of experimental waters were similar to *in situ* conditions.[47, 48] All exposures were conducted under a 16 h:8 h light: dark cycle at $24 \pm 1°$ C.
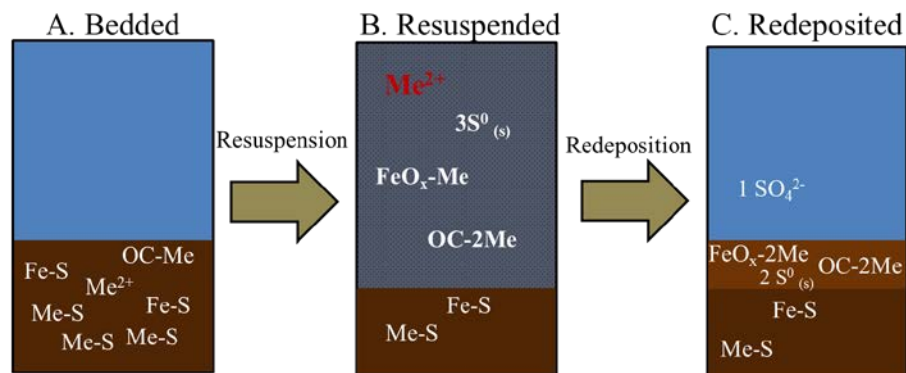
Figure 4-4. Conceptual model of important metal (Me) speciation in various sediment redox states. In bedded sediment (A) the majority of metal is bound as insoluble sulfides or associated with organic carbon (OC). When resuspended, (B) sulfide species are oxidized, mobilizing metals into the overlying water. However, the mobilized metal is scavenged by OC and freshly-precipitated Fe_xO_x. As particles redeposit, and are returned to the benthic environment (C), further oxidation of sulfur to sulfate can occur in the water column or in the aerobic sediment layer over longer durations (10 – 30h). Note that not all potential chemical reactions and species are represented in this schematic, and sulfur stoichiometry is balanced for clarity but speciation may differ depending on environmental conditions.

4.2.3.2 Overlying water comparisons (bedded vs. resuspension)

Experiments with bedded and resuspended sediments were completed in the SeFEC system with water recirculation, either with (resuspension) or without (bedded) induced shear stress from the stir plate. Physicochemical parameters (dissolved O_2, pH, temperature, turbidity, total suspended solids and conductivity) were measured hourly in each exposure chamber. Porewater for metal analysis was sampled from the resuspension chamber before test initiation and overlying water in the exposure chamber was sampled over the experiment duration (0, 1 and 4 h; plus 2 and 3 h for Lake DePue only). Suspended particulate matter was sampled hourly (Lake DePue) or at 1 and 4 h (PNS) during resuspension experiments for determination of total suspended solids, particulate metal concentrations and particulate organic carbon (POC, 4 h only). Turbidity (NTU) was measured with Hach 2100N turbidimeter hourly. Pore and overlying water were filtered (0.2 µm polycarbonate membrane) and acidified to 2% with high purity HNO_3.

For freshwater sediment tests, lab-reared *H. azteca* (10 organisms/replicate, 7–14 d old) and *D. magna* (10 neonates/replicate, < 24 h old) were placed within the inner chambers of the exposure chamber for 4 h. Following exposure, *H. azteca* were transferred into beakers containing 150 mL of clean reconstituted water with a strip of unbleached paper towel and three pre-weighed, preconditioned [50] 1-cm diameter disks of red maple leaf (*Acer rubrum*). Organisms were held for a 7 d recovery period to monitor survival and leaf disk processing. Following either bedded or resuspension exposures, *D. magna* were placed into beakers containing 25 mL of clean reconstituted water and held for a 4 d recovery period to determine survival. At the start of post-

exposure monitoring and on day 3, 0.25 mL of food (*Psuedokirschneriella subcapitata* and wheat grass powder suspension) was added to each beaker as a nutrient source for *D. magna*.

For tests with marine sediments, 10, 2- to 3-week post-emergent *N. arenaceodentata* (sourced from Aquatic Toxicology Support, Bremerton, WA) were placed in the inner chambers. Following the 4-h exposure, 5 organisms from each chamber were transferred to clean seawater for depuration (24 h) prior to tissue metal analysis. The other 5 organisms were transferred to beakers containing 150 mL of clean seawater and held for a 10 d recovery period to monitor survival, and growth was determined by comparing body mass after 10 d to those at test initiation as per standard ASTM methods. *Neanthes arenaceodentata* were fed 10 mg of powdered, commercial rabbit chow at initiation and every third day, after water changes of two-thirds volume. *Pyrocystis lunula* (500 cells/mL test solution, QwikLite Biosensor, Assurance Controls) were exposed to unfiltered (bedded and resuspended) and filtered (0.2 µm, resuspended only) water collected from the exposure chambers after each 4-h experiment. After inoculation, the water-organism mixture was incubated in a 12:12 h light dark cycle for 24 h and the light intensity of the bioluminescent organisms was measured and compared to that of unexposed bioluminescent organisms in controls, with results expressed as a percent bioluminescence inhibition relative to controls. *Pyrocystis lunula* received for MS04 bedded sediment experiments were not viable and therefore excluded from statistical analyses.

Controls for *H. azteca, D. magna,* and *N. arenaceodentata* exposures consisted of four additional replicates that were not exposed to either contaminated water or sediment. Organisms were held in 25 mL of clean water without food during the 4-h tests, but otherwise treated identically through either the depuration and digestion or post-exposure monitoring procedures. Quality of overlying water (dissolved O_2 and pH) was monitored during all control and treatment exposures and remained satisfactory (dissolved $O_2 > 5.2$ mg/L; pH: $7.6 - 8.2$) throughout the experiments.

4.2.3.3 Sediment comparisons (bedded vs. redeposited)

After resuspension experiments, suspended sediments were allowed to settle out over a 20-h period, after which redeposited sediments were subsampled with cores (10-mm depth, sectioned at 5-mm resolution) to investigate effects of resuspension on vertical distributions of acid volatile sulfides (AVS) and simultaneously extracted metals (SEM). Un-manipulated sediment was used to determine pre-resuspension (i.e., bedded) AVS and SEM. Additionally, water for analysis of dissolved metals was sampled from resuspension chambers after the 20-h settling period to determine metal fluxes from the sediment. Filtered water also was sampled before various water changes (described below) to monitor metal concentrations in the test chambers.

Chambers and contained sediment from both resuspension and bedded tests were further used for static-renewal sediment acute toxicity (Figure 4-3). Completing these additional toxicity tests allowed for direct contact between test organisms and the two sediment integrity conditions. Following the 4-h use in the SeFEC system and the 20 h settling period, chambers containing sediment received a 100% water change and organisms were added. For freshwater experiments, 10 each of both *D. magna* and *H. azteca* were included together in the test for 4 and 7 d, respectively, along with three maple leaf disks as a food source. For marine experiments, 5 *N. arenaceodentata* were included for 10 d and fed (10 mg rabbit food in each chamber) every third day. Additionally, *P. lunula* were exposed to filtered marine sediment elutriates (1:4 sediment to water ratio) resulting from bedded and redeposited tests, for determination of sediment acute

toxicity. Control chambers contained clean water and either unbleached paper towel and leaf disks (*D. magna* and *H. azteca*) or clean Ottawa sand (*N. arenaceodentata*). Treatments and controls for freshwater and marine experiments received one water volume (~275 mL) change per day with intermittent sampling of physicochemistry to ensure adequate water quality (neutral pH and > 5.0 mg/L dissolved O_2). Following the described exposure durations, surviving organisms were counted and *N. arenaceodentata* were depurated (24 h) in clean seawater with 10 mg rabbit food prior to weighing (for calculation of growth rates) and metal analysis.

4.2.4 Sample analysis

4.2.4.1 Sediment characterization

Water content of sediments was determined gravimetrically after drying (100°C). Dried sediment was analyzed for total carbon (TC), total organic carbon (TOC), and total recoverable metals. Total organic carbon was measured after pretreatment of 20 mg of sediment in silver capsules with 50 µL 1% HCl, followed by 8 h fumigation with 12 M HCl.[51] Both TOC and TC were determined with a CHN Elemental Analyzer. Total recoverable metals were measured after microwave-assisted acid digestions using a 3:1 ratio of HNO_3: HCl. Digestates were filtered (0.2 µm), diluted with reagent-grade water, and analyzed by ICP-OES. Digestates of PNS sediments and subsamples of wet PNS sediments were sent to Calscience Environmental Laboratories (Garden Grove, CA) for measurement of total recoverable metals (EPA method 6010B) and PAHs (EPA method 3545 followed by method 8270C). AVS and SEM were extracted with standard methods [41] and quantified either colorimetrically (AVS) or by ICP-OES (SEM), and was used as an estimate of bioavailable metals in the subsequent discussions. Total reduced inorganic sulfur (TRIS) was extracted with HCl and Cr powder and measured colorimetrically.[52] Pyrite-S was estimated as the difference between TRIS and AVS.[53] Sediment grain size distributions were determined after wet sieving.[54] Permeability was measured by imposing a constant head difference of 1.6 m on a filtration column (ID 2.5 cm, Omnifit, Danbury, CT, USA) packed with sediment and interpreted according to Darcy's Law.[55]

4.2.4.2 Dissolved and particulate metals and organic carbon

Water samples were filtered through polycarbonate membranes (0.2 µm) and acidified to 2% with high-purity HNO_3. Metals in water were analyzed by either ICP-OES at the University of Michigan (freshwater) or ICP-OES (seawater) following EPA method 6010B at Calscience Environmental Laboratories. Practical Quantitation Limits (PQL) for freshwater samples were conservatively estimated by multiplying the manufacturer determined Instrument Detection Limit (IDL) by a factor of 20. For seawater samples, the detection limits reported by Calscience were determined to be acceptable to be used as quantitation limits, based on the quality control standards used by this laboratory. These Calscience standards are therefore reported as Method Detection Limits (MDL). Separate aliquots of filtered water (0.2 µm) were acidified to pH < 2 for determination of dissolved organic carbon (DOC) on a carbon analyzer. Dried filters containing suspended particles were weighed, acid digested with microwave assistance, filtered, diluted and analyzed as detailed for sediments. Samples for analysis of TOC in SPM were collected by filtering water through pre-ashed (500 °C) 25 mm GF/F glass fiber filters. TOC was determined as described above for sediment TOC. Following acid treatment, filters were dried, rolled in 25 mm tin discs and analyzed on a CHN Elemental Analyzer.

4.2.4.3 Tissue metals analysis

Metal concentrations were measured in depurated *N. arenaceodentata*. Organisms were dried (60 °C), weighed (to nearest 0.001 mg) and digested for 6 d in high-purity 16 N HNO$_3$, followed by addition of 30% ACS-grade H$_2$O$_2$ for an additional 24 h.[56, 57] Digestates were diluted with reagent-grade water and analyzed by inductively coupled plasma mass spectrometry.

4.2.5 Quality Assurance and Data Analysis

Quality control analyses (procedural blanks and spike recoveries) for AVS, SEM, TOC, sediment and tissue metal concentrations were within acceptable ranges (Table 4-2). Statistical analyses were conducted with R 2.14.0.[58] Separate two way ANOVAs were used to investigate differences in toxicity endpoints (i.e., survival, growth, and tissue metal concentrations) for exposures to overlying water (unsuspended v. resuspended) and sediment (bedded v. redeposited). A significant interaction between sediment integrity (e.g., bedded vs. redeposited) and exposure conditions (i.e., control vs. treatment) indicated an effect of resuspension on an endpoint. Two-sample *t*-tests were conducted for experiments with incomplete treatment combinations (e.g., *H. azteca* feeding was not measured from bedded exposures). A nonlinear least squares regression with a Michaelis-Menten kinetics equation was fit to the dissolved metal release data for Lake DePue sediments.[59] One-way ANOVA and *t*-tests were used to determine differences in Qwiklite bioluminescence. Two sample *t*-tests were used to investigate differences in AVS, SEM and $\sum$ (SEM$-$AVS)/fOC between bedded and redeposited sediments. Simple linear regressions were used to examine relationships between pH and dissolved O$_2$ with turbidity. When necessary, data were normalized with appropriate transformations (natural log and arcsine square root) to ensure assumptions of equal variance and normality were met. Non-parametric tests were used when normality could not be achieved with transformations.

Table 4-2. Summary of analyses of procedural blanks and recoveries of known additions with number of replicates in parentheses. ND = not detected. -- = not analyzed.

Analyte	Procedural blank	Recovery of known (%)
AVS	ND (2)	89 ± 3 (3)
SEM$_{Fe}$[a]	71 ± 19 µg/L (2)	--
SEM$_{Zn}$	13 ± 2 µg/L (2)	--
TOC[b]	0.05 ± 0.01% (9)	99 ± 4 (4)
Sediment Zn[c]	5 ± 8 µg/L (10)	93 ± 5 (9)
Sediment Cu	< DL (10)	90 ± 4 (9)
Sediment Cr	< DL (9)	82 ± 6 (8)
Sediment Pb	< DL (9)	99 ± 4 (5)
Sediment Ni	< DL (10)	101 ± 14 (9)
Sediment Fe	9 ± 7 µg/L (10)	92 ± 3 (9)
Sediment Mn	< DL (10)	94 ± 2 (5)
Organism Cu[d]	3 ± 2 µg/L (8)	90 ± 12 (7)
Organism Ni	2 ± 1 µg/L (8)	85 ± 11 (7)
Organism Zn	194 ± 195 µg/L (7)	117 ± 41 (7)

[a] Other SEM metals (Mn, Cu, Ni, Pb and Cd) were less than detection limits.
[b] Total organic carbon (TOC) recoveries based on analyses of caffeine and NIST 2702.
[c] Sediment metal recoveries based on analyses of NIST 2702 and NIST 2781.

[d] Organism recoveries based on analysis of NIST 1570a.

4.3 Effects of Bioturbation and Bioirrigation on Particle Dispersion and Oxygen Redistribution.

4.3.1 Sediment source, collection and characterization.

Both contaminated and reference sediments were collected from Lake DePue for bioturbation and bioirrigation experiments. Contaminated sediments were collected from red dot area and reference sediments were collected in the downstream as shown in the yellow dot area (Figure 4-5). Sediments were collected, transported and stored as described in section 4.1.2.
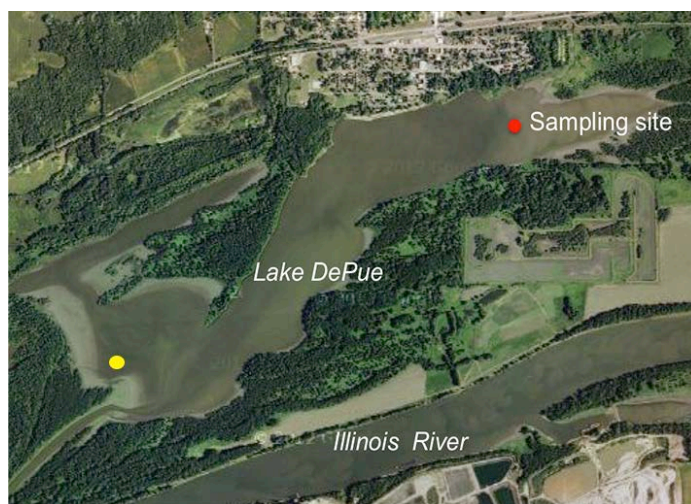
Figure 4-5. Location and aerial photograph of Lake DePue. Red dot represents contaminated sediment sampling site and yellow dot represents reference sediment sampling site.

4.3.2 Experimental setup

Three sets of imaging system were developed to characterize the effect of bioturbation and bioirrigation on sediment structure, particle and solute dispersion in sediments: 1) Bioturbation system used time lapse imaging method to characterize the effect of bioturbation on alteration of sediment structures; 2) LED induced fluorescence bioturbation system (LIF-bioturbation) used fluorescent particles as tracers to characterize bioturbation induced particle mixing; 3) Oxygen optode system was developed to characterize the effects of bioturbation and bioirrigation of oxygen redistribution within sediments. In all these systems, bioturbation chambers ($10 \times 10 \times 22$ cm) were used to contain sediments and harbor the worms.

1) Bioturbation system (Figure 4-6)

Bioturbation chambers ($10 \times 10 \times 22$ cm) were made of acrylic plastics (McMaster Carr). The chambers were filled with LDP sediments to a depth of 8 cm and the headspace of the chamber was filled with ARFW. ARFW was recirculated through a 500 mL water reservoir (HDPE, Nalgene), where the water was oxygenated by an aquarium pump. A mechanical stir (IKA Lab Egg, Cole Parmer) was used to keep the overlying water homogenized but not suspend surficial

sediments. A Nikon D7000 single lens reflex digital CMOS camera (4,928 × 3,264 pixels) equipped with an f2.8 Nikkor 40 mm lens (B&H Photo-Video Inc, NY), an R1 wireless controlled close-up Speedlight system (B&H Photo-Video Inc, NY) was placed in front of the chamber to acquire sequential images. The camera and the flash system were programmed to work every five minutes. The configuration provides an effective image resolution of 20 × 20 μm per pixel.
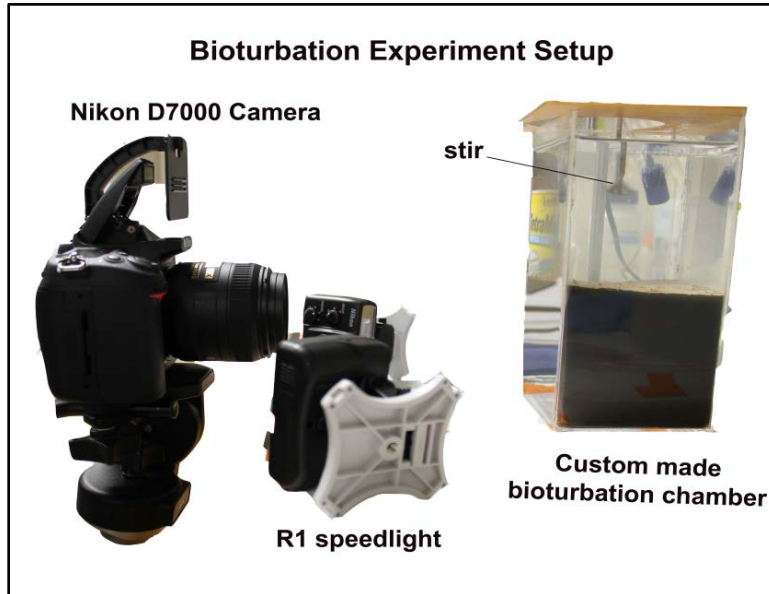
Figure 4-6. Bioturbation experimental setup.

2) LIF-bioturbation system (Figure 4-7)

In LIF-bioturbation experiments, 5 mg of fluorescent particles (ZQ-14, Dayglo Color Corp, OH), which have a size range of 20 to 60 μm and an excitation and emission wavelength of 405 nm and 620 nm, were spread at the sediment water interface to function as tracers. Two UV LED lights (excitation wavelength of 407 nm, Super Bright LEDs, Missouri) and two warm white LED lights (Super Bright LEDs) were connected to a programmable DC power supply (Bell Electronics NW). The UV LEDs were used to excite the fluorescent particles while the warm white LEDs were used to illuminate sediment structures, both sediment water interface and worm burrows. A band-pass emission filter (610 nm wavelength with 10 nm bandwidth, Edmund Optics Inc.) was mounted on the lens of the camera. The camera and DC power supply were programmed to take sequential images with 3 min intervals. Dark images, which serve for background correction, white images, and fluorescent images were taken sequentially.

Figure 4-7. LIF-bioturbation experimental setup.

3) Oxygen optode system (Figure 4-8)

In oxygen optode experiments, planar oxygen optodes were constructed by coating Pt-porphyrin luminophores (excitation 390 nm, emission 645 nm) onto a transparent glass sheet. The planar optode was mounted on the sidewall of bioturbation chambers before emplacement of sediment. 2 UV LEDs (excitation 407 nm) were used to illuminate the optode and a high sensitivity digital video camera (PCO 1600, Cooke Corporation) equipped with a high pass filter (620 nm) was used to acquire fluorescence images. The LEDs and CCD camera were connected to and programmed by a four-channel pulse generator and digital delay circuit (Berkeley Nucleonics). The configuration provides an effective resolution of 70×70 μm per pixel.

Figure 4-8. Oxygen optode experimental setup.

4.3.3 Experimental conditions

Five bioturbation experiments were conducted to study the effects of bioturbation and bioirrigation on sediment structure alteration, sediment mixing and oxygen redistribution (Table 4-3). Experiment B1 and B2 were performed with the bioturbation system. Time series images

were acquired and processed to characterize how the bioturbation process changed the physical sediment properties, such as porosity. Results from experiment B1, with reference LDP sediments, were compared with those obtained from experiment B2, with contaminated sediments, to assess the effects of metal contamination on bioturbation. Experiment B3 and B4 were conducted with LED-Induced Fluorescence (LIF) imaging to characterize the effects of bioturbation and metal contamination on sediment mixing. Experiment B5 was performed with oxygen optode system to characterize the effects of bioirrigation on oxygen redistribution.

Table 4-3. Conditions for bioturbation experiments

	Experiment types	Sediment type	Worm density (ind/m^2)	Image type
B1	Bioturbation	LDP reference		White light
B2	Bioturbation	LDP contaminated		White light
B3	LIF-bioturbation	LDP reference	5000	Fluorescence
B4	LIF-bioturbation	LDP contaminated		Fluorescence
B5	Oxygen optode	LDP contaminated		Oxygen optode

4.3.4 Experimental procedure

Before experiments, bioturbation chambers and 500 mL HDPE bottles were cleaned by soaking into 10% HNO_3 (v/v) for 24 h followed by soaking and rinsing twice with Milli-Q water. 800 cm^3 sediment was emplaced into the bioturbation chamber. ARFW was gently filled into the headspace and was recirculated into the HDPE bottle reservoir by means of peristaltic pump. The whole system was stabilized overnight to allow sediment consolidated.

For LIF-bioturbation experiments, 5 mg fluorescent particles were gently spread at the sediment water interface, and then 0.25 g of *Lumbriculus variegatus* (Aquatic Research Organisms) were added into the chamber. The camera and DC power supply were programmed to take sequential images with 3 min time intervals. Within each 9 min cycle, a dark image, a white-light image and a fluorescent image were acquired.

For oxygen optode experiments, the imaging system was calibrated before each experiment. 2 L fully oxygenated tap water was filled into the chamber to submerge the planar optode. A strong reductant, chemical sodium metabisulfite (Sigma Aldrich), was used to react with the oxygen in the water. The dissolved oxygen (DO) concentration was then measured by an oxygen probe and a fluorescent image was taken by the camera. The optode was calibrated in a stepwise fashion with different volume of reductant solutions added into the water. The optode was then calibrated in pixel-by-pixel fashion, i.e., with an individual calibration curve for each pixel in the image. After calibration, sediment was emplaced into the chamber and filled with ARFW.

4.4 Effects of Flow Hydrodynamics on Cu Efflux in Low Permeability Estuarine Sediments

4.4.1 Field Site.

Metals-contaminated sediments were obtained from the Portsmouth Naval Shipyard (PNS), a U.S. Navy shipyard located on a 276-acre island in the Piscataqua River at the mouth of Portsmouth Harbor. The Piscataqua River is a tidal estuary that forms the southern boundary between Maine and New Hampshire.[48] The water mass in Portsmouth harbor is predominantly saline, with salinity between 30-32‰. The main channel in the harbor has a minimum water depth of 22 m while the Back Channel has a minimum water depth of 6 m (Figure 4-9). Semidiurnal tides with a mean tidal range of 2.5 m occur in the harbor, while the current velocities range from 1.5-2 m/s. Fine-grained sediments occur in the low-flow zone, while coarser-grained sediments occur in regions subject to rapid tidal scouring.

A long history of construction, shipbuilding, and repair of submarines at PNS have resulted in contamination of surface water, soils, groundwater and sediments. Sediment samples for the laboratory experiments presented here were collected from monitoring stations MS3 and MS4, which are located in the eastern portion of the Back Channel (Figure 4-9). Cu is the primary chemical of concern, which is associated with past erosion of the onshore materials.
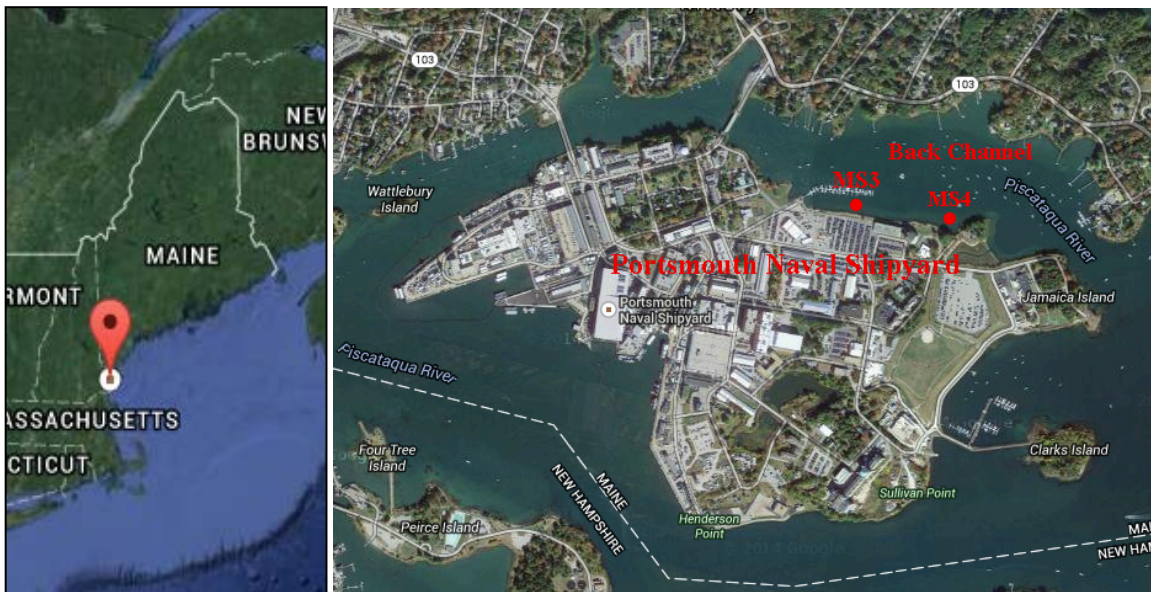
Figure 4-9. Left: Location of PNS. Right: Aerial photography of PNS and the sampling sites MS3 and MS4 as shown by Google Earth (Retrieved on February 24, 2015)

4.4.2 Sample collection.

Sediments were obtained from PNS in September of 2012. ~15 cm of surficial sediments were collected manually by divers and then shipped overnight in coolers to the laboratory, and refrigerated at 4 °C until used in the experiments.

4.4.3 Sediment characterization.

Bulk sediment properties, including porosity, pore water conductivity and salinity, particles size distribution (PSD), permeability, total organic carbon, and total metal concentration, were measured with homogenized sediment samples. To characterize the sulfur composition in the sediments, bulk acid volatile sulfide (AVS), and total reducible inorganic sulfur (TRIS) in sediments were also measured.

Bulk porosity was measured by drying 10 cm^3 of sediments at 70 °C for 48 hours, and then converting the weight loss of water to volume fraction. Porewater was extracted by centrifuging the sediments at 3414g for 20 min (Legend RT plus, Thermo Scientific). Conductivity of the filtered supernatant (0.2 μm nylon filter, VWR International, U.S.A.) was measured with a conductivity probe (Oakton Con 11, Cole-Parmer). 10 mL of the supernatant was dried at 70 °C for 48 hours and the salinity was determined by measuring weight of the remaining solids. Sediment grain size distribution was measured by wet-sieving with 45, 106, 150, 250 and 1000 μm sieves and measuring the dry weight. Permeability was measured in a constant-head permeameter with a test section of 2.5 cm in diameter and 5 cm in length (Chromatography column, Omnifit Ltd). Bulk AVS and SEM were determined by the 1M cold HCl extraction and 0.5 M NaOH trap technique.[60] H_2S produced during the extraction was collected with 0.5 M NaOH and determined colorimetrically by adding mixed diamine reagent and measuring the absorbance with a UV-visible spectrophotometer (Spectronic 20, Spectronic Instrument). Extracted metals were measured using ICP-OES (Vista-MPX, Varian). TRIS was determined by decomposing reduced sulfur species (pyrite, AVS and elemental sulfur) in sediments with a hot acidic $CrCl_2$ solution. [52, 61] Cr powder (Sigma Aldrich, U.S.A.) was added into the digestion flask during the extraction in order to produce a fresh $CrCl_2$ solution.[52] Resulting H_2S was collected and quantified as described above. Total organic carbon was measured by acidifying 80 mg of dry sediments with 1.5 mL of 4N HCl followed by analysis with an Elemental Analyzer (Costech ECS 4010, Costech Analytical Technology Inc., Valencia, CA). Total bulk metal concentrations were measured by ICP-OES after microwave-assisted acid digestion following USEPA method 3051A.[62]

4.4.4 Experimental Setup.

Gust-type mesocosms[63] were used to subject the contaminated sediments from PNS to controlled overlying flow conditions. The Gust chamber (Green Eyes LLC, Cambridge, MD, U.S.A.) (Figure 4-10) uses a combination of a spinning disk and a central suction port to generate a uniform shear stress over the SWI. A DC power supply and a linear motor controller (LSC 30/2, Maxon Precision Motors Inc., U.S.A.) precisely control the rotation rate of the spinning disk, providing a calibrated shear stress between 0.01-0.9Pa. All parts of the Gust chamber were made of polycarbonate to minimize metal contamination. A covered 5 L plastic beaker was used as a reservoir for recirculating water. The inlet and outlet ports of the Gust chamber were connected to the water reservoir by tygon tubing (VWR International, LLC, U.S.A.) and a peristaltic pump (Masterflex, Cole Parmer). Rhizon *in situ* samplers[64-66] (RISS) with 0.15 μm pores (Sunvalley Solutions Inc, Florida, U.S.A.) (Figure 4-10) were installed into the Gust chamber to enable time-series sampling of pore water over the course of the experiments. Experiments were performed with artificial seawater (ASW) made by dissolving 32 g sea salt (Tropic Marin, U.S.A.) into 1 L Milli-Q water (Millipore).
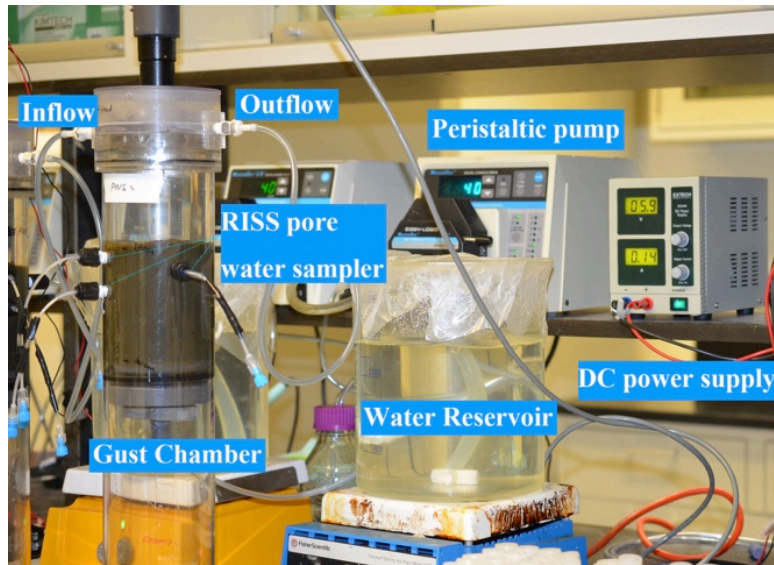
Figure 4-10. Gust chamber system with contaminated sediments.

4.4.5 Hydrodynamic conditions.

Six Gust chamber experiments were performed on PNS sediments. Hydrodynamic conditions for experiments (Table 4-4) were chosen relative to the critical shear (C.S.), which is shear required to cause general sediment resuspension. The critical shear of the test sediments was first characterized by varying the rotation rate of the spinning disk and the recirculation rate in a stepwise fashion until the turbidity of the overlying water increased. The critical shear stress was measured as described in section 4.1.5, and found to be 0.37 Pa for sediments from both PNS locations (MS3 and MS4). Experiments were performed by imposing a constant ("baseline") shear for 14 days. Separate experiments were run at 3%, 50%, and 70% of the critical shear. Experiments run at 70% of the critical shear were also subject to two periods of episodic resuspension of 4 h duration each on days 1 and 8. Resuspension was achieved by subjecting the sediments to a constant shear of 0.9 Pa for 4 h.

Table 4-4. Conditions for Gust chamber experiments. All experiments have durations of 14 days.

Series	#	Sediment location	Baseline shear (Pa)	% of C.S.	Periods of sediment resuspension	
F	F1	MS4	0.011	3%	-	
	F2	MS4	0.185	50%	-	
	F3	MS4	0.262	70%	4 h on day 1	4 h on day 8
C	C1	MS3	0.011	3%	-	
	C2	MS3	0.185	50%	-	
	C3	MS3	0.262	70%	4 h on day 1	4 h on day 8

4.4.6 Experimental procedures.

Before each experiment, all parts of the Gust chamber systems were cleaned by soaking in 10% HNO_3 (v/v) for 24 h. 800 mL of homogenized sediments were then carefully emplaced into the Gust chamber to form a 10 cm deep sediment bed with a flat surface. Three RISS were inserted into the sediment at depths of 1, 2, and 4 cm below the SWI while the sediment was introduced. The 10 cm of headspace was then slowly filled with ASW to avoid disturbance of the sediments. The erosion head was then placed onto the chamber. The system was allowed to stabilize overnight, and then 4.785 L ASW was continuously recirculated for 14 d under the hydrodynamics conditions listed in Table 4-4. The recirculating water was kept oxygenated during the experiments by continuously bubbling water-saturated air into the reservoir.

4.4.7 Sampling and analysis.

Dissolved oxygen (DO), pH, turbidity, conductivity, and dissolved and total metal concentrations in the recirculating water were measured daily. DO was measured directly in the water reservoir with a DO probe (HQ10, Hach). 24 mL of overlying water was sampled from the recirculating flow daily and split into three aliquots. Sampled volumes were compensated with clean ASW to maintain a constant reservoir volume throughout the experiments. One aliquot of the overlying water was used to measure pH (420Aplus, Thermo Orion), conductivity, and turbidity (2100Q, Hach). The other two aliquots were analyzed for dissolved and total metal concentrations. Samples analyzed for dissolved metals were filtered through a 0.2 μm nylon membrane filter (VWR International, U.S.A.) and acidified with concentrated, trace-metal grade HNO_3 (Sigma Aldrich, U.S.A.) to pH<2. Samples analyzed for total metals were acidified to pH<2 without filtration. Samples were stored at 4°C until analyzed. Samples for total metals were filtered just before analysis to remove any residual particulate matter.

Porewater samples were extracted via RISS on days 0, 1, 3, 5, 8, 10, 12, and 14. The first mL of pore water withdrawn from each RISS was discarded and another 2 mL of pore water was collected, acidified to pH<2, and stored for metal analysis.

Cu concentrations in overlying water and pore water samples were analyzed by Zeeman Graphite Furnace Atomic Absorption Spectrometry (Z-GFAAS, Varian SpectrAA-800). UV atomic absorbance of Cu was measured at 248.3 nm. Zeeman background correction overcomes the seawater matrix effects.[67] Ammonium nitrate (5.0% v/v) (catalog no. 256064, Sigma Aldrich) was used as matrix modifier to remove halide salts from the graphite cuvette during ash phase of the furnace program. Standards were prepared from 1000 mg/L Cu stock solution (Sigma Aldrich) diluted with NASS-4 open ocean reference water (National Research Council of Canada) to match sample salinity. 20 μL sample with 20 μL modifier solution were co-injected for each analysis.

Fe concentrations in overlying water samples were analyzed using the ferrozine colorimetric method.[68, 69] 150 μL of hydroxylamine hydrochloride solution (Sigma Aldrich) was added to 1 mL of sample and allowed to react for 10 min to reduce Fe (III) to Fe (II). 100 μL ferrozine (Sigma Aldrich) and 200 μL ammonium acetate buffer solution (Sigma Aldrich) were then added and the absorbance of sample was measured at 562 nm of with the UV-visible spectrophotometer.

At the end of each experiment, the erosion head was removed and dissolved oxygen concentration profiles in porewater were measured with an oxygen microelectrode (OX-50, Unisense, Denmark). The overlying water was then drained, and a set of sediment subcores were obtained for AVS and SEM analysis using modified 60 mL syringes.[70] Sediment subcores were

transferred to a glove box (3% H_2 and 97% N_2) (Coy laboratory products Inc., USA) to avoid oxidation, and sectioned at 0.5 cm intervals for the first 2 cm below the SWI and then at 1 cm intervals for the remainder of the core. Sediment sections were stored in 50 mL polycarbonate centrifuge tubes (VWR International, USA), sealed with vinyl tape (VWR International) and stored at -20°C until analyzed for AVS and SEM using methods described previously.

4.5 Interplay of Hydrodynamics and Bioturbation on Mobility and Efflux of Cu

4.5.1 Sediment source.

A laboratory flume experiment (Figure 4-11) was performed with Cu-contaminated sediments from Portsmouth Naval Shipyard (PNS). PNS is located on an island at the mouth of Piscataqua River, which is a tidal estuary that locates between Maine and New Hampshire.[48] The water in vicinity of PNS has a salinity of 30~32 ‰. The offshore region is subject to strong tidal influences. Fine-grained sediments deposit out of the main flow of Piscataqua River and coarse-grained sediments deposit in regions where strong tides and erosion occurs. The offshore areas provide habitats for a wide variety of biota, including invertebrate worms, mussels, crabs and fishes. Offshore sediments in proximity of PNS received substantial contamination from onshore construction and submarine repair activities. Elevated levels of Cu were detected in the sediments.
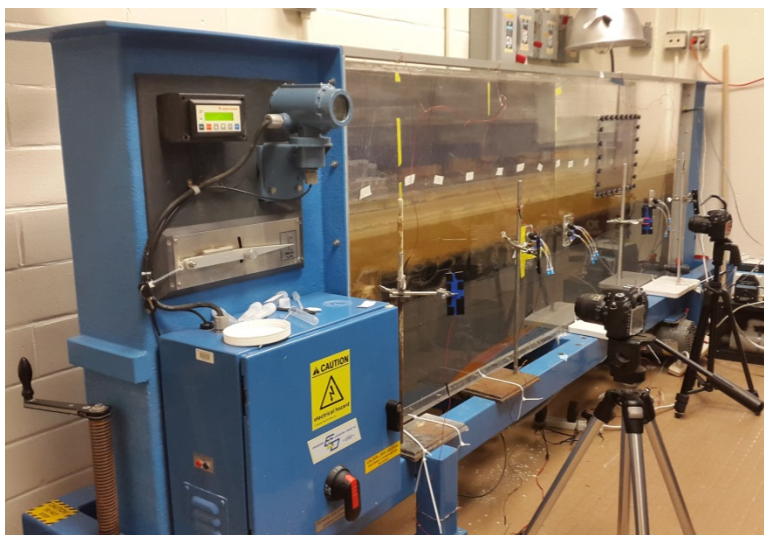
Figure 4-11. Flume experimental setup.

4.5.2 Sample collection

About 100 L Cu contaminated sediments from the site MS3 were supplied by PNS in August 2013. Up to 15 cm surficial sediments were collected and shipped to the laboratory and immediately refrigerated at 4 °C until experiment was performed.

4.5.3 Experimental setup

Due to its full control of stream and sedimentation conditions, laboratory flume has been widely used for study of hyporheic exchanges.[71] A small recirculating flume was used here to study the effects of hydrodynamics and bioturbation on redistribution and mobilization of Cu in sediments. The flume has a test section of 2.5 m in length, 0.2 m in width and 1m in depth. A computer controlled variable speed pump and a vortex shedding flowmeter (Rosemont model 8800, Chanhassen, MN) built into the recirculating loop enable precisely control of the flow hydrodynamic condition. The sidewall of the flume is made of acrylic plastics, which allows visualization of changes taken place inside the flume. An impermeable acrylic plastic ramp was placed at the upstream end to ensure steady and uniform water flow developed over the sediment bed. A porous polyethylene sheet with 90-130 micron pores (Small Parts International) at the downstream end helped retain the sediment bed without restricting the pore water flow. Three sets of rhizon *in situ* samplers (RISS) (Sunvalley Solutions Inc, Florida) were installed along the sidewall for time-series pore water sampling.[64-66] RISS were installed at 0.9 m, 1.2m and 2.1 m longitudinally and at depth 1 cm, 2cm and 4 cm vertically. 180 L artificial seawater (ASW), which was made by dissolving every 32 g sea salt (Tropic Marin, USA) into 1 L reverse osmosis (RO) water, was continuously recirculated over the course of experiment. An acoustic Doppler velocimeter (MicroADV, SonTek, CA) was used to characterize the stream velocity profile.

4.5.4 Experimental Conditions

Individual effects of hydrodynamics and bioturbation, as well as interactions between the two processes, on the mobilization of Cu in sediments were studied by performing a flume experiment. The experiment was run for duration of 26 weeks and subdivided into 14 phases (Table 4-5). At initiation of experiment, the system was stabilized for 4 weeks under baseline shear, which ensured the main stream was in turbulent state that facilitated the oxygen diffusion from air to the main stream. For conditions with higher shear stress, the flow rate was increased and kept for one week and then change back to the baseline condition for another week. Experiment was also subject to episodic resuspension, during which the flume was run on its maximum capability (0.58 Pa) for four hours. 40 *Nereis virens* (Aquatic Research Organisms, NH), corresponding to a density of 800 ind /m^2, were added to the flume on day 134 to study the individual effect of bioturbation and coupling effect between bioturbation and hydrodynamics on the metal efflux.

4.5.5 Experimental procedures

Before experiment, flume was filled with weakly acidic RO water (pH = 2) and run for 24 hours and rinsed with purified RO water twice to remove potential contamination. 50 L of homogenized sediments were emplaced into the flume to form a 10 cm sediment bed. While introducing the sediment, three sets of RISS were installed on the sidewall at 0.9 m, 1.2 m and 2.1 m longitudinally and at depth 1 cm, 2 cm, and 4 cm vertically for pore water collection. 180 L ASW was then carefully filled into the flume to form 10 cm overlying water column. The whole system was allowed to consolidate overnight and the recirculating water was drained and replaced with same volume of clean ASW on the second day before start of the experiment.

Table 4-5. Conditions for flume experiment.

Phase	Time	Duration	Shear stress (Pa)	Bioturbation
1	Day 0-28	4 weeks	0.11	No
2	Day 29-36	1 week	0.22	No
3	Day 36-42	1 week	0.11	No
4	Day 43-50	1 week	0.47	No
5	Day 51-57	1 week	0.11	No
6	4 hours on day 57	4 hours	0.58	No
7	Day 57-133	11 weeks	0.11	No
8	Day 134-148	2 weeks	0.11	Yes
9	Day 148-155	1 week	0.22	Yes
10	Day 155-162	1 week	0.11	Yes
11	Day 162-169	1 week	0.47	Yes
12	Day 169-176	1 week	0.11	Yes
13	4 hours on day 176	4 hours	0.58	Yes
14	Day 176-184	1 week	0.11	Yes

4.5.6 Sampling and analysis

Since in-stream mixing is rapid compared with experiment durations, a single sample at the downstream well can represent the whole recirculated overlying water. Overlying water samples were acquired daily for physicochemical characterization, including dissolved oxygen (DO), pH, turbidity, conductivity and dissolved and total metal concentrations. DO was measured directly at the downstream well of the flume with a DO probe (HQ10, Hach). 24 mL of water samples were collected each time from the recirculating overlying water and split into three aliquots. One aliquot was used for measurement of pH (420Aplus, Thermo Orion), conductivity (Oakton Instruments) and turbidity (2100Q, Hach). The other two aliquots were aimed for dissolved and total metal measurement. 8 mL of the water sample for analysis of dissolved metals was filtered (0.2 μm nylon filter, VWR International), and acidified with HNO_3 (trace metal grade, Sigma Aldrich) to pH <2. The last 8 mL of water sample was acidified with HNO_3 to pH<2 without acidification to capture both dissolved and particulate metals. All water samples were stored at 4 °C before analysis. Cu concentrations in the water samples were analyzed by Zeeman Graphite Furnace Atomic Absorption Spectrometer (Zeeman-GFAAS). Ferrozine colorimetric method was used to characterize Fe concentration in the total metal samples.[68, 69]

Porewater was sampled periodically by RISS over the course of experiments to characterize the Cu concentrations in pore water spatially and temporally. The first 0.5 mL of pore water from RISS was discarded and another 2 mL of water was collected, acidified to pH<2, and stored until Cu analysis.

At the end of each phase, DO concentrations in pore water were characterized by oxygen microsensor system (OX-100, Unisense, Denmark). The microelectrode was mounted on a step motor with computerized depth control (Unisense, Denmark) and driven into sediment with a step size of 125 μm.

Zeeman GFAAS was used to characterize Cu concentrations in all water samples.[67] UV atomic absorbance of Cu was measured at 248.3 nm. NH_4NO_3 (5% v/v) (catalog no. 256064,

Sigma Aldrich) was used as a chemical modifier to remove halide salts during the analysis. Standards were prepared by diluting Cu stock solution (1000 ppm, Sigma Aldrich) with NASS-4 open ocean reference seawater (National Research Council of Canada) to match the sample matrix. 20 μL sample with 20 μL modifier solution was co-injected into graphite cuvette for each analysis.

Fe (III) in water samples was determined by the ferrozine colorimetric method.[69] Fe (III) in 1 mL of sample was first reduced to Fe (II) with 150 μL hydroxylamine hydrochloride solution (concentration, Sigma Aldrich) for 10 min. 200 μL ammonium acetate buffer solution (concentration, pH=9.5) (catalog number, Sigma Aldrich) and 100 μL ferrozine (concentration, Sigma Aldrich) were added and absorbance of the sample was measured at 562 nm with a UV-visible spectrophotometer (Spectronic 20, Spectronic Instrument).

5. Results and Discussion

5.1 Coupled Effects of Hydrodynamics and Biogeochemistry on Zn Mobility and Speciation in Highly Contaminated Sediments

(Results reported in Minwei Xie, Brooke A. Jarrett, Cecile Da Silva-Cadoux, Kyle J. Fetters, G. Allen Burton Jr., Jean-François Gaillard, Aaron I. Packman. 2015. Environmental Science & Technology. 2015. 49: 5346-5353)

5.1.1 Sediment characteristics.

Bulk sediment characteristics are reported in Table 5-1, the sediment particle size distribution in Figure 5-1(a), (b), and sediment microstructure in Figure 5-1(c). The sediment was composed primarily of very fine particles (~80% of particles with diameter <10 μm) and contained, on average, 3% organic carbon. Consequently, the sediment had a very low permeability, $2.0\pm1.2 \times10^{-14}$ m^2. The bulk sediment Zn concentration was very high, on the order of 1.4 % by mass, which is consistent with prior assessments of metals contamination in Lake DePue.[47, 72, 73]

Table 5-1. Bulk characteristics of the Lake DePue sediments used in the experiments.

Porosity	49.3%	Permeability (m^2)	$2.0\pm1.2 \times10^{-14}$
Organic C	3.09%	Zn (mg/kg dry weight)	14,000
Inorganic C	2.65%	Cu (mg/kg dry weight)	410
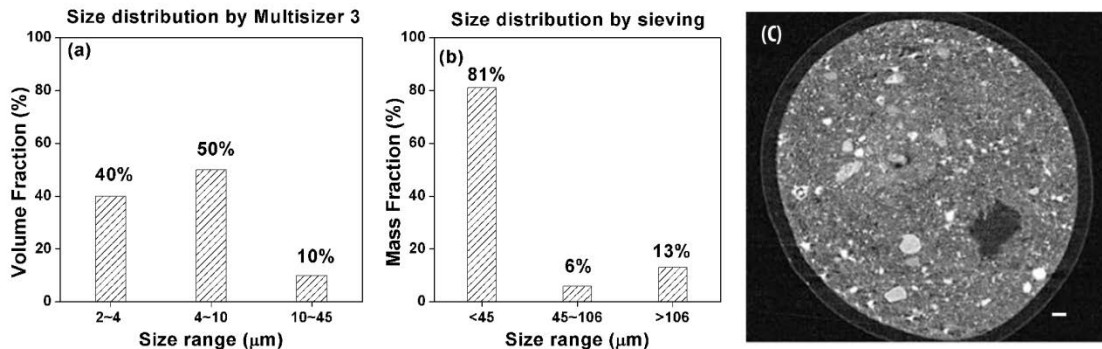
Figure 5-1. (a)(b) Particle size distribution of lake DePue sediments and (c) Microstructure of sediments obtained by XMT imaging. Sample shown has an O.D of 1.9 mm, and was obtained by sub-coring an intact sediment core. The white scale bar represents 100 μm.

5.1.2 Zn concentration in porewater.

Porewater Zn concentrations in experiments with and without sediment resuspension are shown in Figure 5-2. Zn concentrations in porewater from experiment G1 (without resuspension) provide a frame of reference for experiments G2 and G3 (with resuspension). Results from experiment G2 and G3 reflect measurements of porewater Zn concentrations at different times after resuspension: immediately after resuspension and two days later.

Dissolved Zn concentrations at depths greater than 1cm were uniform for all three treatments, suggesting that Zn solubility remained constant with depth. Porewater Zn concentrations near the top of the core, i.e., within the first centimeter, were substantially higher

than those observed at depth and in the overlying water, suggesting that diagenetic processes change the solubility of Zn resulting in its mobilization near the sediment-water interface, making the sediment a source of Zn to the overlying water. Resuspension increased porewater Zn concentration in the first centimeter of the sediments, and these concentrations decreased following cessation of sediment transport. In experiment G2, which was sub-cored immediately after resuspension, the Zn concentration in the porewater within the first centimeter of sediment was 3.04 μM, much greater than the surficial porewater concentration in experiment G3, 1.15 μM, which was sampled two days after resuspension. Both of these porewater Zn concentrations were much higher than those observed in experiment G1, 0.55 μM, which had no resuspension.
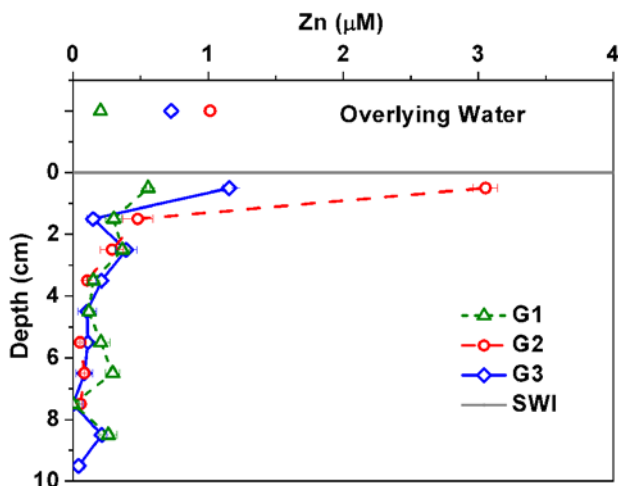
Figure 5-2. Zn concentrations in pore water. G3 was sampled two days after resuspension, G2 was sampled immediately after resuspension, and there was no resuspension in G1. Error bars represent ±1 standard deviation.

5.1.3 SEM and AVS.

SEM and AVS results are presented in Figure 5-3. Extracted Zn, Cu, Pb and Cd concentrations are reported in Table 5-2. Zn was the primary metal present in the sediments: Zn was more than 95% of the total SEM (ΣSEM) for all samples. The AVS profile for experiment G4, with homogenized sediment structure, showed lower concentrations in the surficial sediment and relatively constant concentrations at depth, suggesting oxidation of surficial sediment by diffusion of oxygen from the overlying water.[74] The SEM:AVS molar ratios were all >1, indicating that a signification fraction of metals is bound to other ligands other than volatile sulfides. This condition is generally interpreted to mean that metals toxicity is likely.[75] The maximum SEM:AVS ratio was observed at the SWI, suggesting higher likelihood of metal toxicity to epibenthic organisms.

AVS profiles for experiments G1 and G3, with intact sediment structure, showed higher concentrations at depth 1-2 cm than in both surficial and deeper sediment, suggesting that sulfide production was the greatest at this depth. Lower AVS concentrations in the surficial sediment also suggest oxidation from oxygen diffusion from the overlying water. The SEM:AVS ratio varied dramatically between the two cores, with an average of 6.1 and 20.9 for G1 and G3, respectively, suggesting that there is great spatial variability in sediment metal toxicity at this site.

30
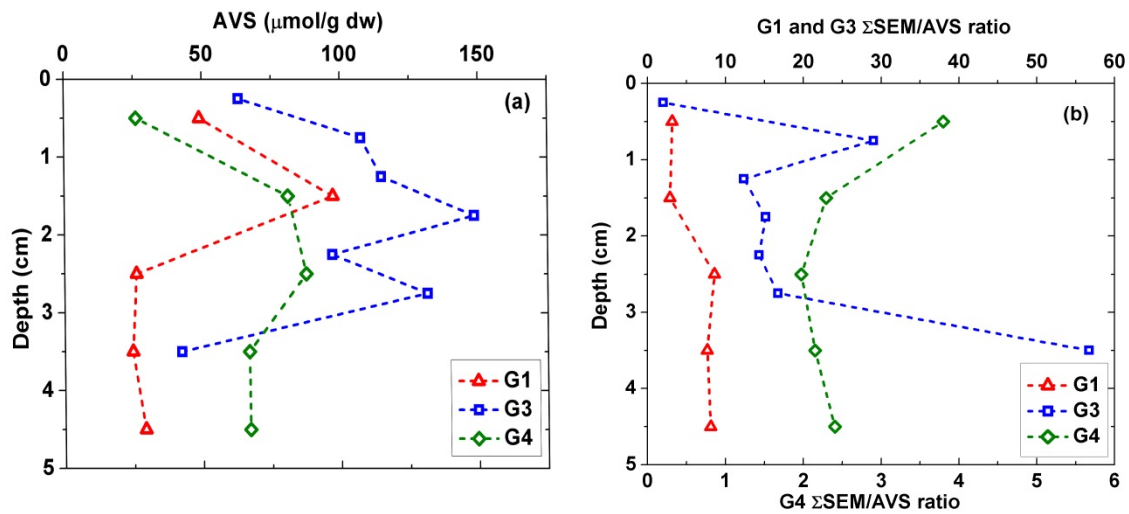
Figure 5-3. Profiles of AVS and SEM:AVS ratio in homogeneous sediments (G4) and intact sediment cores (G1 and G3).

Table 5-2. Depth distribution of SEM and AVS in each treatment.

	Depth (cm)	SEM-Cu (µmol/g dry weight)	SEM-Pb (µmol/ g dry weight)	SEM-Cd (µmol/ g dry weight)	SEM-Zn (µmol/ g dry weight)	ΣSEM (µmol/ g dry weight)	AVS (µmol/ g dry weight)
G1	0-1	4.6	1.6	0.8	147	154	49
	1-2	6.4	2.8	1.5	271	281	97
	2-3	4.0	2.3	1.1	216	224	26
	3-4	2.3	2.2	1.0	183	189	24
	4-5	3.3	2.5	1.1	229	236	29
G3	0-0.5	3.6	1.5	0.8	119	126	63
	0.5-1	56	11	3.8	3047	3118	107
	1-1.5	44	8	2.1	1368	1422	115
	1.5-2	84	13	4.6	2150	2251	148
	2-2.5	27	7	2.2	1354	1389	97
	2.5-3	81	13	3.4	2104	2201	131
	3-4	96	14	3.3	2285	2399	42
G4	0-1	3.5	1.2	0.5	94	99	26
	1-2	6.6	2.2	1.0	176	186	81
	2-3	6.1	2.0	0.9	164	173	88
	3-4	5.1	1.7	0.8	136	144	67
	4-5	5.7	1.9	0.8	153	161	67

31

5.1.4 XAS data processing.

EXAFS spectra and their LCF results for all sediment samples are shown in Figure 5-4. In both experiments G2 and G3, the first two oscillations shifted towards higher k values with depth, while two other oscillations in the region k=7-10 Å^{-1} became more evident (Figure 5-4 a,b), suggesting changes in the average coordination environment of Zn.
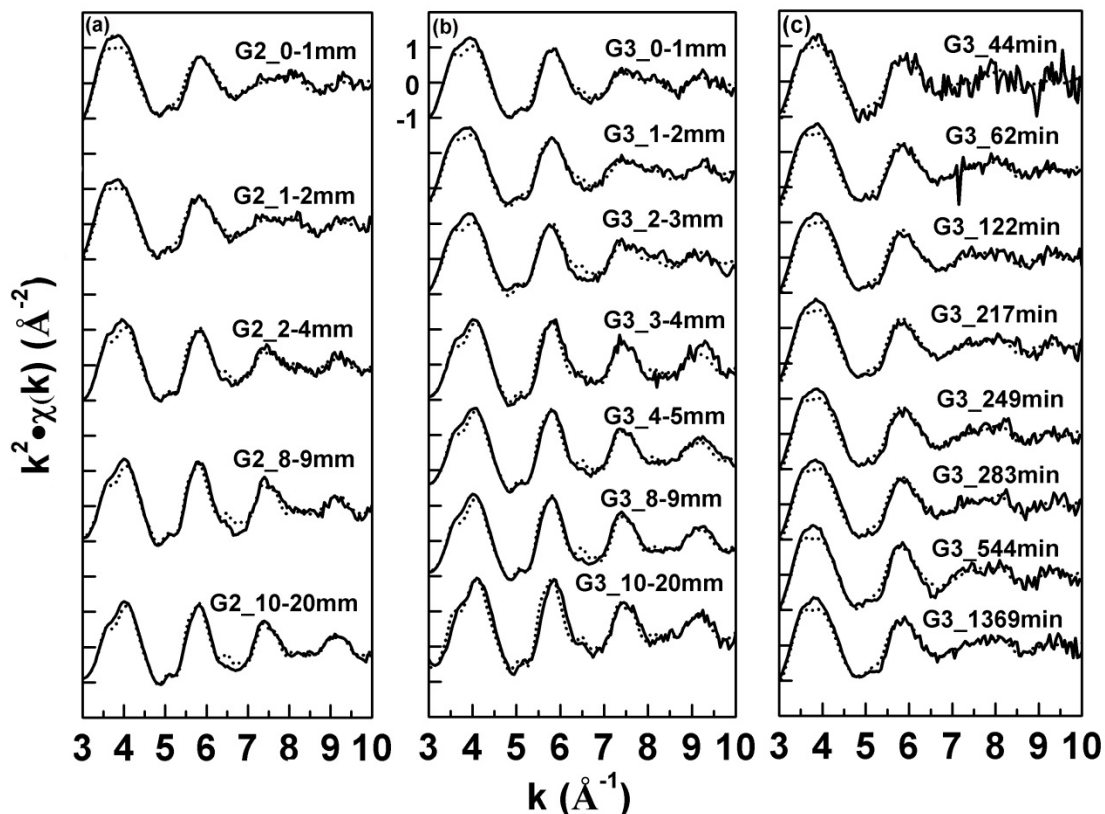
Figure 5-4. EXAFS spectra (full lines) and LCF reconstructed curves (dotted lines) for sediment samples in experiment G2 and G3. (a) Sediment core from experiment G2; (b) Sediment core obtained from experiment G3; (c) Resuspended sediments from experiment G3.

PCA analysis was performed on the complete set of sample EXAFS spectra (Figure 5-5) using Athena software to determine the minimum number of components needed to reconstruct sample spectra. PCA results are shown in Table 5-3 and the first five abstract components (C1-C5) are shown in Figure 5-5. The indicator parameter (IND) reached a minimum for three components, suggesting that the first three principal components are necessary to reconstruct sample spectra.[76, 77] Visual inspections of component spectra also suggest three principal components (Figure 5-5). Component C1 had the highest amplitude among all component spectra, suggesting it represented the primary feature of the sample spectra. C2 was characterized with lower amplitudes but still presented a clear distinction between signal and noise. C3 showed similar noise levels but had amplitude twice the height of the remaining spectra. The remaining component spectra (only C4 and C5 showed) had low signal-to-noise ratios and little meaningful

32

information. C4 and C5 are shown for comparison. Therefore, component C1~C3 were selected for target transformation of reference spectra.

Table 5-3. Principal component analysis results

Component #	Eigenvalue	IND ($\times 10^{-5}$)
C1	18.25	7.079
C2	1.08	5.029
C3	0.21	4.818
C4	0.10	4.965
C5	0.08	5.180
C6	0.05	5.581
C7	0.04	6.066
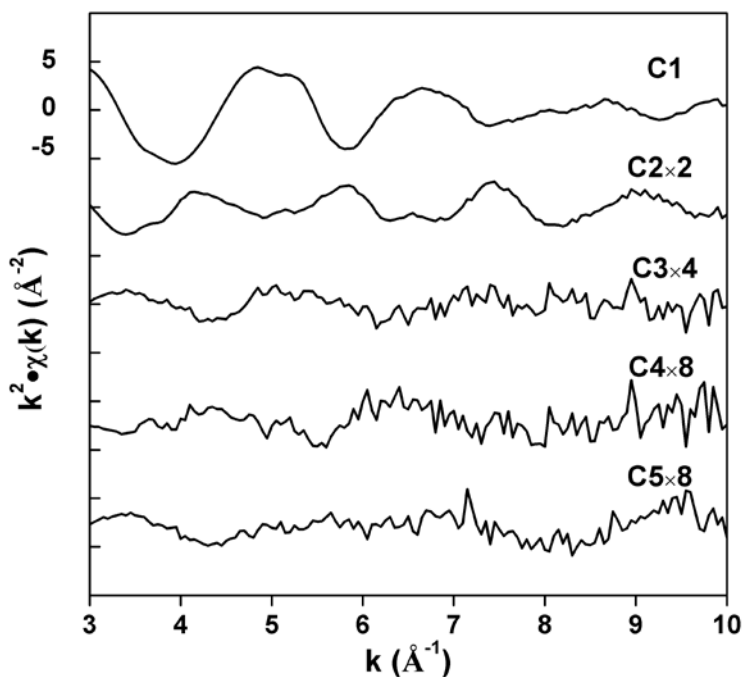
Figure 5-5. The first five components identified by PCA analysis. Amplitudes of C2, C3, C4 and C5 were multiplied by 2, 4, 8, and 8 respectively for clarity.

Target analysis was then performed by reconstructing each reference spectrum (3 to 10 Å^{-1}) individually with the three abstract principal components (C1-C3) to identify reference standards for linear combination fitting (LCF). Normalized sum-square residual (NSS) values of each spectra reconstruction were used as the primary criterion for assessing the quality of target transformation. Prospective reference EXAFS spectra were also visually assessed to ensure they were substantially distinct from each other, which is a requisite for proper selection of reference compounds.[78]

13 reference compounds were investigated and the results are shown in Figure 5-6. Among all reference compounds, Zn(aq), ZnS, and $Zn_5(CO_3)_2(OH)_6$ had the smallest NSS values. Also, their EXAFS spectra showed distinct oscillation structures. The spectrum of $Zn_5(CO_3)_2(OH)_6$ had

a small oscillation near ~7.0 Å^{-1} and wider separation of the first two peaks. The ZnS spectrum was characterized with small peaks either on the shoulder of a large peak or between two oscillations. Therefore, Zn(aq), ZnS and $Zn_5(CO_3)_2(OH)_6$ were selected as references to decompose the sample spectra.
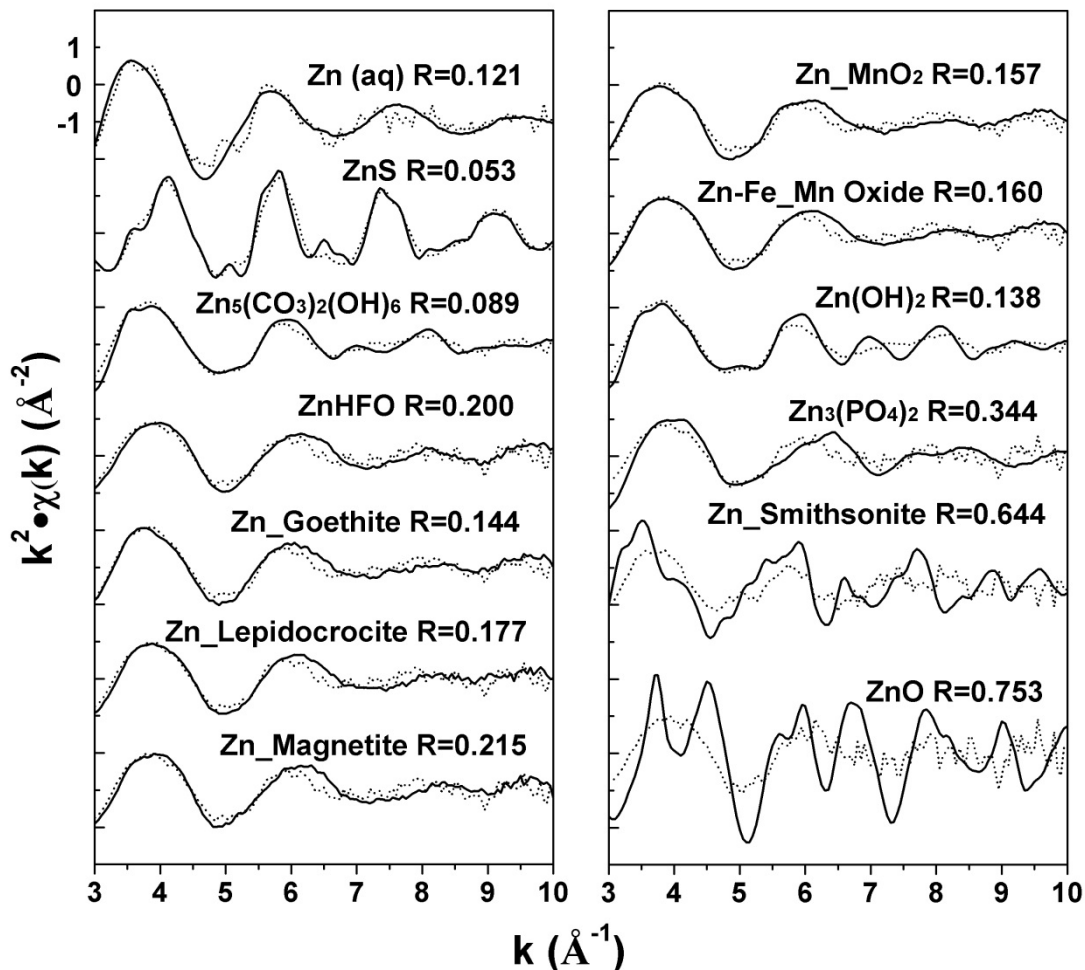
Figure 5-6. Zn K-edge EXAFS spectra (full lines), target transformations (dotted lines), and NSS values of 13 reference compounds. $R = \sum_i [k^2 \chi(k_i)_{data} - k^2 \chi(k_i)_{fit}]^2 / \sum_i [k^2 \chi(k_i)_{data}]^2$.

Least-squares LCF with the three reference standards were performed on EXAFS spectra (3 to 10 Å^{-1}). The EXAFS spectra and fitted curves are displayed in Figure 5-4. Proportions of each Zn species and the associated uncertainties are shown in Figure 5-9 and Table 5-4. Residuals of the fits were calculated, as the sum of squares of residuals normalized to sum of squares of experimental data, R factor (Table 5-4). Reconstructed curves fit the original EXAFS spectra very well. Almost all R values were < 0.1, with the only exception for sample G3_44min due to high levels of noise in the sample spectrum (Figure 5-4).

Table 5-4. Zn speciation determined by LCF with EXAFS spectra

Sample	Zn-S (%)	Zn-CO$_3$ (%)	Zn-aq (%)	R* ($\times 10^{-2}$)
G2_0-1mm	9.6±1.9	72.1±3.1	18.4±3.6	6.59
G2_1-2mm	12.9±1.6	59.8±2.5	27.2±3.0	4.91
G2_2-4mm	39.3±1.7	50.4±2.8	10.3±3.3	5.00
G2_8-9mm	52.8±2.1	31.9±3.3	15.4±3.9	5.59
G2_10-20mm	56.9±1.6	31.0±2.5	12.1±3.0	3.73
G3_0-1mm	30.3±1.7	55.4±2.7	14.3±3.2	4.96
G3_1-2mm	25.8±1.6	47.7±2.6	26.5±3.1	5.01
G3_2-3mm	34.2±2.2	41.6±3.6	24.2±4.2	8.59
G3_3-4mm	57.5±2.3	31.6±3.6	10.9±4.3	6.98
G3_4-5mm	56.9±1.6	31.0±2.6	12.1±3.0	3.80
G3_8-9mm	61.0±1.6	25.9±2.6	13.1±3.1	3.62
G3_10-20mm	66.7±3.5	27.2±2.1	6.2±2.7	5.25
G3_t=42min	6.8±3.6	82.7±5.8	10.4±6.8	**21.60**
G3_t=62min	9.0±2.1	73.5±3.3	17.4±3.9	8.32
G3_t=122min	13.4±1.8	71.0±2.8	15.6±3.4	6.44
G3_t=217min	11.5±2.0	73.4±3.2	15.1±3.7	7.75
G3_t=249min	9.9±1.9	76.0±3.0	14.1±3.6	6.92
G3_t=283min	11.5±1.9	72.6±3.1	15.9±3.6	7.31
G3_t=544min	11.1±2.1	59.9±3.3	29.0±3.9	7.32
G3_t=1369min	9.4±1.9	70.0±3.1	20.6±3.6	6.85

$$^*R = \sum_i [k^2 \chi(k_i)_{exp} - k^2 \chi(k_i)_{reconstr}]^2 / \sum_i [k^2 \chi(k_i)_{exp}]^2$$

LCF was also performed on XANES data (-20 to 100 eV above absorption edge) with the same reference spectra. XANES spectra and reconstructed curves are shown in Figure 5-7. Proportions of Zn species and associated uncertainties obtained from LCF of XANES spectra are also shown in Table 5-5. The percentages of each Zn species derived from XANES spectra correlated well with those calculated from EXAFS spectra (Figure 5-8). All points distributed close to the diagonal line y=x, indicating that both methods yielded equivalent results.

Table 5-5. Zn speciation determined by LCF with XANES spectra.

Sample	Zn-S (%)	Zn-CO$_3$ (%)	Zn-aq (%)	R* ($\times 10^{-3}$)
G2_0-1mm	14.3±2.2	64.0±5.1	21.7±6.6	2.9
G2_1-2mm	23.1±1.6	56.5±3.7	20.3±5.4	1.7
G2_2-4mm	46.4±1.3	38.5±3.0	15.0±4.9	1.1
G2_8-9mm	63.1±2.2	19.0±5.2	17.8±6.6	3.4
G2_10-20mm	69.9±1.3	16.3±2.9	13.7±4.8	1.2
G3_0-1mm	39.4±1.5	44.0±3.4	16.6±5.2	1.5
G3_1-2mm	35.1±1.3	49.0±3.1	16.0±4.9	1.2
G3_2-3mm	48.2±1.8	35.7±4.2	16.1±5.8	2.3
G3_3-4mm	62.4±1.3	24.0±3.0	13.6±4.8	1.1
G3_4-5mm	69.9±1.2	16.7±2.8	13.4±4.7	1.1

G3_8-9mm	71.4±1.3	15.7±3.1	12.9±4.9	1.3
G3_10-20mm	68.3±2.7	16.8±6.3	14.9±7.7	4.7
G3_t=42min	16.5±4.0	72.0±9.1	11.6±10.6	9.7
G3_t=62min	19.9±2.0	65.0±4.7	15.1±6.2	2.7
G3_t=122min	22.1±1.8	63.8±4.2	14.1±5.8	2.1
G3_t=217min	20.9±2.7	62.6±6.2	16.5±7.6	4.5
G3_t=249min	16.3±4.0	60.2±6.9	23.5±5.6	10.3
G3_t=283min	19.9±1.9	65.0±4.3	15.1±5.9	2.3
G3_t=544min	12.8±4.2	57.8±7.3	29.4±5.9	11.0
G3_t=1369min	11.0±4.2	64.5±7.3	24.6±5.9	11.0

$$* R = \sum_{i} [k^2 \chi(k_i)_{\text{exp}} - k^2 \chi(k_i)_{\text{reconstr}}]^2 / \sum_{i} [k^2 \chi(k_i)_{\text{exp}}]^2$$
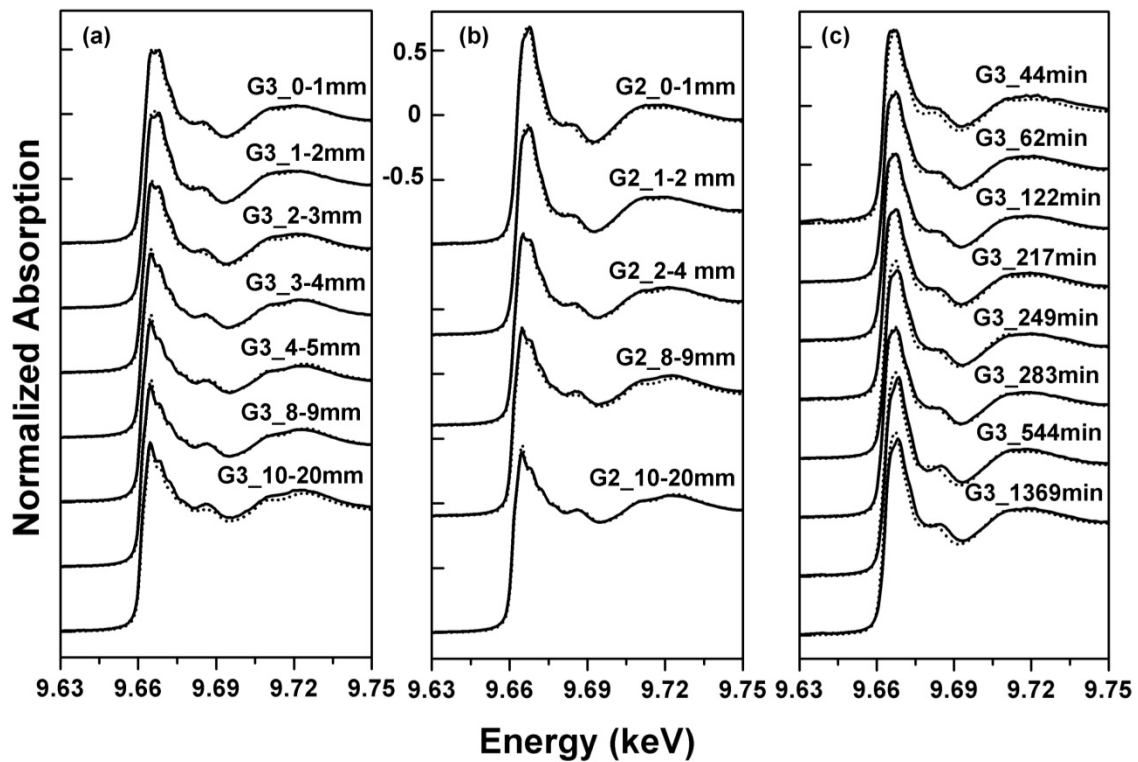
Figure 5-7. XANES spectra (full lines) and reconstructed curves (dotted lines) of sediment samples.
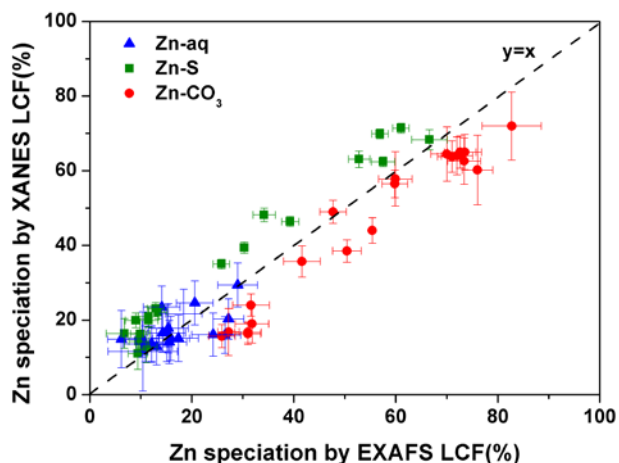
Figure 5-8. Correlation between percentages of Zn species determined by LCF from EXAFS and XANES spectra.

5.1.5 Zn speciation.

Cores from experiments G2 and G3 showed similar speciation profiles (Figure 5-9 a,b). Zn was primarily associated with sulfide at depth (below 1 cm). The fraction of Zn-S increased with depth whereas $Zn-CO_3$ decreased, evidencing a change in Zn coordination as a result of the biogenic formation of sulfides. Experiment G2, sampled immediately after a resuspension event, showed greater abundance of $Zn-CO_3$ and Zn-aq in surficial sediments than experiment G3, sampled two days after a resuspension, indicating that resuspension led to re-partitioning of Zn between oxidized and reduced phases, and liberated Zn(aq) near the SWI. This observation is consistent with the porewater concentration profiles shown in Figure 5-2.

Resuspension events scoured surficial sediments to a depth of just 1-2 mm. Zn-aq, $Zn-CO_3$, and Zn-S were identified in resuspended particles from experiment G3 (Figure 5-9 c). During the period of resuspension, the Zn-S fraction in the resuspended material increased for 2 hours and then slowly decreased, suggesting that a balance was achieved between suspension of the sediment bed and deposition of suspended particles. The Zn-aq fraction increased substantially over the first two hours, indicating ongoing erosion of surficial sediments. After two hours, the Zn-aq fraction continued to increase slowly while Zn-S and $Zn-CO_3$ fractions slowly decreased, suggesting Zn was released from dissolution of these two phases. Experiment G3 also showed that a proportion of Zn-S persisted as function of time in the suspended particles. This indicates that the ZnS phase was not oxidized in presence of dissolved oxygen, as observed previously.[79]
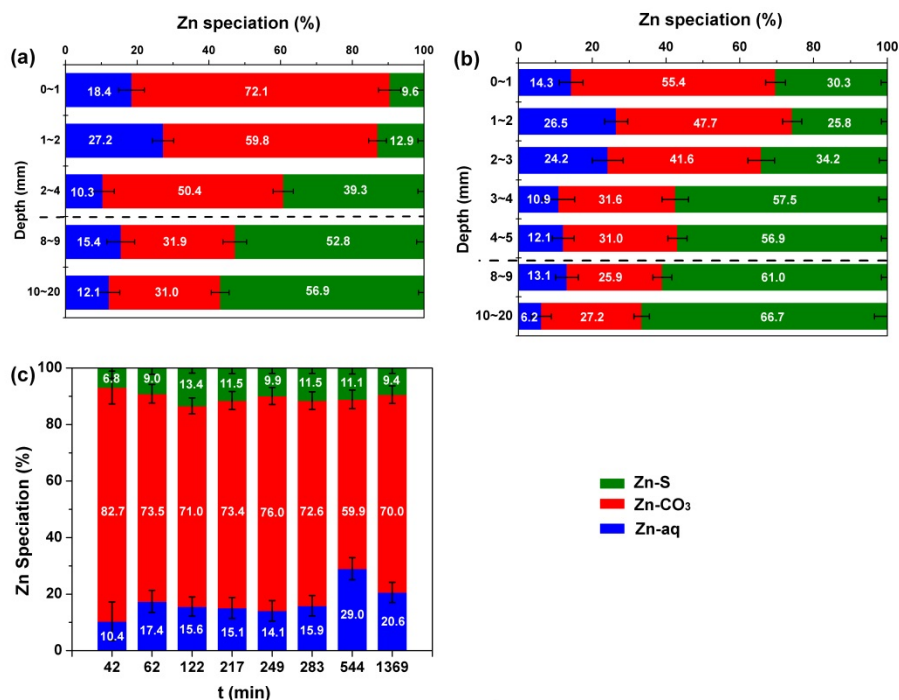
Figure 5-9. (a) Zn speciation in sediment core from experiment G2, obtained immediately after a resuspension event; (b) Zn speciation in sediment core of experiment G3, obtained two days after a resuspension event. (c) Temporal evolution of Zn speciation in resuspended sediments in the water column from experiment G3. t = 0 corresponds to the initiation of resuspension.

5.1.6 Discussion

The mobility and bioavailability of metals in sediments are affected by the solubility of the metal species present.[80] Using XAS, a mixture of three Zn species was identified in bed sediments and resuspended particles: Zn-aq, $Zn-CO_3$, and Zn-S.[11] The Zn-aq fraction represents the most labile form of Zn since it encompasses the hexa-coordinated Zn aqua ion as well as weak outer-sphere Zn surface complexes.[11] Throughout the sediment cores, the solubility of Zn in the porewaters was primarily controlled by the presence of the more soluble $Zn-CO_3$ coexisting with less soluble Zn-S species.

XAS analysis of sediment subcores revealed that Zn sulfide species increased with depth in the sediments. AVS followed similar patterns, as Zn sulfides were the primary components of AVS, resulting in high SEM:AVS ratios near the sediment surface. Lower surficial AVS concentrations have been observed in many other studies, and toxicity is anticipated when the SEM:AVS ratio exceeds one.[74, 81, 82] Here, the combination of XAS, O_2, SEM, and AVS profiles suggests that oxidation reactions near the SWI dissolved binding phases and released weakly-bound Zn-aq to porewater and the water column.

While release of contaminants from fine sediments is normally assumed to occur primarily by diffusion, transient releases induced by sediment remobilization were critical to overall efflux of metals from the sediments in the experiments reported here. The Lake DePue sediment was extremely fine grained and had a very low permeability, in the regime where porewater flow is expected to be negligible and diffusion is the dominant mechanism of solute transport.[83] However, episodic resuspension greatly increased concentrations of Zn both in surficial porewater and

38

overlying water. These elevated concentrations were highly transient, and decreased to near pre-resuspension levels within two days of the cessation of sediment resuspension. XAS analysis also indicated that resuspension led to repartitioning between Zn-aq, Zn-CO$_3$, and Zn-S phases in both sediment cores and resuspended particles. This suggests that resuspension liberated weakly-bound Zn-aq to the overlying water and enhanced dissolution of Zn-sequestering mineral phases, resulting in increased metals mobility and efflux from the sediments. This process is expected to contribute to substantial net Zn release from the sediments in fine-grained natural systems subject to episodic sediment transport.

It is recognized that sediments are extremely complex systems and the fate of metals in sediments varies greatly with sediment properties. The sediments used in this study have very high Zn (~220 µmol/g) and sulfide (25-150 µmol/g) concentrations owing to discharge of waters resulting from the leaching of Zn smelter tailings. Such high concentrations are quite typical of sites with sediments contaminated by mining and smelting activities.[84-86] Mines and smelting plants processing ores of massive metal-sulfide deposits often give rise to contaminated sediment deposits with chemistry similar to that found in Lake DePue.[87-90] In other contaminated sites with higher sulfide and lower Zn concentrations, Zn speciation and mobility also greatly depend on fate of other redox-sensitive metals like Fe and Mn. However, FeS and MnS are readily oxidized whereas the oxidation of ZnS is slow.[91]

5.2 Toxicological Effects of Short-term Resuspension of Metal-contaminated Freshwater and Marine Sediments

(Results reported in *Kyle J. Fetters, David M. Costello, Chad R. Hammerschmidt, G. Allen Burton Jr. (2016) Toxicological effects of short-term resuspension of metal-contaminated freshwater and marine sediments. Environmental Toxicology and Chemistry. 35: 676-686. Doi: 10.1002/etc.3225)*

5.2.1 Sediment characterization

Sediments from the three sites were anoxic (pore water O$_2$ ≤ 1 mg/L), circumneutral (pH = 7.0–7.3), and contained high concentrations of sulfide with moderate organic carbon contents (Tables 5-6 and 5-7). Freshwater sediment from Lake DePue contained more fine particles (< 45 µm, 81% by mass) than the marine sediments from PNS (MS04 = 39%, MS03 = 23% fines; Table 5-8). Despite particle size differences, the permeability of all sediment types was similarly low, from 10^{-15} to 10^{-14} m^2. Porewater DOC was much lower in Lake DePue sediments (15 ± 1 mg/L) than in either MS03 (103 ± 6 mg/L) or MS04 (98 ± 4 mg/L). MS03 and MS04 sediments contained appreciable concentrations of pyrite-S (97 and 91 µmol/g dw, respectively; Table 5-6). Zn was detected in the pore waters of all three sediments (28–146 µg/L), Ni was present at low levels in both marine sediments (18 and 22 µg/L), and other metals (Cu, Cd, and Cr) were at concentrations less than detection limits (Table 5-7).

All three sediments exceeded screening levels, and were therefore potentially toxic. Total recoverable metals in Lake DePue sediment and PNS sediments exceeded effects thresholds based on probable effect levels,[92, 93] and Lake DePue sediments also exceeded bioavailability thresholds (∑SEM-AVS)/fOC > 130–3,000 µmol/g OC).[94] The majority (>85%) of total recoverable Zn and Mn in Lake DePue was extractable with 1M HCl (i.e., SEM) while Cu, Ni, and Fe were less reactive (Table 5-9). In PNS sediments, Zn was also labile (~60% of total recoverable as SEM),

whereas the concentration of Fe, Mn, Cu, Ni, Pb, and Cr in the SEM fraction was less than 30% of total, indicating the recalcitrance of these metals (Table 5-9). PAHs were present in PNS sediments but at concentrations unlikely to cause acute toxicity (< effects range-low 4,022 µg/kg dw; Table 5-6).[95]

Table 5-6. Mean geochemical characteristics of three test sediments. -- = not analyzed.

	Total recoverable metal (mg/kg dw)								TOC (%)	AVS (µmol/g dw)	TRIS (µmol/g dw)	Σ(SEM-AVS)/ƒOC (µmol/g OC)	ΣPAHs (µg/kg dw)
	Fe	Mn	Cd	Cr	Cu	Pb	Ni	Zn					
PNS MS03	39,600	332	--	96	575[a]	181[a]	69[a]	533[a]	1.6	20	117	−921	3180
PNS MS04	24,900	289	--	114	364[a]	83	48[a]	223	2.0	9	98	−267	2050
Lake DePue	36,600	1,130	109[a]	84	403[b]	--	49[a]	13,900[a]	2.7	60	--	4,970	--

[a] Exceeds recommended probable effect levels (PELs; MacDonald et al. 1996, Smith et al. 1996)

Table 5-7. Initial physicochemistry of Lake DePue and Portsmouth Naval Shipyard (MS03 and MS04) pore waters (mean ± 1 SD, n = 3–12). ND = not detected. -- = not analyzed.

Sediment	pH	DO (mg/L)	DOC (mg/L)	Dissolved metals (µg/L)[a]						
				Zn	Cu	Ni	Cd	Cr	Fe	Mn
Lake DePue	7.32	1.01	15	146	ND	ND	ND	ND	1010	913
	(0.03)	(0.13)	(1)	(37)					(771)	(178)
MS03	7.05	1.04	103	28	ND	22	--	ND	14100	351
	(0.02)	(1.00)	(6)	(10)		(19)			(3810)	(93)
MS04	7.08	0.81	98	40	ND	18	--	ND	14000	103
	(0.04)	(0.52)	(4)	(18)		(18)			(5760)	(34)

[a] Means between experiments (resuspension and bedded) analyzed on separate ICP-OES runs, resulting in large standard deviations for certain metals.

Table 5-8. Particle size distribution (%) with Lake DePue and Portsmouth Naval Shipyard (MS03 and MS04) sediments. -- = not analyzed.

Sediment	Particle size distribution (%)					
	< 45 µm	45–106 µm	106–150 µm	150–250 µm	250–1000 µm	>1000 µm
Lake DePue	81	6	13[a]	--	--	--
PNS MS03	23	17	12	6	16	26
PNS MS04	39	37	11	12[b]	--	--

[a] > 106 µm largest fraction analyzed for Lake DePue
[b] > 150 µm largest fraction analyzed for MS04

Table 5-9. Fraction of total recoverable metals as 1M HCl extractable (SEM) in bedded Lake DePue and Portsmouth Naval Shipyard (MS03 and MS04) sediments. -- = not analyzed.

	[SEM]/ [total recoverable metals] (%)		
	Lake DePue	**MS03**	**MS04**
Fe	36	14	22
Mn	86	12	11
Zn	95	55	65
Cu	25	9	15
Ni	45	29	26
Pb	--	6	7
Cr	--	30	27
[AVS]/[TRS]	--	17	9

5.2.2 Overlying water comparisons (bedded vs. resuspension)

5.2.2.1 Geochemistry

During resuspension events, SPM concentrations in the organism exposure chambers were maintained between 0.2 to 1.0 g/L in most replicates (Table 5-10). Resuspension of Lake DePue sediments was consistently associated with a pH decrease in overlying water by approximately 0.4 units; pH changed mostly rapidly during the first hour of resuspension (Figure 5-10A and Table 5-10). The pH of overlying water in Lake DePue exposure chambers without resuspension

declined less than 0.05 units (Table 5-11). Resuspension of Lake Depue sediment also consumed dissolved O_2 from overlying water but the water remained oxic ($\geq$ 6.2 mg/L, Figure 5-10B and Table 5-10). Dissolved oxygen in overlying water was inversely correlated with turbidity (NTU) after 4 h of resuspension of Lake DePue sediment ($p <$ 0.001, r = 0.94). In contrast, pH was not related to turbidity ($p =$ 0.17, r = 0.53).

In contrast to Lake DePue sediments, resuspension of PNS sediments was associated with a more modest decrease of pH (~0.2 units) that occurred more linearly during the 4 h exposure period (Figure 2A and Table 5-10). Without resuspension, pH of overlying water decreased less than 0.05 units over 4 h (Table 5-11). Turbidity was inversely correlated with pH ($p =$ 0.02, r = 0.80) during resuspension of MS03 sediment but not for MS04 sediment ($p =$ 0.84, r = 0.08). Similar to Lake DePue tests, resuspension of PNS sediments was associated with a decrease of dissolved O_2 in overlying water but the water remained oxic ($\geq$ 4.7 mg/L, Fig 1B and Table 5-10) and there was a strong inverse relationship between turbidity and O_2 after 4 h of resuspension (p < 0.001, r > 0.93).

Resuspension of Lake DePue sediment increased the concentration of dissolved Zn (Figure 5-11A) and Mn in overlying water compared to bedded sediment experiments. Concentration of dissolved Zn in overlying water increased during the first 2 h of resuspension to a maximum of 83 ± 11 µg/L, and remained constant during the following 2 h, approximating a Michaelis-Menten kinetic function ($R^2 =$ 0.73, p < 0.0001, Figure 5-11A). Nearly all (> 98%) of the Zn in the water column during periods of resuspension was bound to particles (Figure 5-11B) and remained below USEPA acute aquatic life criteria (120 µg/L).[96] In tests with bedded Lake DePue sediment, Zn diffused into the overlying water and reached a maximum of 20 ± 3 µg/L after 4 h (Figure 5-11A). Dissolved Mn behaved similarly to Zn, with a rapid increase during the first 2 h to approach a steady-state concentration of approximately 120 µg/L ($R^2 =$ 0.90, p < 0.0001). Dissolved manganese also diffused from bedded sediment and reached a maximum concentration of 4.8 ± 0.3 µg/L in overlying water after 4 h. Other dissolved metals (Fe, Cu, Cd, Cr and Ni) were either near or below detection limits (Table 5-12) in both resuspension and bedded exposures. Dissolved zinc concentrations in overlying water continued to increase after Lake DePue sediment experiments during a 20-h settling period, and Zn concentrations in the resuspension chambers remained significantly elevated compared to the bedded exposures (144 ± 3 versus 59 ± 8 µg/L; p = 0.029). The increase of dissolved Zn in overlying water during the 20-h post experiment period was similar for the resuspension (62 ± 13 µg/L) and bedded sediment tests (39 ± 10 µg/L), which suggests that deposition of resuspended particles did not either scavenge Zn from the water or affect diffusion of Zn from sediments. Manganese behaved similarly, with greater concentrations of dissolved Mn remaining in the overlying water after settling of resuspended particles (126 ± 7 µg/L) compared to bedded sediments (86 ± 9 µg/L, $p <$ 0.001). However unlike Zn, dissolved Mn in overlying water of the resuspension chambers did not increase during the 20-h settling period, whereas Mn continued to increase in water overlying the bedded sediment. This suggests that resuspension and the settling of sediments inhibits diffusive mobilization of Mn.

Resuspension of both MS03 and MS04 sediments from PNS resulted in minimal release of dissolved metals to overlying water, with metal concentrations below method detection limits (Table 5-13 and 5-14). Resuspension of MS03 sediment resulted in Ni and Mn reaching maximum concentrations of 6 ± 1 µg/L and 16 ± 2 µg/L respectively after 4 h (bedded Ni = < DL, Mn = 9 ± 0 µg/L). During resuspension of MS04 sediment, dissolved Mn was the only metal detected in

overlying water, with a maximum concentration of 10 ± 1 µg/L (bedded Mn = 8 ± 0.1 µg/L). In both MS03 and MS04 bedded exposures, dissolved Zn concentrations in water increased marginally through time (Tables 5-13 and 5-14). After settling for 20 h, there was no additional release of metals into overlying water from either sediment (Tables 5-13 and 5-14).

Metal concentrations in suspended particles were generally similar to those in bedded sediment among all metals (Table 5-15). Enrichment factors (EF; e.g., Zn_{SPM}/Zn_{BEDDED}) of metals were similar between samples collected after 1 and 4 h of resuspension for each of the three sediments (Table 5-16). When Lake DePue sediment was resuspended, Zn and Mn were the only metals for which EF was less than one (Figure 5-12) and Ni, Cr and POC had the greatest EF (1.5, 1.5, and 1.3, respectively). The EF was greater than one for all metals when MS03 and MS04 sediments were resuspended. In both PNS resuspension experiments, SPM was greatly enriched with organic carbon, although EF values were highly variable (Figure 5-12).
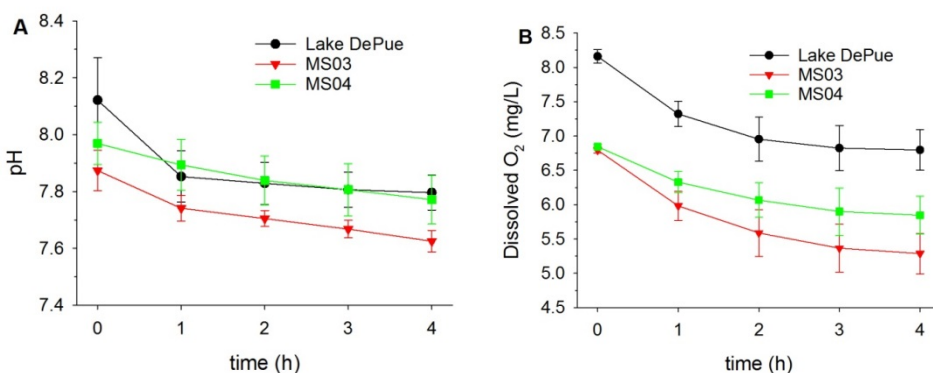
Figure 5-10. Mean ($\pm$ 1 SD, $n = 8$) pH (A) and dissolved O_2 (B) in overlying water during 4-h resuspension experiments with Lake DePue and PNS (MS03 and MS04) sediments. pH and DO remained stable through time for all bedded experiments (data not shown).

Figure 5-11. Mean ($\pm$ 1 SD, $n = 4$ to 8) dissolved Zn (A) and particulate Zn, Cu and Ni (B) during 4-h resuspension and bedded experiments with Lake DePue sediment. Equation in panel A represents nonlinear least squares regression fit model for dissolved metal release during sediment resuspension. Dissolved Cu, Ni, Cr, and Pb were not detected for the duration of experiments.

Figure 5-12. Mean ($\pm$ 1 SD, $n = 4\text{–}8$) calculated enrichment factors (e.g., Zn_{SPM}/Zn_{BEDDED}) after 4-h resuspension experiments of Lake DePue and Portsmouth Naval Shipyard (MS03 and MS04) sediments (POC = particulate organic carbon).

Table 5-10. Mean ($\pm$ 1 SD, n = 8) physicochemistry of overlying water during resuspension experiments with Lake DePue and Portsmouth Naval Shipyard (MS03 and MS04) sediments. -- = not analyzed.

Sediment	Time (h)	pH	Temp. (ºC)	DO (mg/L)	Turbidity (NTU)	Specific conductance (µS/cm)	TSS (mg/L)
Lake DePue	Source	8.16 (0.04)	22.7 (0.1)	8.12 (0.11)	0.1	361 (7)	--
	0	8.12 (0.15)	22.5 (0.1)	8.16 (0.10)	0.1 (0.07)	351 (1)	--
	1	7.85 (0.09)	23.0 (0.1)	7.32 (0.18)	383 (150)	366 (3)	439 (159)
	2	7.83 (0.07)	23.6 (0.1)	6.95 (0.32)	529 (275)	372 (3)	599 (223)
	3	7.81 (0.06)	24.0 (0.1)	6.82 (0.33)	598 (322)	375 (3)	626 (222)
	4	7.80 (0.06)	24.2 (0.2)	6.80 (0.30)	658 (330)	378 (4)	643 (284)
	24	--	--	--	50 (19)	--	--
PNS MS03	Source	7.92 (0.03)	23.0 (0.1)	6.75 (0.07)	0.6	--	--
	0	7.87 (0.07)	23.1 (0.3)	6.80 (0.04)	0.6 (0)	--	--
	1	7.74 (0.05)	23.8 (0.4)	5.98 (0.21)	171 (68)	--	387 (171)
	2	7.71 (0.03)	24.4 (0.3)	5.59 (0.34)	240 (111)	--	--
	3	7.67 (0.03)	24.7 (0.2)	5.37 (0.35)	259 (117)	--	--

	4	7.63 (0.04)	24.8 (0.2)	5.29 (0.29)	265 (126)	--	576 (281)
	24	--	--	--	--	--	--
	Source	8.02 (0.10)	22.7 (0.2)	6.85 (NA)	0.5	--	--
	0	7.97 (0.07)	23.0 (0.2)	6.84 (0.04)	0.5 (0)	--	--
	1	7.89 (0.09)	23.3 (0.2)	6.33 (0.16)	150 (70)	--	337 (166)
PNS MS04	2	7.84 (0.09)	23.8 (0.1)	6.07 (0.25)	246 (143)	--	--
	3	7.81 (0.09)	24.0 (0.1)	5.90 (0.34)	266 (197)	--	--
	4	7.77 (0.09)	24.0 (0.2)	5.85 (0.28)	294 (235)	--	686 (438)
	24	7.66 (0.07)	23.3 (0.1)	--	--	--	--

Table 5-11. Mean (± 1 SD, n = 4) physicochemistry of water during bedded experiments with Lake DePue and Portsmouth Naval Shipyard (MS03 and MS04) sediments. -- = not analyzed.

Sediment	Time (h)	pH	Temp (°C)	DO (mg/L)	Turbidity (NTU)	Specific Conductance (μS/cm)
Lake DePue	Source	7.98	22.9	8.40	0.1	347
	0	8.06 (0.02)	22.7 (0.2)	8.38 (0.08)	0.1 (0)	349 (1.4)
	1	8.02 (0.02)	23.2 (0.2)	8.37 (0.05)	2 (1)	353 (1)
	2	8.04 (0.01)	23.8 (0.2)	8.38 (0.02)	2 (1)	354 (1)
	3	8.02 (0.01)	24.1 (0.1)	8.34 (0.05)	2 (1)	354 (1)
	4	8.03 (0.01)	24.3 (0.2)	8.35 (0.04)	2 (1)	355 (1)
PNS MS03	Source	8.17	22.5	7.08	1.0	--
	0	8.11 (0.02)	23.4 (0.1)	7.13 (0.03)	1.0 (0)	--
	1	8.10 (0.01)	23.9 (0.1)	7.05 (0.02)	1.0 (0.2)	--
	2	8.09 (0.02)	24.5 (0.1)	6.98 (0.03)	0.9 (0.1)	--
	3	8.08 (0.01)	24.8 (0.1)	6.94 (0.02)	0.8 (0.1)	--
	4	8.07 (0.01)	24.8 (0.1)	6.87 (0.04)	0.7 (0.1)	--
	24	7.96 (0.00)	23.4 (0.1)	6.50 (0.07)	--	--
PNS MS04	Source	8.03	22.7	7.19	0.8	--
	0	8.00 (0.02)	23.3 (0.1)	7.18 (0.03)	0.8 (0.0)	--
	1	8.00 (0.01)	23.6 (0.1)	6.95 (0.04)	0.8 (0.1)	--
	2	7.99 (0.01)	24.2 (0.1)	6.89 (0.03)	0.7 (0.0)	--
	3	7.99 (0.01)	24.5 (0.2)	6.86 (0.04)	0.6 (0.0)	--
	4	7.98 (0.01)	24.6 (0.1)	6.84 (0.05)	0.6 (0.0)	--
	24	7.96 (0.01)	23.3 (0.1)	6.60 (0.10)	--	--

Table 5-12. Mean ($\pm$ 1 SD, n = 4 and 8) dissolved metal concentrations (µg/L) in water during tests with resuspended and bedded Lake Depue sediments. EPA's acute ambient water quality criteria (AWQC) is presented for comparison.[96] All measurements of Cu, Ni, Cd, Cr, and Pb were less than practical quantitation limits (PQL = instrument detection limit $\times$ 20). PQLs (µg/L) were Cu = 8, Ni = 10, Cd = 2, Cr = 4, Pb = 20.

Test	Hour	Zn	Fe	Mn
	PQL	4	2	2
	AWQC	120	-	-
Resuspended	Source water	<PQL	<PQL	2
	0	17 (14)	<PQL	2 (0)
	1	63 (11)	6 (3)	72 (15)
	2	81 (8)	6 (1)	100 (16)
	3	83 (11)	8 (4)	106 (17)
	4	76 (12)	6 (1)	101 (17)
	24	144 (3)	<PQL	126 (7)
Bedded	Source water	<PQL	<PQL	<PQL
	0	13 (4)	3.5 (1)	<PQL
	1	18 (4)	2 (1)	4 (0)
	4	20 (3)	<PQL	5 (0)
	24	59 (8)	<PQL	86 (9)

Table 5-13. Mean ($\pm$ 1 SD, n = 4) concentrations of dissolved metals (µg/L) in water during tests with resuspended and bedded Portsmouth Naval Shipyard MS03 sediments. EPA's acute ambient water quality criteria (AWQC) is presented for comparison.[96] All measurements of Cr, Pb and Fe were less than method detection limit (MDL). MDLs (µg/L) were Cr = 2.7, Pb = 4.1 and Fe = 10.

Test	Hour	Zn	Cu	Ni	Mn
	MDL (µg/L)	3.5	2.7	3.0	2.7
	AWQC	90	4.8	74	-
Resuspended	Source water	<MDL	<MDL	<MDL	7
	0	<MDL	4 (1)	<MDL	7 (0)
	1	6 (NA)	ND	4 (1)	12 (1)
	4	<MDL	<MDL	6 (1)	16 (2)
	24	5 (0)	3 (0)	7 (1)	20 (2)
Bedded	Source water	<MDL	<MDL	<MDL	7
	0	13 (5)	3 (NA)	<MDL	8 (0)
	4	32 (7)	<MDL	<MDL	8 (0)
	24	36 (7)	<MDL	<MDL	9 (0)

Table 5-14. Mean (± 1 SD, n = 4) concentrations of dissolved metals (µg/L) in water during tests with resuspended and bedded Portsmouth Naval Shipyard MS04 sediments. EPA's acute ambient water quality criteria (AWQC) is presented for comparison.[96] All measurements of Cr, Pb and Fe were less than method detection limit (MDL). MDLs (µg/L) were Cr = 2.7, Pb = 4.1 and Fe = 10.

Test	Hour	Zn	Cu	Ni	Mn
	MDL (µg/L)	3.5	2.7	3.0	2.7
	AWQC	90	4.8	74	-
	Source water	<MDL	4	<MDL	7
Resuspended	0	20 (16)	<MDL	<MDL	7 (0)
	1	7 (NA)	<MDL	<MDL	9 (1)
	4	ND	<MDL	3 (NA)	10 (1)
	24	31 (43)	<MDL	3 (0)	10 (1)
	Source water	ND	<MDL	<MDL	7
Bedded	0	5 (1)	<MDL	<MDL	8 (0)
	4	17 (5)	<MDL	<MDL	8 (0)
	24	22 (12)	<MDL	<MDL	8 (0)

Table 5-15. Mean (± 1 SD, n = 4–8) concentrations of metals (µg/g dw) and particulate organic carbon (POC, % mass basis) on suspended particles during tests with resuspended Lake DePue and Portsmouth Naval Shipyard (MS03 and MS04) sediments. -- = not analyzed.

Sediment	Hour	Zn	Cu	Fe	Mn	Ni	Pb	Cr	POC (%)
Lake DePue	1	10100 (345)	432 (19)	40500 (1800)	682 (35)	79 (19)	--	142 (7)	--
	2	10200 (446)	439 (13)	42000 (767)	689 (36)	60 (6)	--	--	--
	3	10500 (324)	440 (18)	42500 (1400)	710 (24)	66 (8)	--	--	--
	4	10500 (335)	437 (17)	41600 (11800)	731 (38)	75 (17)	--	127 (8)	3.6 (0.1)
PNS MS03	1	720 (30)	911 (43)	42000 (1100)	372 (18)	82 (8)	299 (24)	200 (5)	--
	4	771 (31)	961 (51)	45100 (2700)	394 (27)	79 (6)	312 (3)	215 (14)	4.2 (1.2)
PNS MS04	1	367 (44)	325 (10)	36100 (4900)	349 (63)	65 (8)	168 (19)	218 (16)	--
	4	430 (35)	384 (36)	43300 (3100)	407 (24)	66 (5)	139 (52)	245 (17)	4.8 (0.8)

50

Table 5-16. Mean (± 1 SD, n = 4 to 8) enrichment factors of metals and particulate organic carbon (POC) on suspended particles during resuspension tests with Lake DePue and Portsmouth Naval Shipyard (MS03 and MS04) sediments. -- = not analyzed.

Sediment	Hour	Enrichment Factor							
		Zn	Cu	Fe	Mn	Ni	Pb	Cr	POC
Lake DePue	1	0.72 (0.02)	1.07 (0.05)	1.11 (0.05)	0.60 (0.03)	1.64 (0.39)	--	1.68 (0.08)	--
	2	0.74 (0.03)	1.09 (0.03)	1.15 (0.02)	0.61 (0.03)	1.25 (0.13)	--	--	--
	3	0.76 (0.02)	1.09 (0.04)	1.16 (0.04)	0.63 (0.02)	1.37 (0.16)	--	--	--
	4	0.75 (0.02)	1.08 (0.04)	1.13 (0.05)	0.65 (0.03)	1.54 (0.35)	--	1.51 (0.10)	1.31 (0.02)
PNS MS03	1	1.35 (0.06)	1.58 (0.07)	1.06 (0.03)	1.12 (0.05)	1.18 (0.11)	1.65 (0.13)	2.09 (0.05)	--
	4	1.45 (0.06)	1.67 (0.09)	1.14 (0.07)	1.18 (0.08)	1.14 (0.09)	1.72 (0.02)	2.24 (0.14)	2.62 (0.78)
PNS MS04	1	1.65 (0.20)	0.89 (0.03)	1.45 (0.20)	1.21 (0.22)	1.36 (0.16)	2.02 (0.23)	1.91 (0.14)	--
	4	1.93 (0.16)	1.06 (0.10)	1.74 (0.13)	1.41 (0.08)	1.38 (0.11)	1.98 (0.20)	2.14 (0.15)	2.38 (0.42)

5.2.2.2 Toxicity

For all toxicological endpoints, no differences in acute toxicity were observed between the bedded and resuspended Lake DePue sediment treatments. *Daphnia magna* survival was not affected by exposure to overlying water from Lake DePue bedded (100%) or resuspension (96 ± 11%) tests (Figure 5-13). Survival of *D. magna* was lower (70%) in one of the replicate chambers that had the greatest concentration of SPM (1,010 mg/L), but concentrations of dissolved metals in this replicate were similar to those in other replicates, which suggests physical stress as a potential cause. No further mortality was observed when *D. magna* were held for an additional 3 d under either exposure scenario (Figure5-13). *Hyalella azteca* survival was not affected by exposure to overlying water from either bedded (98 ± 5%) or resuspended sediment (98 ± 5%) even after a 6-d post-exposure hold (Figure5-13). *Hyalella azteca* feeding rates were not different between organisms exposed to resuspended sediment (0.65 ± 0.12 mg/mg/d) and unexposed controls (0.56 ± 0.03 mg/mg/d; $p = 0.25$, t = 1.35).

Similar to tests with Lake DePue sediment, resuspension of the two marine PNS sediments was associated with limited acute toxicity. *Pyrocystis lunula* exhibited only minimal bioluminescence inhibition in response to exposure to overlying water in resuspension tests with MS03 and MS04 sediments, relative to water from bedded chambers (Figure 5-14). There were no differences in bioluminescence among organisms exposed to bedded, filtered resuspension, or unfiltered resuspension overlying water (MS03; $p = 0.114$) or filtered resuspension compared to unfiltered resuspension overlying water (MS04 ($p = 0.07$). *Neanthes arenaceodentata* survival was

100% following exposure to overlying water from MS03 and MS04 resuspension and bedded treatments and > 95% after the 10-d post exposure recovery period (Figure 5-13). During tests with MS03 and MS04, there was no significant difference in *N. arenaceodentata* relative growth rates between any of the exposure treatments ($p > 0.29$, Figure5-15). Organisms exposed to sediment resuspension had slightly reduced growth rates compared to control and bedded exposures, but effects were not statistically significant (Figure 5-15). Also, *N. arenaceodentata* exposed to resuspension had slightly elevated concentrations of Zn, Cu, and Cr compared to bedded and control exposures; however, these differences were not statistically different due to large variability and low power ($p > 0.05$, Table 5-17). Exposure to MS03 and MS04 resuspensions increased *N. arenaceodentata* Zn tissue concentrations by 20% and 37% over controls, respectively. Ni, Pb, and Cr tissue concentrations were very low in all exposure scenarios, typically < 5 mg/kg dw.

The toxicity results were as expected given that concentrations of dissolved metals during resuspension were below EPA's acute AWQC (Tables 5-12 to 5-14).[96] Additionally, observed concentrations, with the exception of Cu in MS03, were below more stringent chronic AWQC, although chronic effects were not likely to be observed in the experiments describe here given the short duration of these exposures.[96]
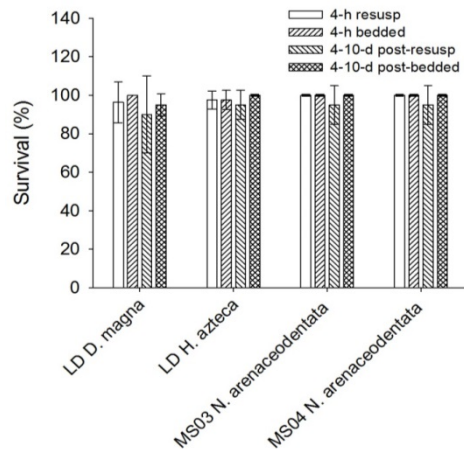
Figure 5-13. Mean (± SD, n = 4-8) organism survival following resuspension and bedded experiments, and subsequent post-exposure hold. Note: *Hyalella azteca* held for 7 d, *Daphnia magna* 4 d and *Neanthes arenaceodentata* 10 d.
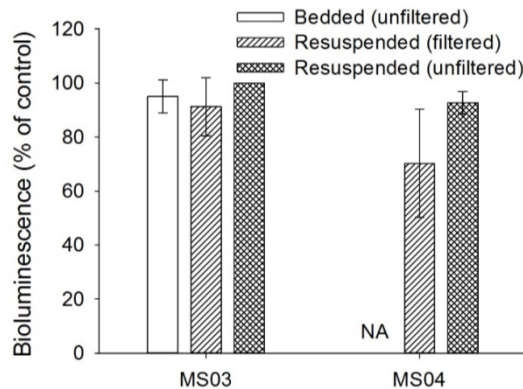
Figure 5-14. Mean (± 1 SD, *n* = 4) bioluminescence response of *Pyrocystis lunula* following 4-h exposure to unfiltered and filtered overlying water in resuspension and bedded experiments with

Portsmouth Naval Shipyard MS03 and MS04 sediments, expressed as % of control. Percentages > 100 were reduced to 100% to allow for arcsine square root transformations. MS04 bedded results not available due to receiving non-viable organisms from supplier.
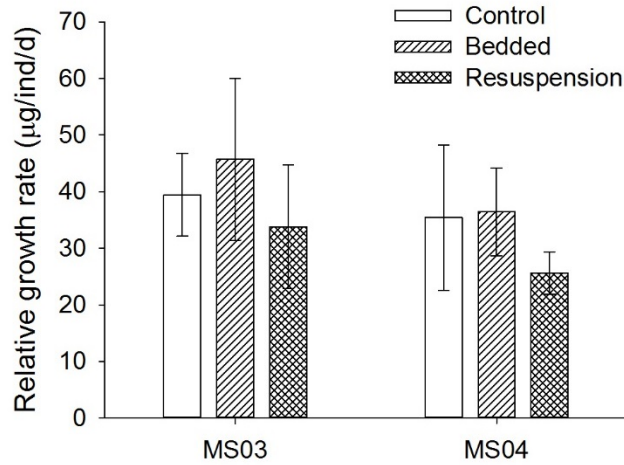
Figure 5-15. Mean ($\pm$ 1 SD, $n = 4$ for bedded and resuspension, $n = 8$ for controls) relative growth rates of *Neanthes arenaceodentata* following 4-h exposure to overlying water from control, bedded and resuspension experiments and after 10-d post-exposure recovery period. Bedded and resuspension controls for each sediment type are depicted as a single bar but were analyzed separately.

Table 5-17. Mean ($\pm$ 1 SD, n = 4) concentrations of metals (mg/kg dw) in *Neanthes arenaceodentata* following 4-h experiments with resuspended and bedded Portsmouth Naval Shipyard sediments.

Sediment	Exposure	Zn	Cu	Ni	Pb	Cr
PNS MS04	Bedded control	137 (8)	24 (2)	3.1 (0.2)	0.8 (0.2)	2.5 (0.3)
	Bedded	159 (23)	24 (2)	3.5 (0.5)	0.8 (0.1)	2.7 (0.5)
	Resusp. control	130 (32)	26 (4)	3.9 (1.2)	0.8 (0.2)	3.9 (0.2)
	Resuspended	156 (23)	29 (4)	3.6 (1.0)	1.1 (0.4)	5.2 (1.9)
PNS MS03	Bedded control	180 (36)	23 (2)	3.3 (0.7)	0.6 (0.1)	2.4 (0.4)
	Bedded	185 (21)	24 (2)	3.8 (0.6)	0.7 (0.1)	2.4 (0.4)
	Resusp. control	124 (20)	26 (1)	3.7 (0.3)	0.8 (0.2)	2.8 (0.9)
	Resuspended	170 (50)	25 (2)	4.0 (0.9)	0.9 (0.2)	3.9 (1.2)

5.2.3 Sediment comparisons (bedded vs. redeposited)

5.2.3.1 Geochemistry

Concentrations of AVS and SEM did not differ significantly between bedded and redeposited sediments ($p > 0.05$; Table 5-18). Surface sediment (top 2 – 3 mm) color was visibly lighter as a result of resuspension (Figure 5-16), which suggests oxidation, but this visual change was not reflected in geochemical measurements, possibly due to coarse core sectioning (5 mm depth). Metal bioavailability (i.e., $\sum$(SEM−AVS)/fOC) in MS04 sediment was increased slightly by resuspension relative to bedded controls ($p = 0.041$, t = 2.59) but resuspension did not affect metal bioavailability in Lake DePue and MS03 sediments ($p > 0.19$, Table 5-18). The small changes in metal bioavailability related to resuspension did not result in changes in predicted acute toxicity based bioavailability thresholds.

On day 7 of Lake DePue exposures, porewater dissolved Zn was elevated above USEPA acute aquatic life criteria (120 µg/L)[96] in both the bedded (451 ± 51 µg/L) and redeposited sediment treatments (493 ± 72 µg/L), while all other metals were below detection limits (Table 5-19). Concentrations of dissolved metals in water overlying MS03 and MS04 sediments were typically below detection limits after the 10-d period (Table 5-20).
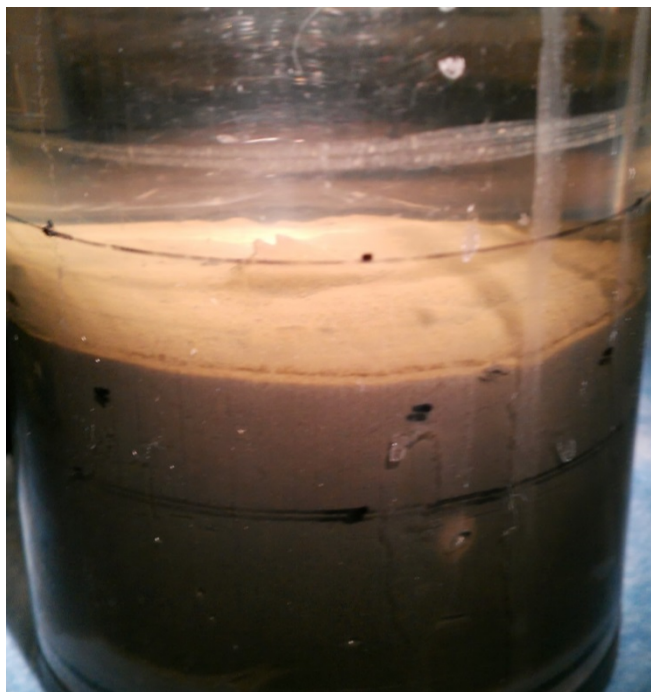
Figure 5-16. MS03 surficial sediment oxidation and color change following resuspension and redeposition.

Table 5-18. Mean (± 1 SD, n = 4) concentrations of AVS, SEM and ∑(SEM-AVS)/ƒOC (µmol/g OC) in bedded and redeposited surface (0–0.5 cm) sediments with Lake DePue and Portsmouth Naval Shipyard sediments (MS03 and MS04).

Sediment type	Integrity condition	AVS (µmol/g)	SEM (µmol/g)	∑(SEM-AVS)/ƒOC (µmol/g OC)
Lake DePue	Bedded	60 (3)	196 (7)	4970 (251)
	Redeposited	60 (3)	207 (18)	5380 (631)
PNS MS03	Bedded	20 (1)	6 (1)	−921 (74)
	Redeposited	19 (4)	8 (2)	−701 (288)
PNS MS04	Bedded	9 (1)	3 (0)	−267 (49)
	Redeposited	7 (1)	4 (1)	−140 (84)

Table 5-19. Mean (± 1 SD, n = 4) dissolved metal concentrations (µg/L) in water overlying redeposited and bedded Lake DePue sediment after 7 d. All measurements of Cr, Cu, Pb, Ni, Cd, and Fe were less than practical quantitation limits (PQL = instrument detection limit × 20). PQLs (µg/L) were Cr = 4, Cu = 8, Pb = 20, Ni = 10, Cd = 2, Fe = 2.

Test		Mn	Zn
	PQL	2	4
Lake DePue redeposited	Control	<PQL	<PQL
	Treatment	108 (12)	493 (72)
Lake DePue bedded	Control	<PQL	<PDL
	Treatment	144 (11)	451 (51)

Table 5-20. Mean (± 1 SD, n = 4) dissolved metal concentrations (µg/L) in water overlying redeposited and bedded Portsmouth Naval Shipyard sediments after 10 d. All measurements of Cr, Pb, and Ni were less than method detection limits (µg/L), which were Cr = 2.7, Pb = 4.1, Ni = 3.0.

Test		Cu	Mn	Zn
	MDL	2.7	2.7	3.5
PNS MS03 redeposited	Control	<MDL	120 (13)	24 (11)
	Treatment	<MDL	23 (1)	20 (18)
PNS MS03 bedded	Control	4 (1)	182 (19)	9 (1)
	Treatment	4 (1)	26 (2)	7 (2)
PNS MS04 redeposited	Control	4 (1)	111 (32)	<MDL
	Treatment	5	16 (1)	6 (1)
PNS MS04 bedded	Control	<MDL	135 (46)	8 (1)
	Treatment	3 (0)	15 (1)	8 (3)

5.2.3.2 Toxicity

Daphnia magna exhibited no differences in survival between control ($89 \pm 12\%$), bedded ($90\pm 8\%$) and redeposited Lake DePue sediment exposures (100%; $p = 0.11$). Survival of *H. azteca* in both bedded ($40 \pm 18\%$) and redeposited ($10 \pm 12\%$) Lake DePue exposures was less than in controls (100%; $p < 0.001$). *Hyalella azteca* exposed to redeposited sediments had significantly lower survival than those exposed to bedded sediment ($p < 0.01$).

Pyrocystis lunula exposed to MS03 and MS04 sediment elutriates of bedded and redeposited sediment showed minimal inhibition of bioluminescence. There were no differences in bioluminescence inhibition between bedded and redeposited MS03 exposures ($p = 0.74$, Figure 5-17), with both treatments near 100% of controls. The bioluminescence response of *P. lunula* exposed to redeposited MS04 elutriates ($75 \pm 14\%$) was not significantly different from exposure to bedded sediment elutriates ($89 \pm 19\%$, $p = 0.14$, Figure 5-17).

Minimal mortality of *N. arenaceodentata* was observed following 10-d exposure to bedded and redeposited PNS sediments and associated controls (all survival > 95%). For MS03 sediments, there was no difference in relative growth rates due to sediment exposure ($p = 0.49$, Figure 5-18) and no differences between bedded and redeposited exposures ($p = 0.40$). For MS04 sediments, exposure to bedded and redeposited sediments reduced relative growth rates compared to controls ($p = 0.017$), but there was no difference between bedded and redeposited experiments ($p = 0.35$).

Exposure of *N. arenaceodentata* to MS04 sediment resulted in elevated Cu tissue concentrations compared to controls ($p < 0.01$), while no differences were observed for Zn, Cr, Ni and Pb ($p > 0.05$, Table 5-21). No differences between sediment exposure and controls were observed for MS03 ($p > 0.05$), with the exception of Ni, which was elevated in controls ($p < 0.001$) and Cu, which was marginally greater in sediment exposures compared to controls ($p = 0.053$, Table 5-21). *Neanthes arenaceodentata* exposed to bedded and redeposited PNS sediments had similar tissue metal concentrations ($p > 0.05$), with the exception of Pb in organisms exposed to MS03 ($p < 0.001$), which was low (< 5 mg/kg) but slightly elevated in redeposited compared to bedded exposures.
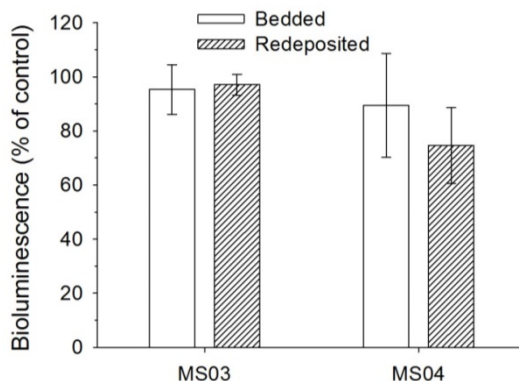
Figure 5-17. Mean ($\pm$ 1 SD, n = 4) response of *Pyrocystis lunula* exposed to filtered sediment elutriates (1:4 sediment to water) of Portsmouth Naval Shipyard MS03 and MS04, expressed as % of control. Percentages > 100 were rounded down to 100% to allow for arcsine square root transformations.
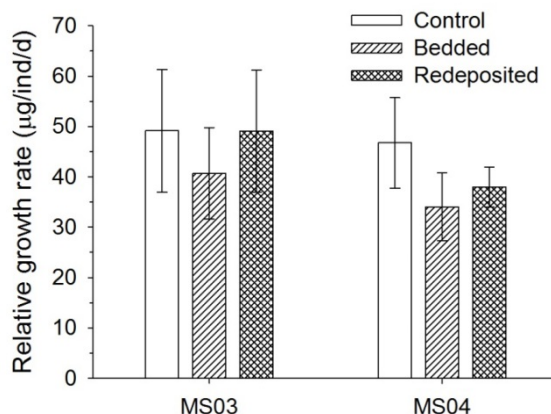
Figure 5-18. Mean ($\pm$ 1 SD, n = 4 and 8) relative growth rates between 10-d control, bedded and redeposited Portsmouth Naval Shipyard sediment toxicity exposures. Bedded and redeposited controls for each sediment type are depicted as a single bar but were analyzed separately.

Table 5-21. Mean ($\pm$ 1 SD, n = 4) metal tissue concentrations (mg/kg dw) in *Neanthes arenaceodentata* following 10-d bedded and redeposited sediment toxicity tests with Portsmouth Naval Shipyard sediments.

Sediment	Exposure	Zn	Cu	Ni	Pb	Cr
MS03	Bedded control	159 (10)	44 (16)	14 (2)	2.6 (0.3)	4.0 (1.0)
	Bedded	146 (18)	82 (54)	5 (2)	1.6 (0.2)	3.3 (0.7)
	Redeposited control	196 (25)	36 (1)	12 (2)	2.2 (0.3)	4.5 (1.3)
	Redeposited	189 (29)	62 (20)	6 (1)	2.8 (0.2)	3.8 (0.9)
MS04	Bedded control	161 (20)	28 (1)	11 (1)	1.9 (0.1)	3.2 (0.9)
	Bedded	128 (42)	54 (30)	8 (3)	1.5 (0.5)	2.3 (0.8)
	Redeposited control	176 (29)	31 (8)	12 (3)	1.6 (0.5)	2.5 (0.5)
	Redeposited	157 (21)	51 (9)	10 (2)	1.6 (0.5)	3.5 (0.9)

5.2.4 Discussion

Environmentally relevant SPM concentrations used in the resuspension experiments resulted in modest pH and dissolved O_2 declines in overlying water. Other short-term resuspension studies have reported pH changes similar to those observed here (typically < 1.0 pH unit) but O_2 declines ranged from no change to anoxia.[53, 97-100] Decreases of pH and O_2 during the first few hours of resuspension, like those observed in the present study, have been attributed to aerobic respiration and oxidation of reduced inorganic ions and molecules (e.g., Fe^{2+}, FeS); however, protons liberated during oxidation can be buffered by suspended sediment and overlying water.[101] The relatively high dissolved O_2 concentrations ($\geq$ 4.7 mg/L) maintained in the overlying water were distinctly different from the low O_2 concentrations in pore water (< 1.0 mg/L), which has implications for metal mobilization from resuspended sediments. Thus, it appears that the oxic, circumneutral conditions maintained during the short-term resuspension tests, which are representative of most natural events, promote metal scavenging by suspended particles and minimize the net release of bioavailable metals.[102, 103]

57

Minimal mobilization of metals occurred during sediment resuspension. Concentrations of dissolved Zn and Mn in water increased during resuspension of Lake DePue sediment to levels greater than would be expected from diffusion alone; however, the vast majority of Zn remained sorbed to particles. The distribution coefficient (K_D, L/kg) of Zn in overlying water remained consistently between $10^{5.1}$ and $10^{5.2}$ throughout the 4-h resuspension period. Solubilization of Zn from suspended particles likely was not from dissolution of zinc sulfide, given that metal sulfides can take more than 8 h to oxidize [104] and that approximately half of the Zn in Lake DePue sediment is associated with carbonates and other inorganic ligands.[105] Concentrations of Cu, Ni, Cd and Cr in pore water were near detection limits. That neither dissolved Cu, Cd, nor Pb were measured in water overlying both Lake DePue and PNS sediments may be attributed to either their high affinities for particulate organic matter [106, 107] or their presence as metal sulfides, which may not be oxidized during short-term sediment resuspensions.[104, 108] Metal mobilization from PNS sediment may have been limited by the greater relative abundance of pyrite, which is more resistant to oxidization compared to AVS, and can co-precipitate trace metals during formation.[53, 109] Porewater Fe^{2+}, which was abundant in all sediments, provided a substrate for the formation of iron oxides while pore water was oxidized during resuspension;[110] particulate and colloidal Fe oxides may act as an additional sink for any potentially mobilized trace metals.[111, 112] Significant fluxes of metals to overlying water were observed only from Lake DePue sediments, and even after resuspension, concentrations of dissolved Zn and Mn did not exceed acute aquatic life criteria (120 and 1,600 µg/L, respectively).[96, 113]

Coincident with changes in overlying water chemistry, resuspension changed the chemistry of suspended and redeposited sediment particles. Enrichment factors between suspended and bedded sediments were >1 for a majority of the metals, indicating that either sediment particles with greater metal concentrations (i.e., fine-grained particles) were preferentially suspended or particles in oxic overlying water scavenged previously dissolved metals. Suspended particles with metal concentrations greater than bulk sediment can result in a metal-concentrated layer at the sediment surface upon redeposition. The current study showed consistent, but non-significant increases of metal bioavailability in surface sediment following resuspension and redeposition of all sediments. The change in metal bioavailability was likely small due to 1) low sediment permeability, 2) a thin layer of surficial sediment resuspended and redeposited (~2 – 3 mm) and/or 3) coarse core sectioning (5 mm depth resolution). Despite consistent increases in metal bioavailability, the change was not large enough to alter the acute toxicity predictions. Following resuspension and redeposition of Lake DePue sediment, diffusion of Zn and Mn into the overlying water was neither inhibited nor promoted compared to undisturbed sediments. Therefore, systems subjected to sediment resuspensions would not be expected to have higher concentrations of dissolved metals due strictly to such events.

Despite elevated concentrations of dissolved Zn and metals associated with SPM, exposure of *D. magna* and *H. azteca* to resuspended Lake DePue sediments resulted in few observed adverse effects. *Hyalella azteca* exposed to resuspended sediment did not exhibit either increased mortality or reduced feeding rates during post-exposure monitoring. Absence of Zn toxicity could be explained by dissolved concentrations below the acute criteria and not available as free ions (i.e., bound to Fe colloids or organic matter).[114] *Pyrocystis lunula* bioluminescence (Qwiklite) was not inhibited from exposure to overlying water from PNS bedded and resuspended exposures. *Pyrocystis lunula* exposed to unfiltered water samples generally showed less adverse impacts compared to filtered samples, suggesting that metals associated with SPM were not bioavailable

58

to this organism. Neither acute mortality nor latent growth effects were observed for *N. arenaceodentata* exposed to resuspended sediment. Although *Neanthes arenaceodentata* likely consumed suspended particles during resuspension, because they excreted particles during depuration, these organisms did not accumulate metals in their tissues, which suggest that metals were neither liberated nor absorbed in the gut. Uptake from the dissolved phase is the most important route for Zn and Cd bioaccumulation in this species [115] so an absence of elevated tissue metal concentrations was not surprising. Other studies have shown synergistic effects between particulate and dissolved metals, with bioaccumulation being metal and species specific.[116-119] Despite high concentrations of metals associated with suspended particles, the metals apparently were not bioavailable and did not elicit adverse effects.

Metal bioavailability predictions accurately separated non-toxic from potentially toxic conditions for each of the sediments tested under bedded and redeposited conditions. Bioavailable metal concentrations for bedded and redeposited Lake DePue sediments were > 3000 µmol/g OC and acute toxicity to *H. azteca* was observed, but *D. magna* were not negatively affected by elevated concentrations of Zn in either sediment or water. An absence of *D. magna* acute toxicity during bedded and redeposited sediment exposures may have been due to behavior: the organisms are planktonic and therefore had limited contact with contaminated sediment. *Hyalella azteca* exhibited greater sensitivity to redeposited compared to continuously bedded sediment, suggesting the proposed changes in metal speciation of SPM during resuspension and oxidation may increase bioavailability and toxicity of metals bound to solids. These results contrast those of Bonnet and colleagues,[120] who found no differences in toxicity between perturbed and non-perturbed sediments. In a separate study with Lake DePue sediment, resuspension resulted in a greater abundance of oxidized Zn species ($ZnCO_3$, $Zn_3(PO_4)_2$ and Zn^{2+}) in the upper 1 mm of sediment compared to sediment at depth immediately following disturbance, but two days post-disturbance, these Zn species had declined with increases in ZnS abundance, indicating that resuspension had a transient effect on metal speciation.[121] Despite potentially short-term changes in metal speciation, net negative effects on *H. azteca* survival were detected. In general *N. arenaceodentata* exhibited little acute toxicity to either bedded or redeposited PNS sediment. Differences in acute toxicity between bedded and redeposited conditions were relatively strong and weak for *H. azteca* and *N. arenaceodentata*, respectively, which likely reflects differences in behavior and feeding strategies. *Neanthes arenaceodentata* burrows were observed to extend 2–3 cm below the sediment-water interface, to depths that were not likely physically and chemically altered by sediment resuspension, whereas *H. azteca* foraged at the sediment surface where most of the chemical oxidation due to resuspension had occurred. These behavioral and foraging differences highlight the importance of interactions between life history and sediment disturbance when assessing risks to ecosystems.

Simulating environmental relevance of natural phenomena under controlled laboratory conditions is a persistent challenge in toxicological studies, and the current study attempted to mimic environmental conditions during sediment resuspension events. The duration and suspended sediment concentration of the resuspension events as well the use of field-contaminated sediments were intended to simulate stress conditions that organisms would experience in their natural habitat. Despite these efforts to replicate environmental relevance, the present study was designed to isolate the toxicological effects from a single resuspension event, but in reality organisms likely experience multiple events per day, which could result in pulsed metal exposures, creating the potential for additive toxicological effects.[122] In addition, use of intact sediment cores

rather than homogenized sediments would have improved environmental realism of the present study. In natural systems, surficial sediment is typically oxic, and resuspension of this layer into oxic waters may result in different degrees of metal bioavailability than resuspension of homogenized, anoxic sediments. Use of anoxic sediments with limited water exchange likely created more extreme changes in metal speciation than would be anticipated in the field, thus the experimental conditions created a greater potential for changes in metal bioavailability as a result of redox reactions. Given the observed absence of acute toxicity, resuspension of oxic surface sediments is not expected to pose a greater direct risk. The results of the present study support the conclusions of the literature review by Eggleton and Thomas,[14] which suggested that metal mobilization is not significant enough to be acutely toxic, although chronic effects have been observed.

The present study highlights the importance of fully characterizing sediment and water geochemistry, and also understanding disturbance regimes, which are paramount in predicting potential metal mobilization and assessing ecological risks due to resuspension events. Resuspension of contaminated sediments is important because even infrequent resuspension events can negate improvements made by remediation, restoration and management activities.[123, 124] Further research is needed to examine ecologically relevant endpoints, including community-level responses, predator-prey interactions, recruitment and reproduction under sediment resuspensions of varying frequencies, durations, intensities and overlying water dilutions.

5.3 Effects of Bioturbation and Bioirrigation on Particle Dispersion and Oxygen Redistribution.

5.3.1 Burrow structures and sediment mixing.

Lumbriculus variegatus burrow networks were primarily observed near the SWI (Figure 5-19). Burrows are highly branched and interconnected. While new burrows were constructed, worms also tend to revisit the old burrows (Movie B1_reference sediments, B2_contaminated sediments, Supporting information). The abundance of burrows progressively increased over the time, leading to increasing sediment porosity. The abundance and spatial distribution of burrows in reference and contaminated sediments were assessed visually (Figure 5-19, 5-20, Movie B1_reference sediments, B2_contaminated sediments, Supporting information). *L. variegatus* constructed more burrows and perturbed a wider area of sediments without contamination, suggesting that *L. variegatus* was more active in these sediments.
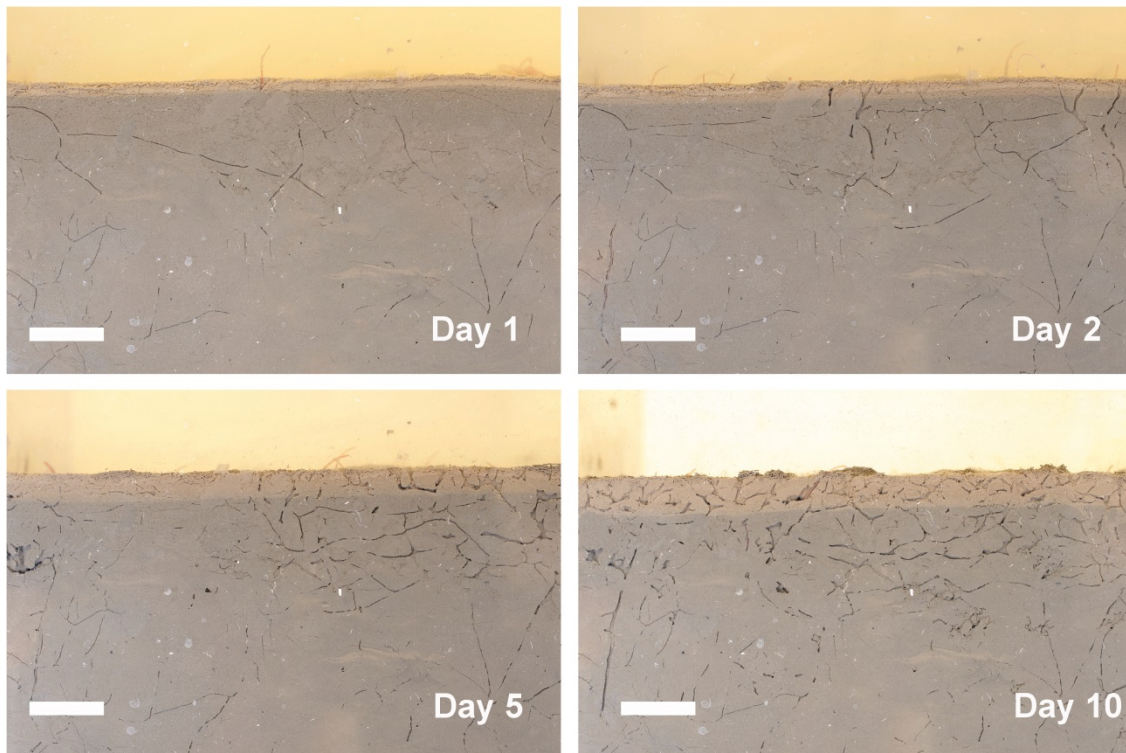
Figure 5-19. Evolution of sediment structures in experiment with reference sediment (B1). Scale bars = 1 cm.
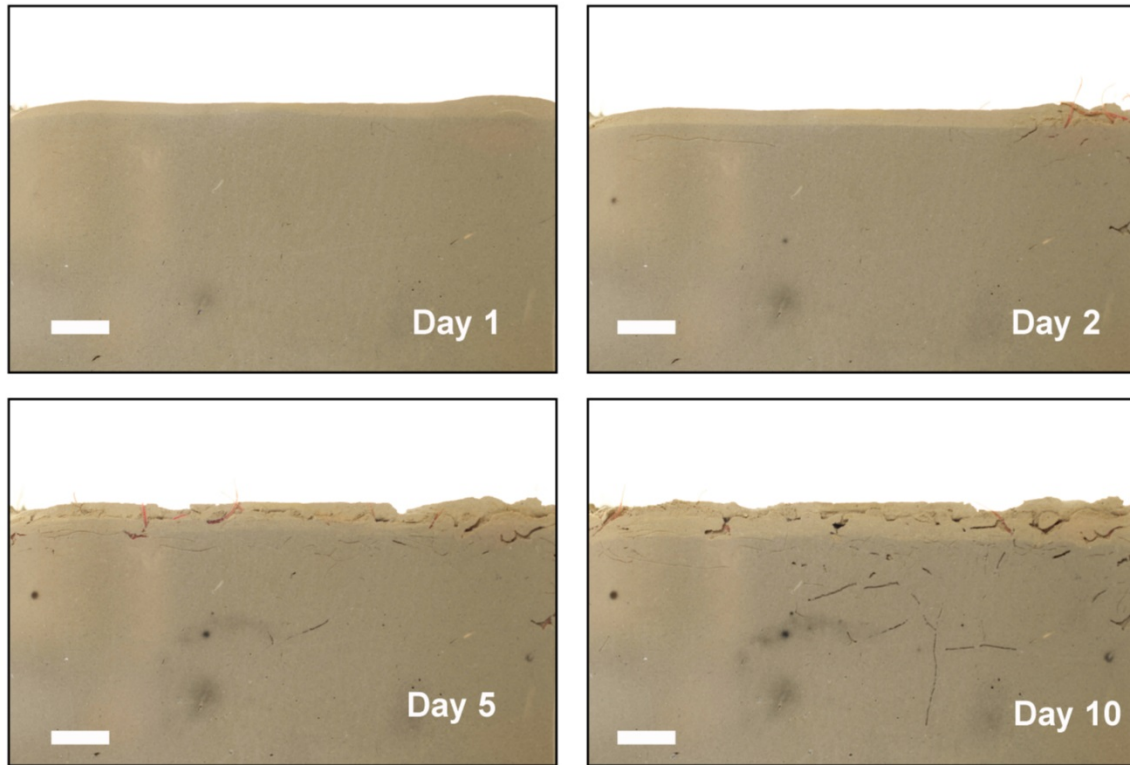
Figure 5-20. Evolution of sediment structures in experiment with contaminated sediment (B2). Scale bars = 1 cm.
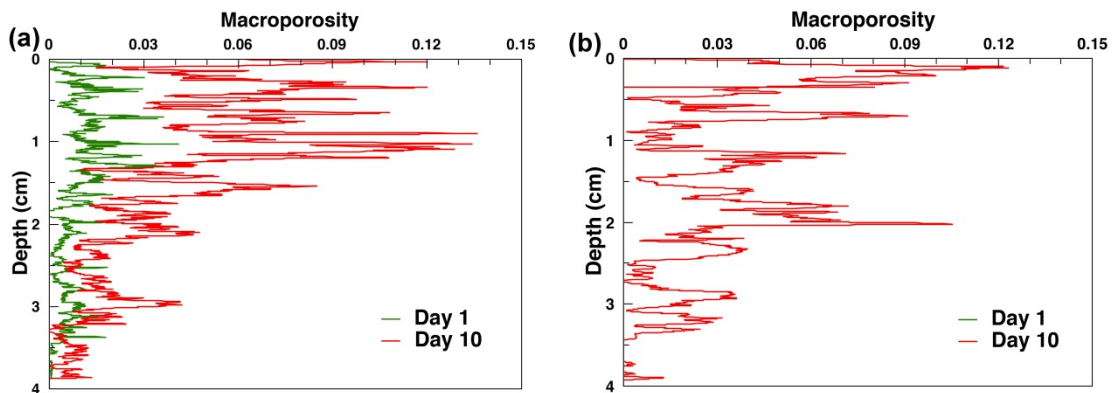
Figure 5-21. Distribution of macroporosity in sediments. (a) Experiment B1 with reference sediment. (b) Experiment B2 with contaminated sediment.

Mixing of sediment particles were also observed in LIF-bioturbation experiments. Movement of fluorescent particles was primarily associated with activities of the worms (Movie B3_reference sediments, Movie B4_contaminated sediments, Supporting information). During the early stage of experiments, when worms were actively constructing burrows, fluorescent tracers were progressively redistributed downward. The initial sharp boundaries of fluorescent particles became less evident over the course of the experiment. When burrow networks approached

completion, particles were moved less frequently. The effects of sediment contamination on mixing of fluorescent particles by *L. variegatus* were also assessed by comparing the temporal evolution of distribution of fluorescent particles in two sediments (Figure 5-22, 5-23, Movie B3_reference sediments, Movie B4_contaminated sediments, Supporting information). In contaminated sediments, the mixing of fluorescent particles was nearly stagnant after day 2 (Figure 5-23), while in reference sediments, mixing of fluorescent particles could still be clearly observed later in the experiments (Movie B4). However, horizontally-averaged vertical profiles of tracer particle distributions were not significantly different between experiments with reference sediments and contaminated sediments owing to high variability in the observed mixing profiles (Figure 5-24).
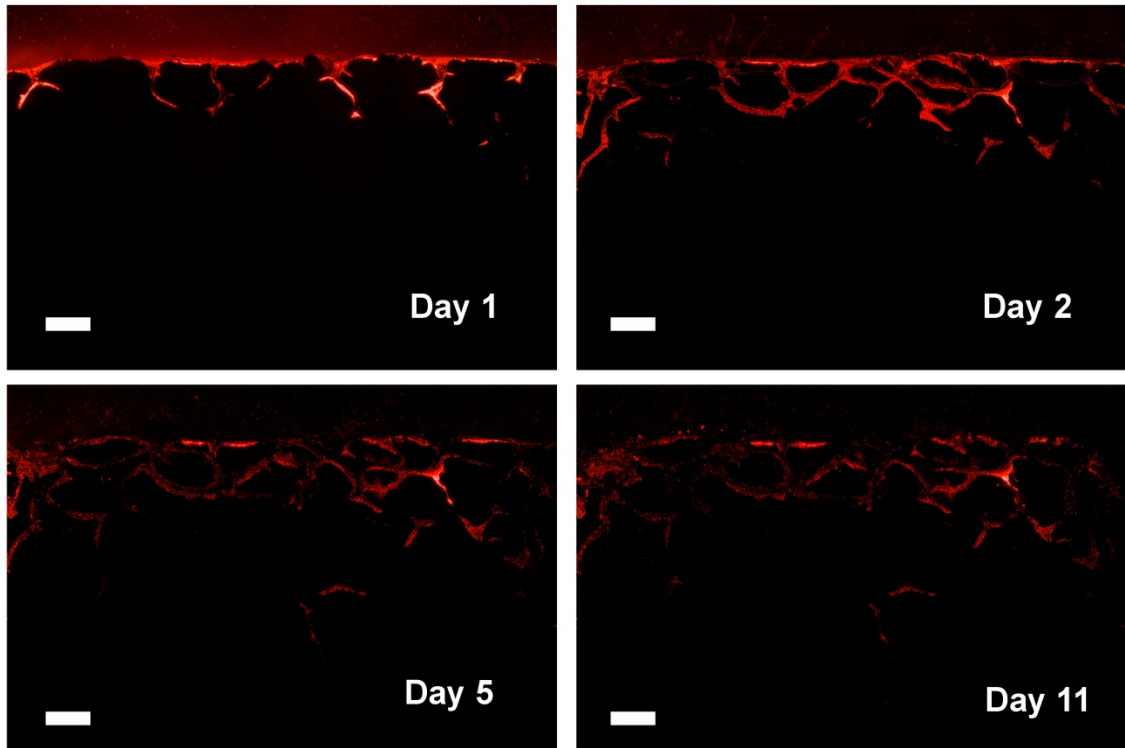
Figure 5-22. Sediment mixing by bioturbation in experiment with reference sediments (B3). Scale bars = 1 cm.
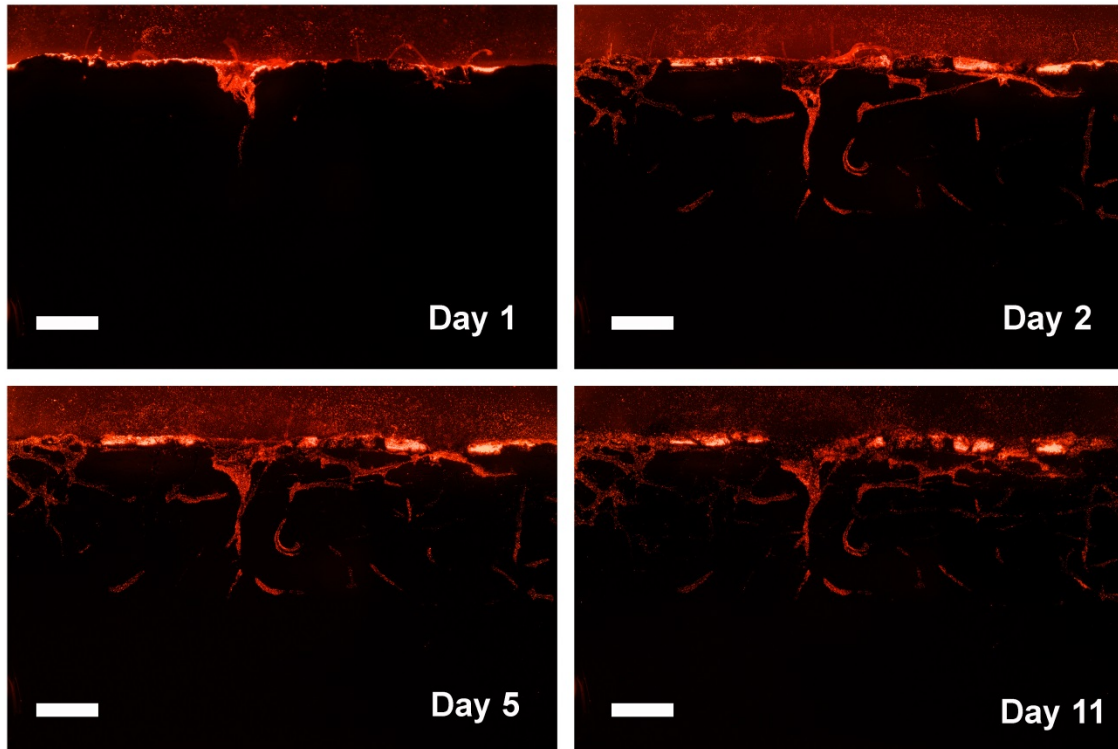
Figure 5-23. Sediment mixing by bioturbation in experiment with contaminated sediments (B4). Scale bars = 1 cm.
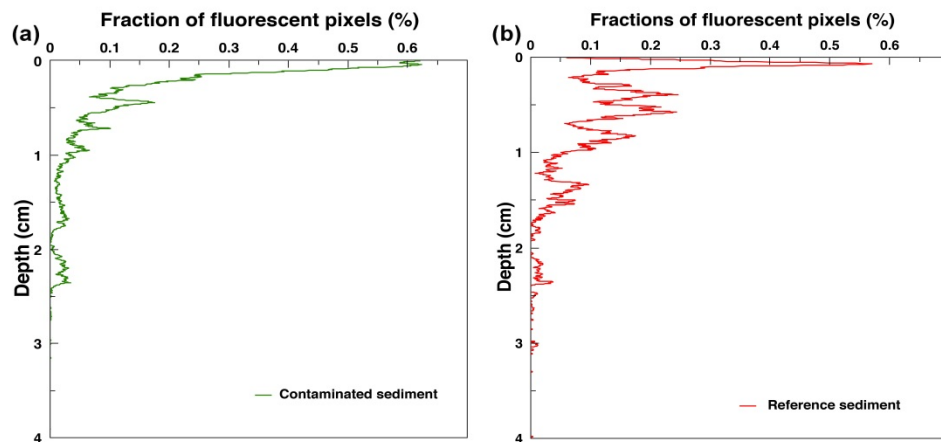
Figure 5-24. Distribution of fluorescent particles on day 11 for experiments B4 (a) and B3 (a).

5.3.2 Discussion

Bioturbation altered the sediment structure and physicochemical properties. Bioturbation clearly increased the complexity of the sediment-water interface and the heterogeneity of near-surface sediments. Burrow networks also increased the porosity and permeability of sediments, which obviously facilitate exchange between overlying water flow and hyporheic flow.

Bioturbation also changed the residence time of solute and particles in the sediment bed. Hyporheic flow in streams is known to deliver solutes and particles into streambeds, where they were stored and retained for a long time compared with the in-stream transport.[24, 125] Solutes and particles also behaved differentially, as particles rapidly deposit along hyporheic flow paths while solutes can propagate deep into sediment beds.[126] By enhancing exchanges between overlying water and hyporheic flow, bioturbation could potentially decrease the residence time of solutes inside the sediments. By transporting surficial sediments downward, fine particles originally immobilized in shallow surficial regions may be delivered deeper, leading to longer-term storage. In contrast, sediment particles that reside in deep sediments can also be transported to the surface or even released to the stream.

5.3.3 Oxygen optode results

1) Calibration of oxygen optode

Optode images were acquired with spatial resolutions of 28 µm/pixel. Each pixel was calibrated by applying the Stern-Volmer equation (1).[127]

Stern-Volmer equation:

$$I = I_0\left[\alpha + (1 - \alpha)\left(\frac{1}{1 + K_{sv}C}\right)\right] \quad (1)$$

Where α is the non-quenchable fraction of the fluorescence including scattered stray light and I_0 is the fluorescence intensity in the absence of O_2. The overall calibration is shown in Figure 5-25.
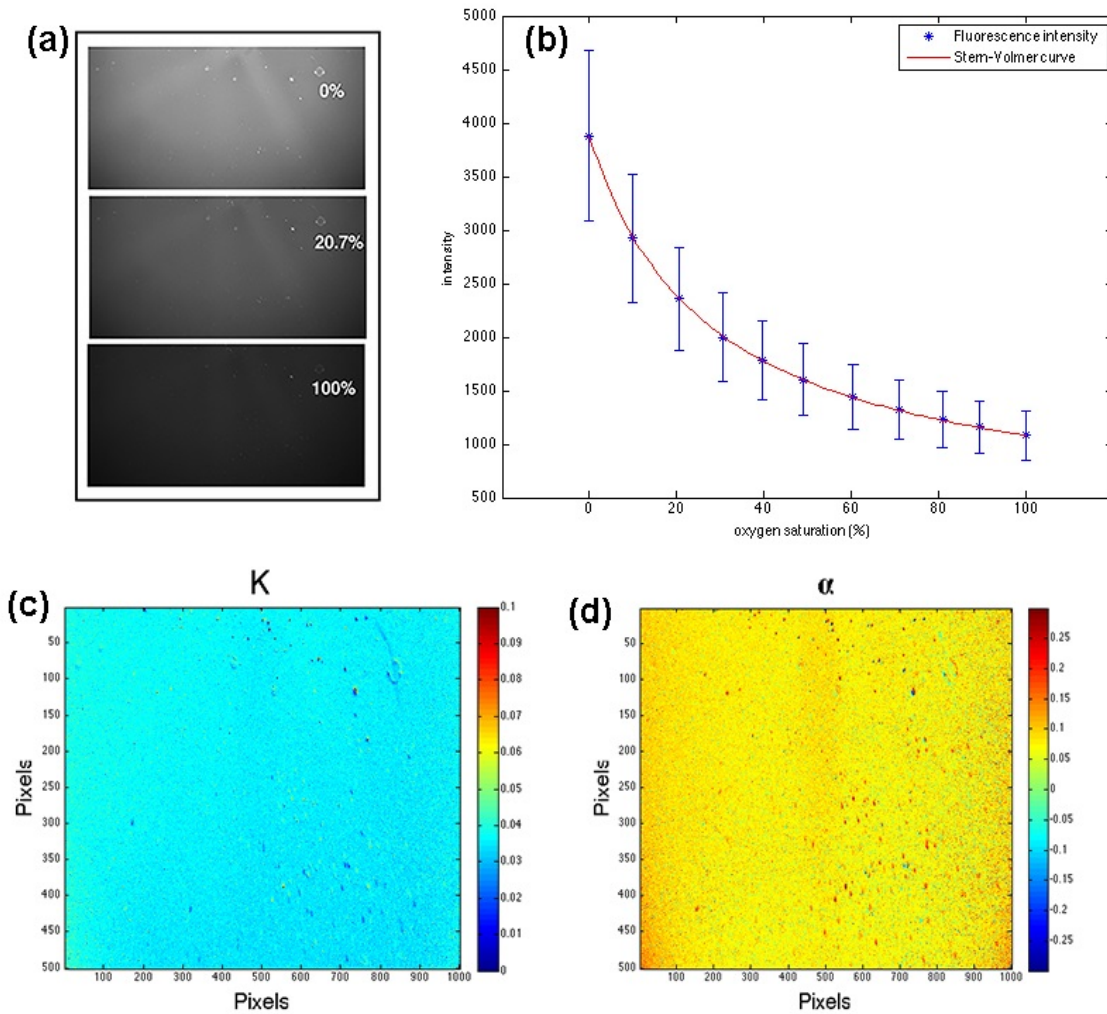
Figure 5-25. (a) Optode images under different O_2 concentrations, reported as percentage of oxygen saturation. (b) The Stern-Volmer equation showed good performance for calibration of optode data under different oxygen concentrations. (c) (d) Distributions of Stern-Volmer equation constants in each pixel across the field of view.

2) Dissolved oxygen redistribution by bioturbation

Dissolved oxygen distributions in sediments are shown in Figure 5-26. Steady diffusion of oxygen from the oxygenated overlying water column led to oxygen penetration to depths as large as 3 mm in sediments. Sediment reworking by bioturbation caused tremendous variability in porewater oxygen distributions. Sediment reworking altered the sediment structure and modified the morphology of the SWI, which led to redistribution of oxygen in the sediment. Ventilation of oxygenated water into anoxic burrows produced deep penetration of oxygen into the sediments. High porewater oxygen concentrations were observed in burrows up to 2 cm beneath the SWI (Figure 5-26 l). By irrigation, the worms also eject reduced burrow water into the water column (Figure 5-26 c). Oxygenated water that penetrated into burrows was reduced over ~10 min following irrigation events, indicating high temporal variations of porewater oxygen distributions induced by bioirrigation (Figure 5-27, Movie B5_oxygen optode, Supporting information).
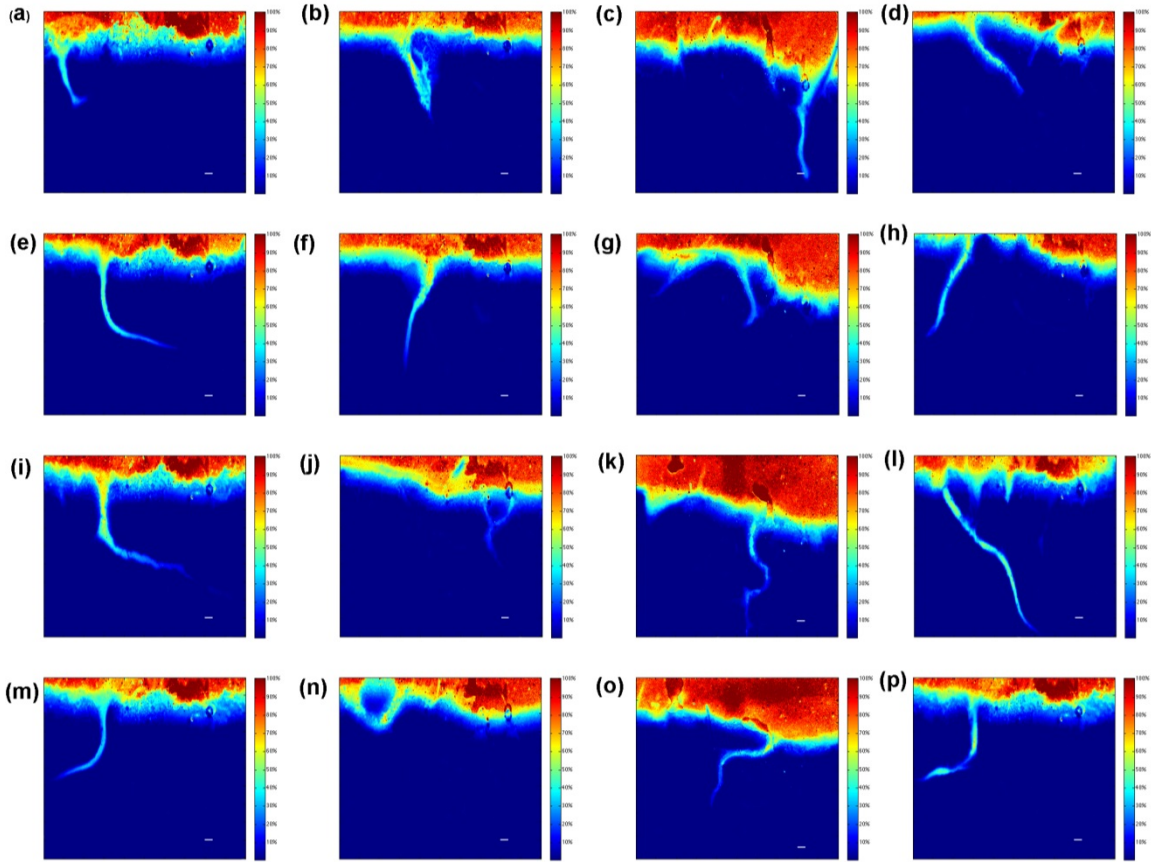
Figure 5-26. Spatial patterns of bioturbation-induced oxygen redistribution. Scale bars = 1 mm and fields of view are 26 mm × 23 mm.
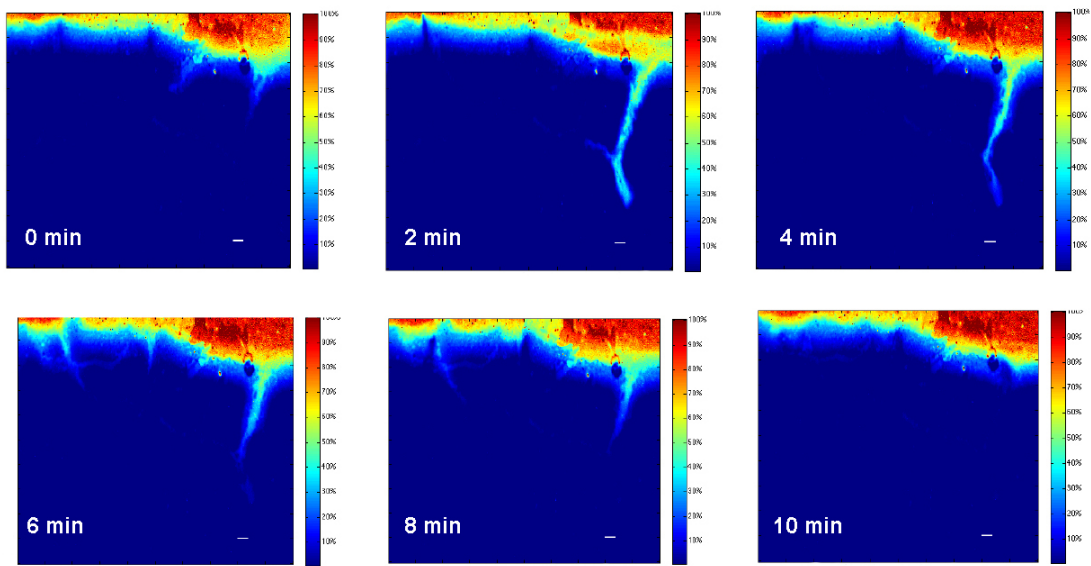
Figure 5-27. Temporal variation of oxygen distribution. Scale bars = 1 mm and fields of view are 26 mm × 23 mm.

67

5.3.4 Discussion

An oxygen optode enabled 2D visualization of oxygen distributions in sediments. Oxygen distributions obtained by 1D profiling method, such as microelectrodes, provide an incomplete picture of redox conditions as they are restricted to a single point, which may not be representative. Examination of 1D vertical profiles in optode measurements reveals that there is considerable variability in oxygen distributions through and across burrows (Figure 5-28). Subsurface sediments are broadly subdivided into oxic, suboxic and anoxic regions based on the extent of oxygen penetration from the overlying water column.[8, 128] The extent of penetration depends on the balance between downward transport of oxygen in porewater, aerobic metabolism in the sediments, and reactions with reduced materials in the sediments. In suboxic and anoxic regions, NO_3^-, Mn^{4+}, Fe^{3+}, SO_4^{2-}, and organic matter function as terminal electron acceptors for diagenesis reactions. Optode results showed that the thickness of oxic region varied from millimeters to centimeters between and within burrows. However, sediment reworking by bioturbation and ventilation of oxygenated water by bioirrigation obscured the boundaries of the oxic, suboxic and anoxic regions. Oxygen distributions induced by bioirrigation were also highly transient, as the introduced oxygen was consumed within several minutes. The continuous reworking of burrows and ventilation of oxygen produced cyclic redox oscillations within sediments. Such redox oscillations have been observed to alter sedimentary bacterial communities and chemical composition of porewaters.[129, 130]
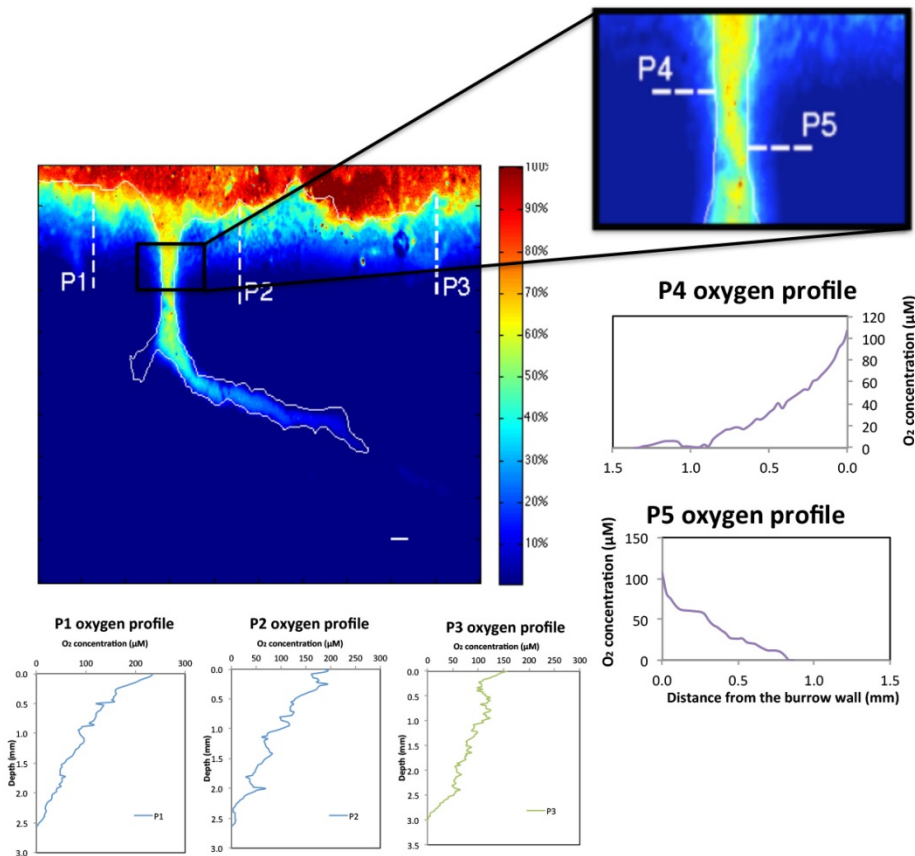
Figure 5-28. Vertical oxygen profiles at multiple locations within an optode image. Scale bar = 1 mm and main image field of view is 26 mm × 23 mm.

5.4 Effects of Flow Hydrodynamics on Cu Efflux in Low Permeability Estuarine Sediments

(Results reported in Minwei Xie, Ning Wang, Jean-François Gaillard, Aaron I. Packman. Hydrodynamic forcing mobilizes Cu in low-permeability estuarine sediments. Environmental Science & Technology. 2016. 50 (9): 4615-4623)

5.4.1 Sediment characteristics.

Bulk sediment properties are shown in Table 5-22 and Figure 5-29. Both sediments had a moderate fraction of very fine particles (<45 μm). Sediments are identified by their relative size: C series sediments are coarser ($d_{50} \approx 150$ μm), while F series are finer ($d_{50} \approx 60$ μm). However, both sediments had very low permeability, on the order of 10^{-15} m^2. This indicates that the fine fractions dominate the permeability of both sediments. Bulk sediment metal concentrations were slightly higher in C series sediments than in F series sediments.

Table 5-22. Bulk characteristics of PNS sediments.

Experimental runs	F1-F3	C1-C3
Porosity (%)	46.9±0.3	37.0±1.2
Porewater salinity (‰)	29.5	29.3
Permeability (m^2)	$1.3\pm1.2\times10^{-15}$	$1.3\pm0.3\times10^{-15}$
Organic C	1.94 %	1.77 %
AVS (μmol/g dry weight)	9.5±1.9	22.2±1.4
Cu (mg/kg dry weight)	256±34	646±76
Zn (mg/kg dry weight)	270±67	618±7
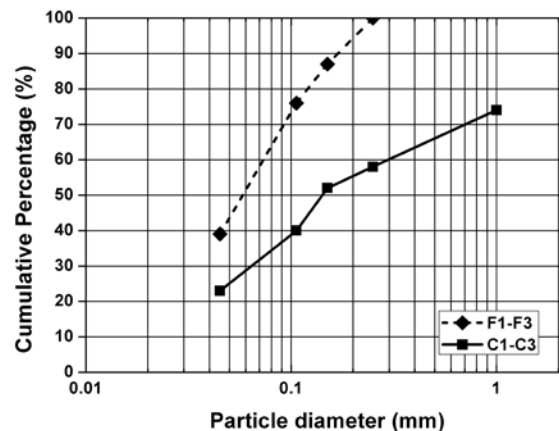
Figure 5-29. Sediment particle size distributions.

5.4.2 Metal efflux to the overlying water.

Overlying flow conditions exerted complicated impacts on the efflux of metals to the overlying water. In experiments with the finer-grained sediments (F series), dissolved Cu showed similar temporal patterns under all hydrodynamic conditions tested (Figure 5-30a). Dissolved Cu started at less than 15 nmol/L and gradually approached ~50 nmol/L in experiments F1, F2 and F3. Dissolved Cu concentrations in experiments with coarser-grained sediments (C series) differed with overlying flow conditions (Figure 5-30b). In experiment C1 (3% of critical shear), dissolved

Cu gradually increased from 3 to 78 nmol/L. In experiment C2 (50% critical shear), dissolved Cu rapidly increased from 18 to 123 nmol/L within the first 8 days and then increased further to 140 nmol/L over the remaining 6 days of the experiment. In experiment C3 (baseline 70% of critical shear, plus episodic resuspension), dissolved Cu increased rapidly from 40 to 120 nmol/L before the resuspension event on day 8 and then declined to 88 nmol/L at day 14.

Total Cu in the overlying water showed identical trends with dissolved Cu during all periods of steady flow, but differed greatly during periods of resuspension (Figure 5-30c, d). Resuspension mobilized Cu-rich sediment particles (Figure 5-33). The total Cu concentration in the water column thus increased substantially during periods of resuspension. However, these perturbations were highly transitory. Total Cu decreased rapidly following the cessation of sediment transport, and returned to pre-resuspension concentrations within 24 hours.

4-day running average fluxes of dissolved Cu across the SWI were calculated from the rate of change of dissolved Cu concentrations in the overlying water by linear least squares fitting of 4 days of dissolved Cu concentration data. Associated fluxes were then calculated by normalizing with the volume of recirculating water and SWI area. Temporal variations of 4-day running average fluxes of dissolved Cu in all six experiments are shown in Figure 5-31. Fluxes of Cu remained similar over the course of experiments with finer grained sediments (F1-F3), with an overall average flux of ~1.8 μmol/m^2/d for the three experiments (Figure 5-31a). In contrast, 4-day running average fluxes in experiments with coarser grained sediments (C1-C3) showed substantially different trends (Figure 5-31b). Both experiments C2 and C3 had higher fluxes than experiment C1 early in the experiments. The fluxes in C1-C3 were highest at the initiation of experiments and then decreased with time, indicating dissolved Cu in overlying water approached equilibrium concentration late in the experiments. The fluxes in experiment C3 were constantly positive before the sediment resuspension at day 8 and then became negative after the resuspension event, corresponding to the decrease of Cu concentrations in the overlying water (Figure 5-30b,d).

Fe concentrations were also analyzed for overlying water samples from experiments with coarser grained sediments. All Fe in the overlying water was particulate (dissolved Fe concentrations were below detection limit). Total Fe concentrations in the overlying water sample for experiment C1-C3 were shown in Figure 5-32. In experiment C1 and C2, total Fe remained at low concentrations, corresponding to low levels of turbidity in the overlying water (Figure 5-33). In experiment C3, sediment resuspension greatly increased Fe concentrations in the overlying water, which rapidly decreased to the pre-resuspension levels following reduction of the shear to baseline shear stress. Particulate Fe concentrations were strongly correlated with particulate Cu concentrations (total Cu- dissolved Cu) (Figure 5-31b), proving Fe and Cu were co-associated in the particles.
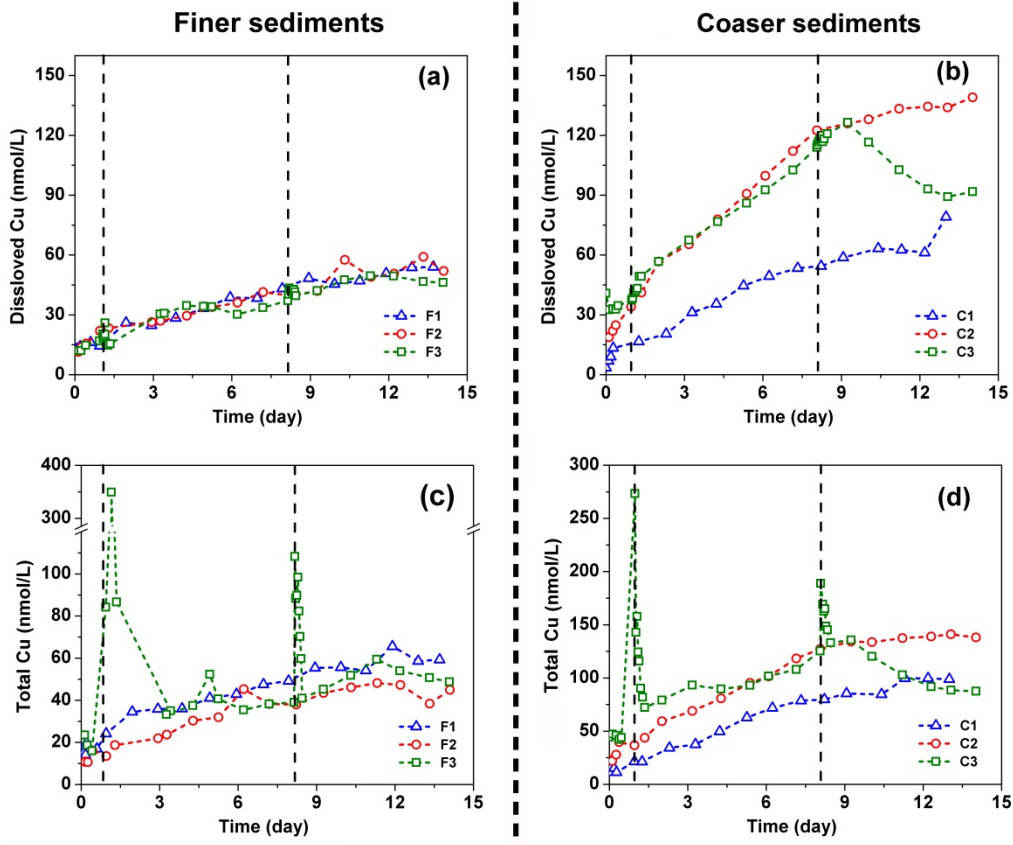
Figure 5-30. Time course of release of Cu to the overlying water under varied hydrodynamic conditions. (a) Efflux of dissolved Cu in experiments with finer-grained sediments. (b) Efflux of total Cu in experiments with finer-grained sediments. (c) Efflux of dissolved Cu in experiments with coarser-grained sediments. (d) Efflux of total Cu in experiments with coarser-grained sediments. Episodic sediment resuspension events in experiments F3 (a, b) and C3 (c, d) are indicated by vertical dashed lines. Each sediment resuspension lasted 4 hours (0.17 day).
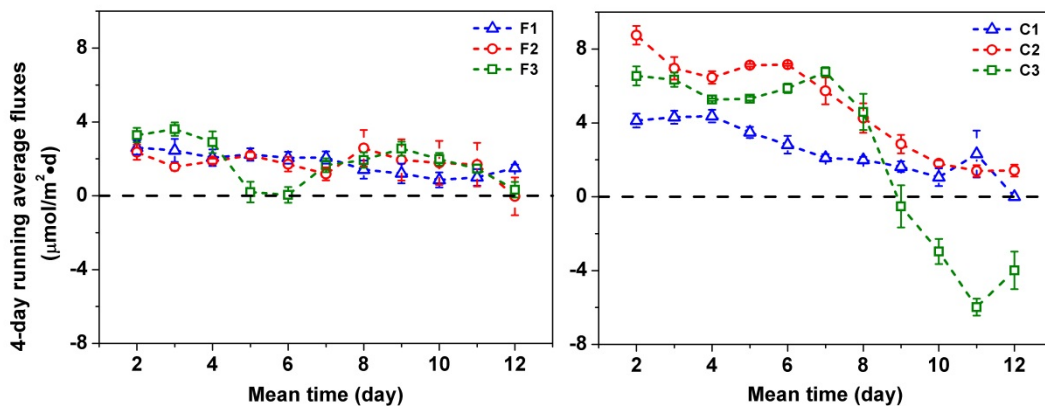
Figure 5-31. 4-day running average fluxes of dissolved Cu in experiments with (a) finer-grained sediments and (b) coarser-grained sediments.
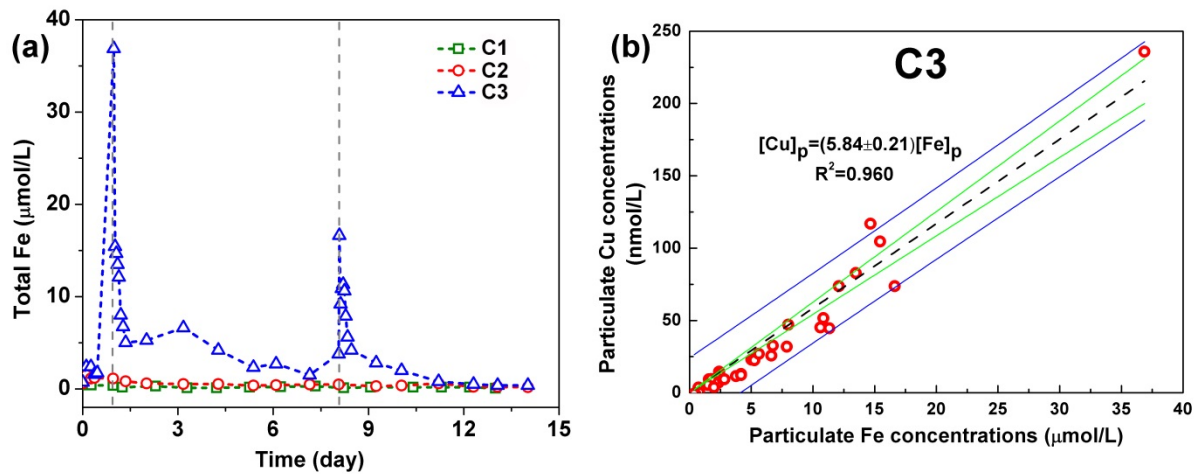
Figure 5-32. (a) Total Fe concentrations in experiments with coarser grained sediments. (b) Particulate Cu and particulate Fe in overlying water samples showed strong correlations. The black dashed line, green curves, and blue curves represent the best linear fit, the 95% confidence interval, and the 95% prediction interval of the fit, respectively.
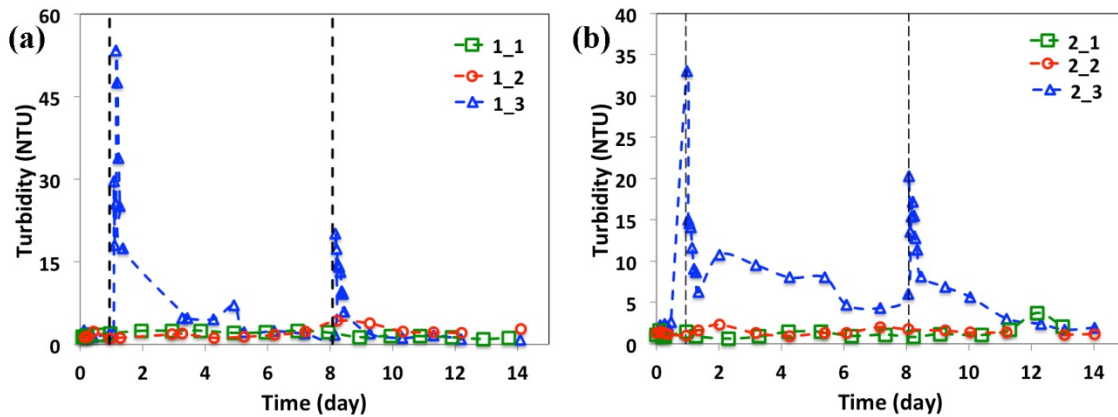
Figure 5-33. Overlying water turbidity. (a) Experiments with fine grained sediments; (b) Experiments with coarser-grained sediments.

5.4.3 Temporal variations of metals in pore water.

Porewater Cu concentrations in two sets of experiments showed similar response to hydrodynamic forcing from the overlying water column. In experiments F1-F3 with finer-grained sediments (Figure 5-36 a,b,c), Cu concentrations in pore water were uniform at all depths and were not substantially different between each treatment, suggesting that Cu mobilization and transport within the sediments was unaffected by flow hydrodynamics. In experiments C1-C3 with coarser grained sediments (Figure 5-34 d,e,f), Cu concentrations showed higher temporal and spatial variability. Cu concentrations in 2 cm and 4 cm porewater remained uniform throughout the experiments and treatments, suggesting constant solubility of Cu minerals. However, Cu concentrations in 1 cm porewater were substantially different. In experiment C1 with 3% of C.S., Cu concentrations in 1 cm porewater were constant with time. In experiment C2 with 50% of C.S., Cu concentrations in 1 cm porewater increased rapidly from 20 to 200 nmol/L. In experiment C3 with 70% C.S. and plus resuspension, Cu concentrations increased from 10 to 80 nmol/L for the first 8 days and then decreased to 25 nmol/L after the second resuspension event.

Dissolved Fe concentrations in porewater samples in experiment C1-C3 also showed varied patterns. In all three experiments C1-C3, pore water Fe concentrations at three depths were uniform at the initiation of experiments as a result of sediment homogenization (Figure 5-35). Dissolved Fe in the top 2 cm rapidly decreased (within two days) after the initiation of experiments whereas dissolved Fe at 4 cm depth remained approximately constant throughout the course of experiments. In experiment C3, dissolved Fe at 1 cm porewater remained constant between the two resuspension events on day 1 and day 8, but increased after the second resuspension (Figure 5-35 c). Fe concentrations also differed substantially at 1 and 2 cm of porewater in experiment C3, suggesting high Fe concentration gradients between 1 and 2 cm. The high Fe concentration gradients between 1 and 2 cm, and increasing Fe concentrations at 1 cm suggested efflux of dissolved Fe to the overlying water.
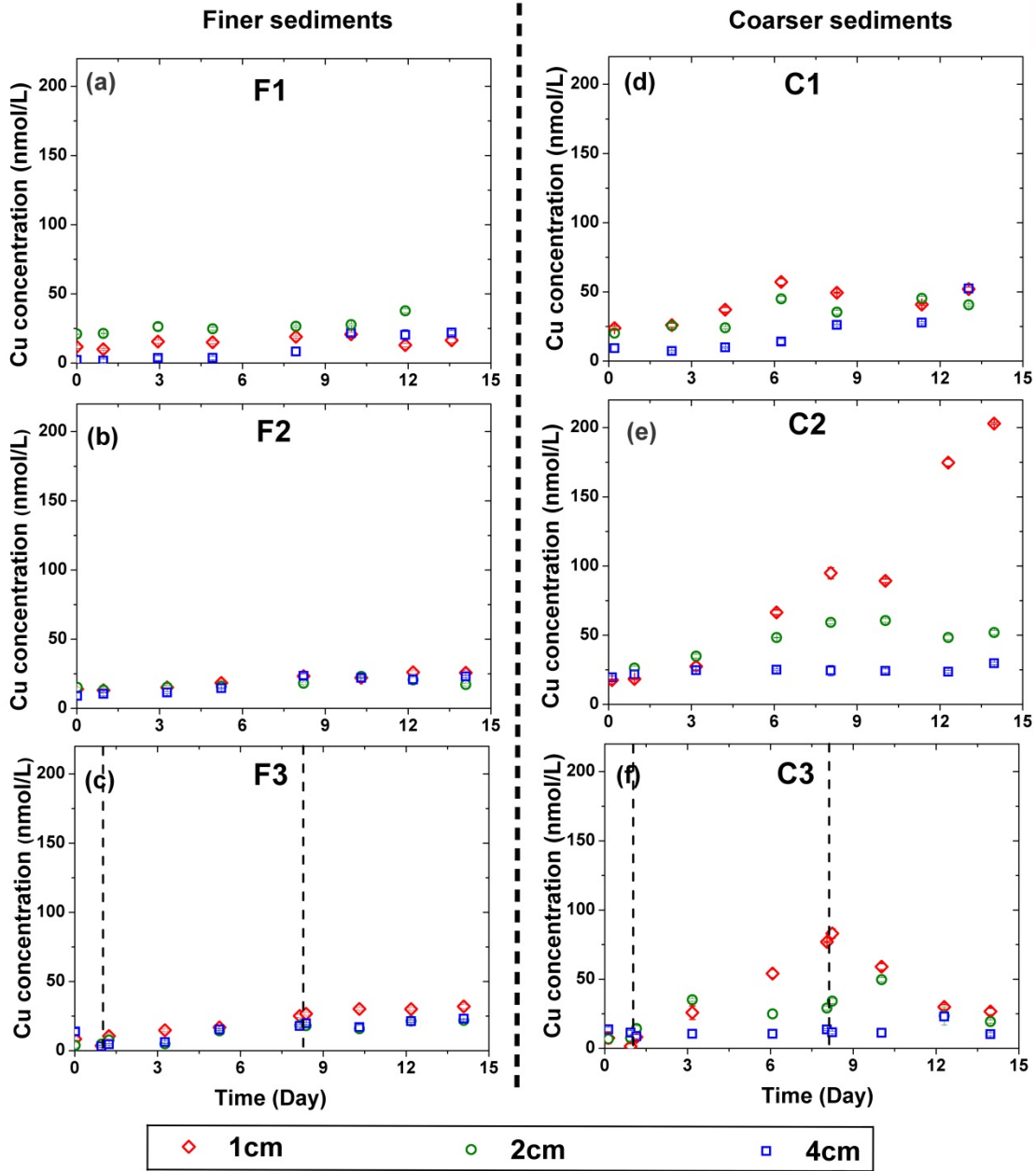
Figure 5-34. Temporal variations in pore water Cu concentrations in experiments with finer-grained sediments (a, b, c) and coarser grained sediments (d, e, f). Episodic sediment resuspension events in experiments F3 (c) and C3 (f) are indicated by vertical dashed lines. Each sediment resuspension lasted 4 hours (0.17 day).
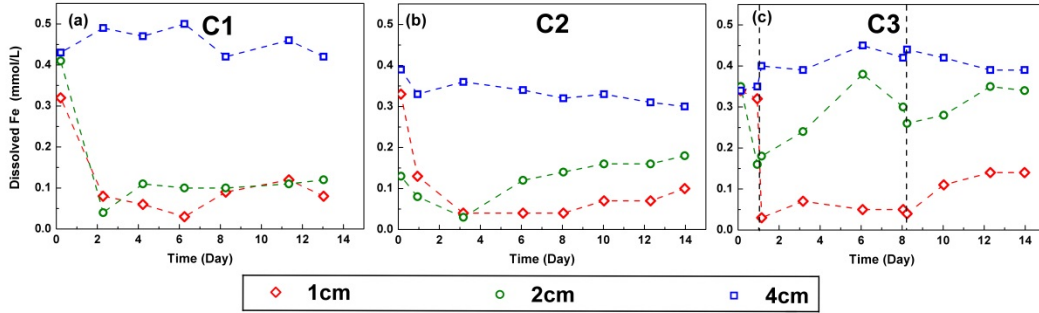
Figure 5-35. Temporal variations of porewater Fe concentrations in experiment C1-C3. Vertical dashed lines represented 4-h resuspension events for experiment C3.

5.4.4 Dissolved oxygen profiles.

Porewater dissolved oxygen profiles in experiments with coarser-grained sediment are shown in Figure 5-36. Oxygen penetrated less than 5 mm into the sediments in all three experiments. Oxygen penetration depth increased with imposed shear stress, indicating that hydrodynamic shear enhanced oxygen transport to and within the sediments. In contrast, DO profiles in finer-grained sediments did not vary substantially with imposed shear, suggesting that hydrodynamic shear did not enhance oxygen transport in the finer sediments (Figure 5-37).
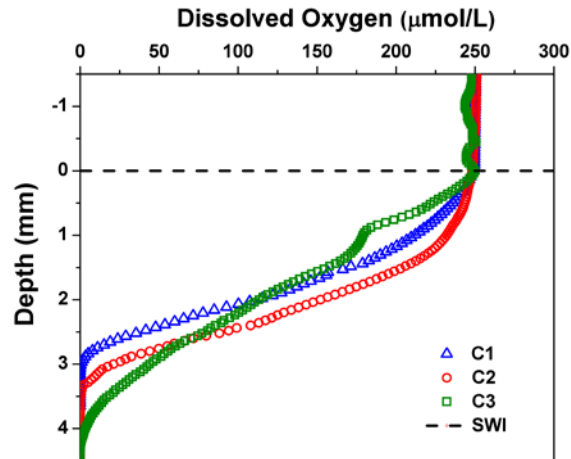
Figure 5-36. Hydrodynamic forcing enhanced the penetration of dissolved oxygen into coarser-grained sediments.
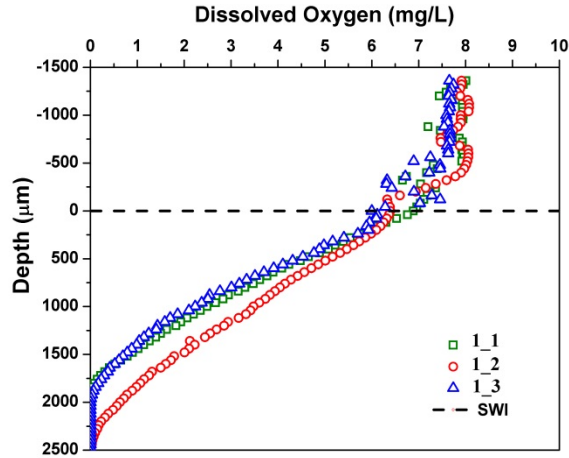
Figure 5-37. Dissolved oxygen concentration profiles in experiments with finer-grained sediments did not vary substantially with overlying flow conditions.

5.4.5 AVS and SEM-Cu

AVS and SEM-Cu profiles showed consistent trends in all treatments (Figure 5-38). AVS concentrations were substantially higher than SEM-Cu concentrations at all depths. AVS profiles showed lower concentrations in the surficial sediment than those at depth, suggesting oxidation of surficial sediments by oxygen diffused from overlying water. In contrast, SEM-Cu profiles showed higher concentrations in surficial sediments than those at depth, suggesting oxidation of surficial sediment increased the extractability of SEM-Cu at surficial sediments.
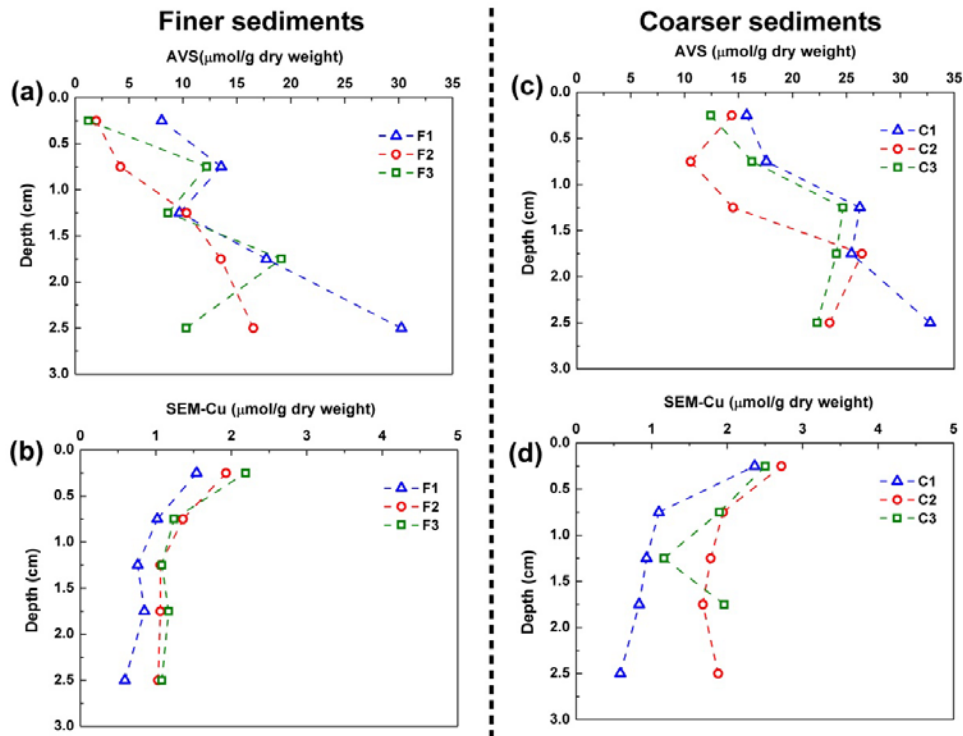
Figure 5-38. AVS and SEM-Cu profiles in experiments with finer and coarser sediments.

5.4.6 Discussion

Previous studies have demonstrated that oxygen diffusion from the overlying water column oxidizes surficial sediments, changes the solubility of metal associated minerals, and releases metals to pore water and overlying water.[121, 131] Here, oxygen penetrated less than 5 mm into the sediments (Figure 5-36), which led to a great decrease in AVS in the surficial sediments (depth < 0.5 cm) (Figure 5-38 a,c). Oxidation of AVS increased the extractability of SEM-Cu at the surficial sediments and liberated Cu to the porewater and overlying water.[40] Cu concentrations in both surficial pore water (Figure 5-34) and overlying water (Figure 5-30) steadily increased over the 14 d duration of the experiments, indicating ongoing mobilization of Cu from anoxic sediments to the pore water and overlying water.

Overlying hydrodynamics has been shown to influence surface-porewater exchange, modify biogeochemical zonation, and affect the fate of contaminants.[28, 132, 133] Enormous efforts have been particularly placed in fluvial systems, where the sediments are typically highly permeable. However, in sediments with permeability less than 10^{-12} m^2, solute transport in sediments is generally considered to be dominated by diffusion, and thus the effects of overlying hydrodynamics are often negelected.[28] However the current study demonstrates that increasing hydrodynamic shear on the SWI increased Cu concentrations in surficial pore water, facilitated the release of dissolved Cu to the overlying water, and also enhanced the penetration of oxygen into sediments in experiments even in the coarser of the two sediments tested (C1-C3). This observation indicates that hydrodynamic shear can play an important role in controlling the mobilization and overall efflux of metals even in sediments with permeability as low as 10^{-15} m^2. This effect could result either directly from porewater transport or by changes in the hydrodynamics of the diffusive boundary layer (DBL). The DBL is the thin layer of water immediately above the SWI, where solute transport is predominantly diffusive and driven by concentration gradients.[134] The DBL is strongly influenced by overlying hydrodynamics, as increasing shear over SWI decreases the thickness of DBL, sharpens the solute concentration gradients within DBL, and thus increases the solute flux.[135] In addition, turbulence in the bulk flow forms vortices that sweep and eject water parcels into and out of DBL, which also increases flux across the DBL.[136, 137]

Unlike experiments with coarser sediments, Cu concentrations in overlying water and porewaters remained unaffected by the changing hydrodynamic conditions in experiments with finer-grained sediments (F1-F3). These finer-grained sediments had a narrower particle size distribution than the coarser C-series sediments, and thus are expected to have a smoother sediment water interface.[138] Surface roughness of sediments plays important roles in both the thickness and stability of DBL.[139, 140] Therefore, it appears that sediment particle size distribution influences the mobilization of Cu both by controlling pore water fluxes and the structure of the DBL.

Sediment resuspension exerted diverse effects on metal mobilization. During resuspension, overlying water turbidity and total Cu concentrations increased dramatically as a result of mobilization of sediment particles to the overlying water (Figure 5-30 and Figure 5-33). However, this change was highly transitory as the turbidity and total Cu concentrations quickly returned to pre-resuspension levels when resuspension ceased. Resuspension also caused variable residual effects in the overlying water and pore water chemistry. In experiments with coarser sediments, Cu concentrations in both overlying water and porewater dropped gradually after the second resuspension (Figure 5-30b, d and Figure 5-34f), likely due to the release of dissolved Fe and

subsequent Cu precipitation and adsorption processes. Increasing dissolved Fe concentrations in near-surface porewater and high concentration gradients of dissolved Fe between 1 and 2 cm depth suggested efflux of dissolved Fe to the overlying water after the second resuspension in experiment C3 (Figure 5-35). Oxidative precipitation of Fe(II) to Fe(OH)$_3$ was thermodynamically and kinetically favorable in oxygenated overlying water.[141] The freshly precipitated Fe(OH)$_3$ thus provided reactive surfaces for adsorption and sequestration of Cu in particulate phases.[15] In the overlying water, concentrations particulate Fe and Cu were highly correlated, indicating that Fe and Cu were co-associated in suspended particles. Therefore, it appears that the dissolved Fe released from the sediment during and after the resuspension event rapidly oxidized in the overlying water and formed Fe(OH)$_3$ precipitates, which scavenged dissolved Cu from the overlying water.

5.4.7 Implications for assessment of contaminated sites

In low permeability sediments, such as the PNS sediments, it is generally considered that solute transport in porewaters occurs predominately by diffusion[22, 25, 28]. However, the results presented here clearly show that increased hydrodynamic shear is likely to enhance the transport of oxygen into sediments, the mobilization of Cu to porewater, and also the overall efflux of dissolved Cu to the overlying water even in these low permeability sediments.[140] Many estuarine sediments are subject to a high degree of variability in overlying hydrodynamic conditions, including both regular tidal fluctuations and episodic floods and storms that can increase both current and wave activity.[142] Therefore, overlying hydrodynamic processes, including variation of hydrodynamic shear and sediment resuspension, should be expected to strongly influence the mobility and efflux of metals in estuarine sediments.

Investigation of contaminated sediment sites typically involves a sequence of four approaches: development of a conceptual site model (CSM), screening assessment, characterization of exposure and effects, and identification of remedial actions.[4] Identifying the critical processes that influence the mobility of metals is an essential step in developing a CSM. This is complicated in dynamic sites exhibiting spatially and temporally variable patterns of metals fluxes, as site assessments typically use a low density and frequency of sampling.[15] Effects of time-variable flow forcing on the release and effects of contaminants from sediments are thus likely to be omitted from CSMs. In addition, current approaches for assessing bioavailability and toxicity of metals in sediments generally employ bulk sediment characterizations and batch organism exposure in a laboratory setting in combination with equilibrium partitioning models that attribute toxicity to the presence of dissolved metals in porewaters.[5] These approaches will miss ecological uptake and risk factors that result from interactions between flow, metals chemistry, and biological processes. Based on the results obtained in this study, time-variable flow and sediment resuspension should be considered in CSMs, and assessments of contaminated sediment bioavailability and toxicity should also include measurements of the effects of flow forcing in concert with bioturbation and bioirrigation in characterizations of exposure and effects.

5.5 Interplay of Hydrodynamics and Bioturbation on Mobility and Efflux of Cu

5.5.1 Particle dynamics and total Fe concentrations in the overlying water with and without bioturbation

Total Fe concentration and turbidity in the overlying water column reflect fine particle dynamics under variable flow forcing and bioturbation (Figure 5-39). Total Fe was dominated by particulate Fe in the overlying water column and showed similar trends to turbidity. Following initiation of the experiment, Fe and turbidity steadily increased in the overlying water (Figure 5-39 a). Fe (II) was produced in the sediments by reduction of Fe (III) and released to the overlying water, where it was quickly oxidized by oxygen to form Fe oxy-hydroxide precipitates. The Fe concentration substantially increased just after the flow shear increased to 0.22 Pa, suggesting upwelling of reduced Fe (II) from the sediment to overlying water by the increased hydrodynamic forcing. Fe concentrations and turbidity then decreased (Figure 5-39 b), indicating deposition of these particles by some combination of gravitational settling, attachment, filtration and trapping within the sediment bed.[143-145] Fe concentrations and turbidity remained at low levels when the flow shear was increased from 0.22 to 0.47 Pa (Figure 5-39 b). The short-term flow increase to 0.58 Pa to induce sediment resuspension caused a transitory increase in particle concentration in the overlying water (Figure 5-39 c). Total Fe and turbidity increased substantially during the period of resuspension but then decreased rapidly following cessation of the resuspension event.

Introduction of 40 *Nereis virens* at day 138 caused small increases in overlying water turbidity and total Fe (Figure 5-39 d). Bioturbation (worm burrowing) produced large heterogeneity in both sediment structure and chemistry. The worms burrowed into the sediment within 1 hour after they were introduced to the flume, and created mound structures and extensive branched burrow networks (Figure 5-40). Subsequently the worms also egested sediment particles at the sediment surface (Figure 5-40 b). The worms formed >100 burrows within 24 hours of introduction, and new burrows continued to be formed for 10 days, yielding ~160 burrow openings at steady state (Figure 5-46). The burrows represented a substantial perforation of the sediment, yielding substantial macroporosity both at the SWI and within the bed (Figures 5-40, 5-46). Worm burrow openings ultimately comprised 0.5% ± 0.2% of the surface area. Note that the number of burrow openings was 3-4 times the number of worms, reflecting the fact that the burrows were highly branched.

These sediment-reworking activities caused a net remobilization of particles to the overlying water (Figure 5-39 d). This effect became more obvious in concert with perturbations of the overlying flow (Figure 5-39 e,f). Flow perturbations produced greater increases in particle resuspension and metals release following bioturbation. Following bioturbation, total Fe and turbidity became substantially elevated under shear stresses of 0.22, 0.47, and 0.58 Pa, indicating bioturbation destabilized the sediments and favored both sediment resuspension and remobilization of metals.
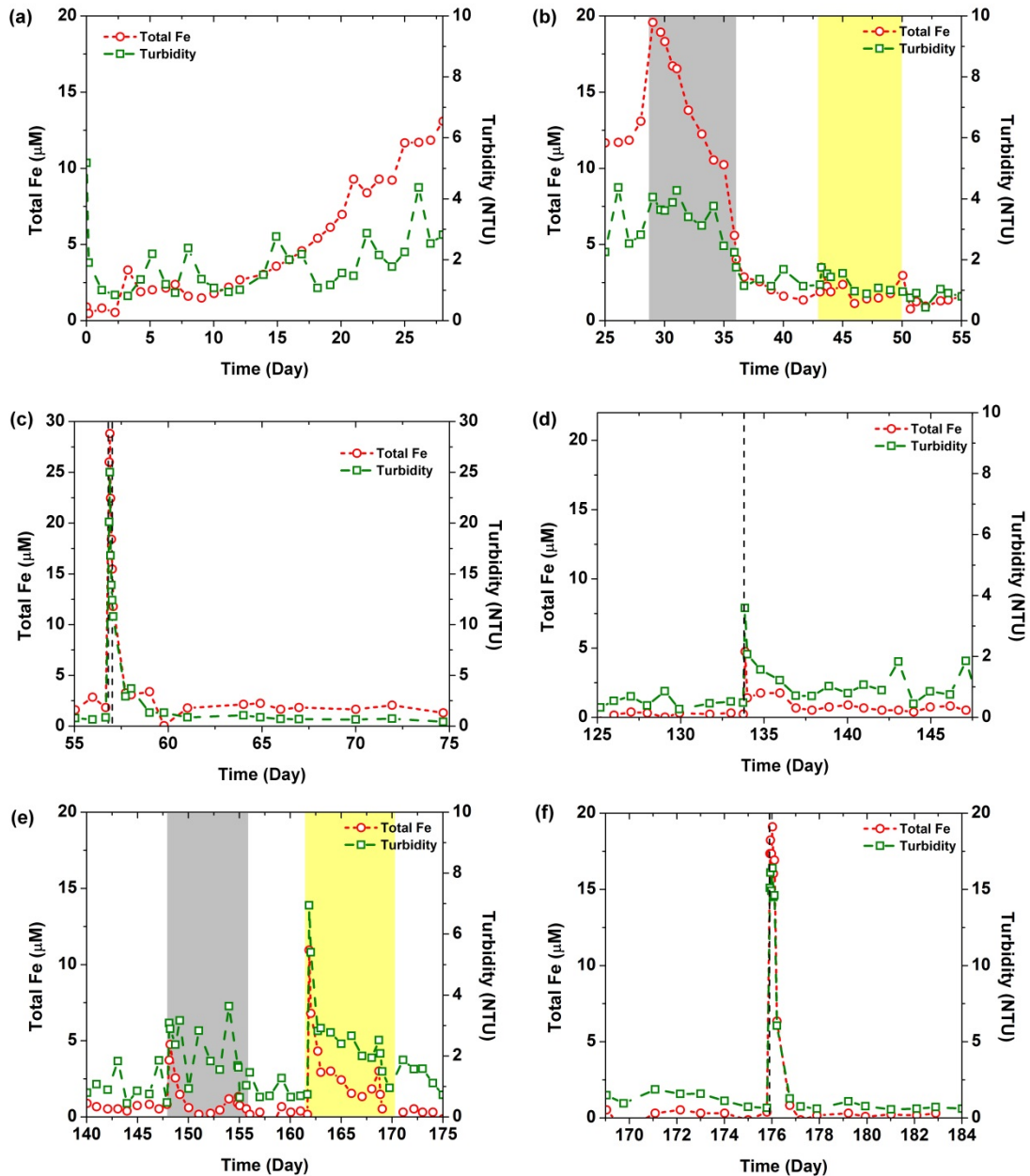
Figure 5-39. Fe concentration and turbidity in the water column in long-term flume experiment. (a) Stabilization period under baseline shear stress. (b) Increased hydrodynamic forcing. (c) Sediment resuspension. (d) Bioturbation with baseline shear. (e) Bioturbation with increased hydrodynamic shear. (f) Bioturbation with resuspension. Light gray area and light yellow area indicate imposed shear stress of 0.22 and 0.47 Pa, respectively. Dashed lines in (c) and (f) indicate sediment resuspension. Dashed line in (d) indicates introduction of 40 *Nereis virens*.
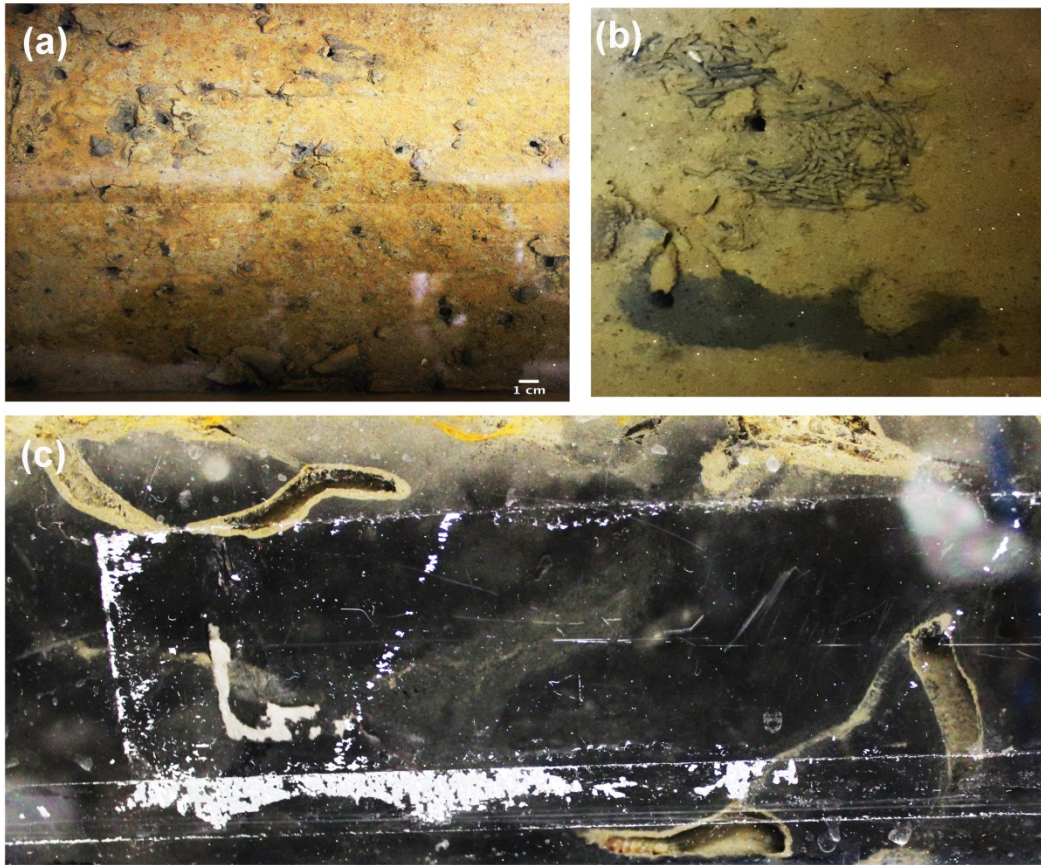
Figure 5-40. Images of sediment features produced by bioturbation in flume experiments. (a) Burrow openings at sediment water surface. Scale bar = 1 cm. (b) Egested sediments deposited outside of the burrow at SWI. (c) Side view of branched burrow networks showing oxidation of sediments along burrows (compare with black color of undisturbed sediments).
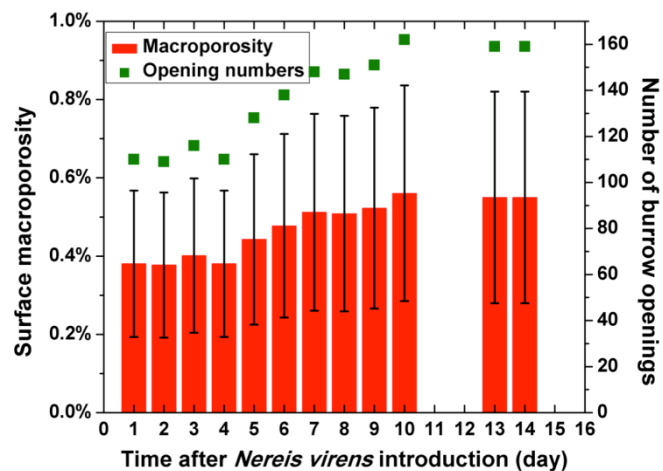
Figure 5-46. Development of worm burrow openings and surface macroporosity associated with burrows. Images of the sediment surface were taken daily and burrow openings were identified and counted using ImageJ. Macroporosity was calculated as the ratio of open burrow area to the total surface area of the sediment bed.

5.5.2 Cu concentrations in the overlying water.

Both dissolved and total Cu gradually released to the overlying water after the initiation of experiment and plateaued after ~5 days (Figure 5-41 a). Previous studies have found that oxidation of anoxic sediment is the principal mechanism for mobilization of metals (Zn and Cu) to pore water and overlying water.[128] Oxidation of reduced Cu species occurs near the SWI while diagenetic reactions using Fe^{3+} as the terminal electron acceptor occurs beneath the oxic zone. After reaching a maximum at 5 days, dissolved Cu for several weeks, most likely due to sorption of Cu ions to Fe oxy-hydroxide particles produced by liberation of reduced Fe from the sediments. When the shear was increased to 0.22 Pa, Fe-rich fine particles were removed from suspension and total Cu also decreased (Figure 5-41 b). Dissolved Cu first decreased and then increased, suggesting ongoing competition between Cu scavenging by Fe-rich particles and efflux of dissolved Cu from the sediments under higher shear. When flow shear was increased to 0.47 Pa, both dissolved and total Cu increased, indicating further mobilization of dissolved Cu from porewater and remobilization of particulate Cu. Total Cu increased dramatically after initiation of sediment resuspension and decreased rapidly after sediment resuspension ceased (Figure 5-41 c). Resuspended particles strongly scavenged dissolved Cu, while dissolved Cu continued for several days following the flow perturbation, resulting in elevated the overall dissolved Cu concentrations in the overlying water after the resuspension event (Figure 5-44 a).

Bioturbation further perturbed the sediments and overlying water chemistry. Ventilation of oxygenated water into anoxic burrows oxidized the sediments around the burrows (Figure 5-40 c).[19] Both dissolved Cu and total Cu concentrations gradually increased after the introduction of *Nereis virens* (Figure 5-41 d). Increased shear (0.22 Pa) caused small perturbations in total Cu concentrations associated with the remobilization of fine particles from the bed. Dissolved Cu concentrations increased at the same rate as in the baseline condition (Figure 5-41 e). When flow shear was increased to 0.47 Pa, both dissolved and total Cu substantially increased and then gradually decreased. Sediment resuspension consistently produced strong increases in particulate and total Cu. Consistent patterns for dissolved and total Cu were also observed when a sediment resuspension event occurred (Figure 5-41 f).
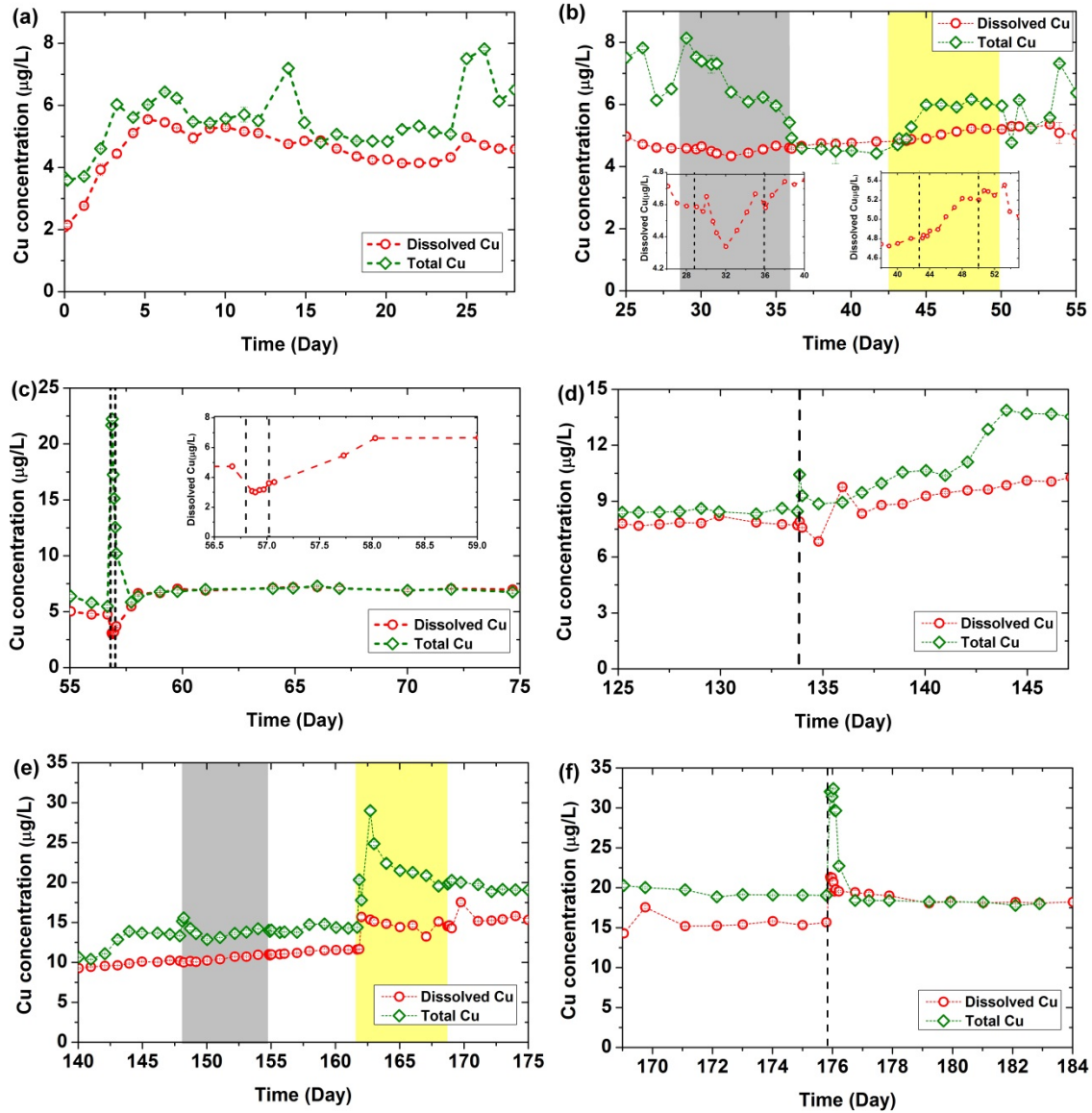
Figure 5-41. Dissolved and total Cu concentrations in the overlying water under varied conditions. (a) Stabilization period with baseline shear stress. (b) Increased hydrodynamic forcing. (c) Sediment resuspension. (d) Bioturbation with baseline shear. (e) Bioturbation with increased hydrodynamic shear. (f) Bioturbation with resuspension. Light gray area and light yellow area indicate 0.22 Pa shear stress and 0.47 Pa shear stress, respectively. Dashed lines in (c) and (f) indicate sediment resuspension. Dashed line in (d) indicates 40 *Nereis virens* introductions. Error bars represent one standard deviation from Cu analysis.

5.5.3 Cu concentrations in the pore water.

Diagenetic reactions strongly regulate the redistribution of metals between sediment particles and pore water.[146, 147] Oxygen diffusion from overlying water oxidizes surficial sediments and mobilizes metals into surficial pore water, while metals in deeper sediments are bound to reduced sulfide minerals. Hydrodynamics and bioturbation highly influenced the transport of oxygen and thus played key roles in the redistribution and mobility of Cu (Figure 5-42, 43). Before the introduction of *Nereis virens*, Cu concentrations in the uppermost 1 cm of pore water were higher than those in the overlying water and in the deeper porewater, suggesting that oxidation of surficial sediment was the primary source of Cu efflux to the overlying water (Figure 5-42). Cu concentrations in the uppermost 1 cm of pore water were influenced by overlying water hydrodynamics and thus showed high temporal and spatial variability.

When worms were introduced into the sediment, bioturbation and bioirrigation dominated the distribution of Cu in these pore waters (Figure 5-43). In one porewater profile, Cu concentrations in pore water at 2 cm depth were much higher than those observed at 1 cm, 4 cm, and in overlying water (Figure 5-43 a). In addition, Cu concentrations were similar in overlying water and 1 cm pore water, suggesting that surficial pore water and the water column were more mixed following bioturbation, and that worm burrows accumulated high concentrations of Cu, either bond to Fe-rich fine particles or organic matter, and become a pool and also a source of Cu to pore water and overlying water. Porewater sampled in a second location showed comparable but different patterns (Figure 5-43 b). Cu concentrations in the 4 cm pore water steadily increased after worm introduction. Cu concentrations at 2 cm increased slightly and had similar concentrations as 1 cm pore water. Cu concentrations in the overlying water were higher than those in 1 cm pore water, also suggesting surficial pore water was less likely to be the primary source of Cu to the overlying water. These results indicate spatial heterogeneity caused by bioturbation, with worm burrows increasing exchange with the overlying water, thereby oxidizing sediments near the burrows and liberating dissolved Cu.
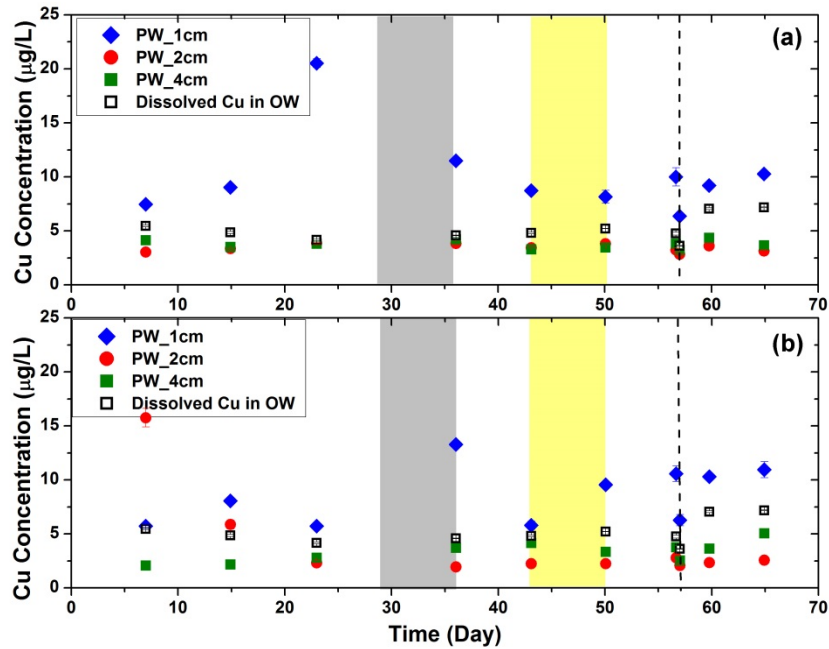
Figure 5-42. Cu concentrations in pore water and overlying water before introduction of *Nereis virens* at two sampling locations (a,b). Black dashed lines represent sediment resuspension events that lasts for four hours. Error bars represent one standard deviation of replicate measurements.
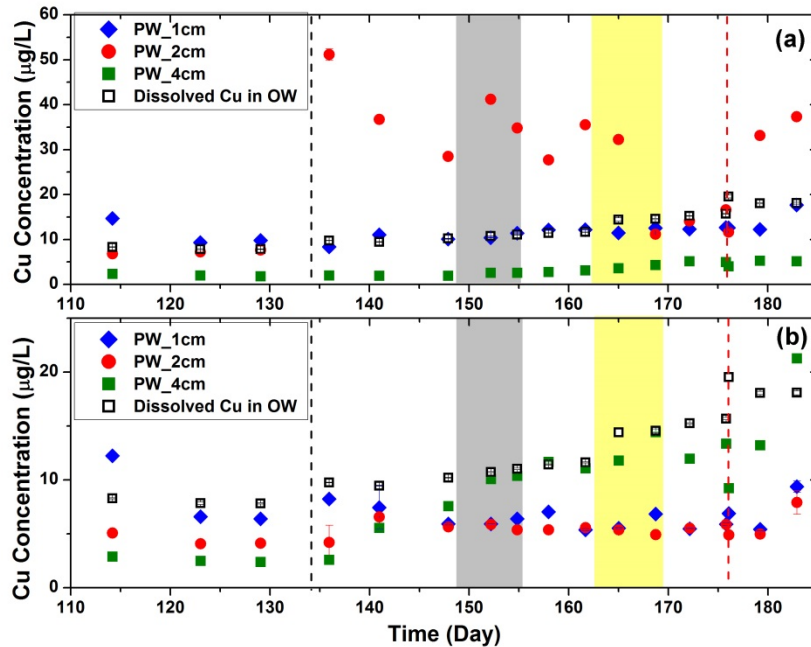
Figure 5-43. Cu concentrations in the pore water and overlying water following bioturbation at two sampling locations (a,b). Black dashed line represents the introduction of *Nereis virens*. Light gray area indicates period of 0.22 Pa shear stress and light yellow area indicates period of 0.47 Pa shear stress. Red dashed line indicates a sediment resuspension event that lasted for four hours. Error bars represent one standard deviation of replicate measurements.

5.5.4 Dissolved oxygen profile.

Penetration of oxygen into the sediment is regulated by the dynamic balance between diffusion of oxygen from overlying water and consumption within the sediment bed.[34] Observed oxygen profiles in pore water show the effects of hydrodynamic forcing and bioturbation on oxygen penetration within sediment bed (Figure 5-44). Porewater oxygen profiles typically approach to steady state rapidly, within a few days.[148] Here, hydrodynamic forcing substantially enhanced the transport of oxygen into sediment (Figure 5-44 a). The penetration depth increased from 1.5 mm for the baseline condition to 5 mm immediately after the sediment resuspension event. Bioturbation also enhanced oxygen penetration into the sediments (Figure 5-44 b).
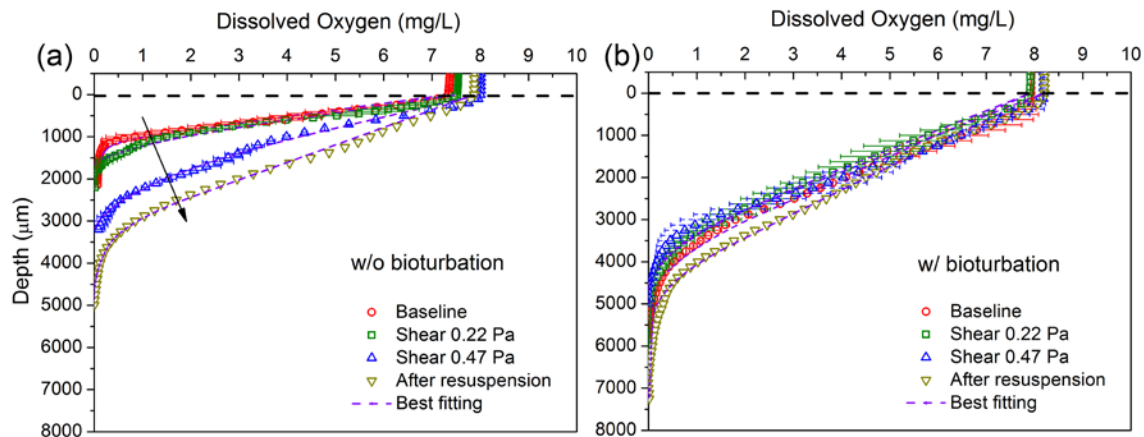
Figure 5-44. Figure 6. Dissolved oxygen profiles under varied hydrodynamic conditions without and with bioturbation. (a) Hydrodynamic forcing enhanced the delivery of oxygen into sediments. (b) Bioturbation also enhanced the transport of oxygen into sediment. Oxygen profiles on each hydrodynamic condition represent average of two individual replicate measurements, and error bars represent the standard deviation. Only one replicate profile was measured for "after resuspension" condition (Dark yellow triangles). Black horizontal dashed curves represent sediment water interface. Purple dashed lines represent the best fitting profiles calculated using the numerical interpretation method by Berg *et al.*[149]

5.5.5 Effects *of physical, chemical and biological processes on metal mobility.*

This flume study highlights that the fate of metal contaminants are strongly regulated by the interplay between physical, chemical and biological processes. Within sediment beds, diagenetic reactions controlled the redistribution of metals between pore water and sediment particles.[7] Increased hydrodynamic forcing delivered additional oxygen into the sediment and enhanced the mobilization of metals. Hyporheic flow hydrodynamics also played an important role in the dynamics of fine particles by facilitating the delivery and retention of suspended particles in the sediment bed.[150] Fine, Fe-rich sediment particles strongly influenced Cu dynamics, but this behavior changed over the course of the experiment. Particulate Cu and Fe concentrations were highly correlated throughout the experiment, but the slope of the linear regression changed substantially during different phases of the experiment (Figure 5-45). Under baseline conditions, low Cu/Fe ratios were observed in suspended particles, suggesting scavenging of dissolved Cu by Fe oxy-hydroxide particles. During periods of sediment resuspension, a medium Cu/Fe ratio was observed, reflecting the composition of the resuspended sediments (i.e., reflecting the Cu/Fe ratio

in the surficial sediments). After introduction of *N. virens*, a much higher Cu/Fe ratio was observed in suspended particles, indicating that bioturbation either changed the speciation of Fe particles that scavenged Cu or liberated Cu-rich sediments from within burrows.
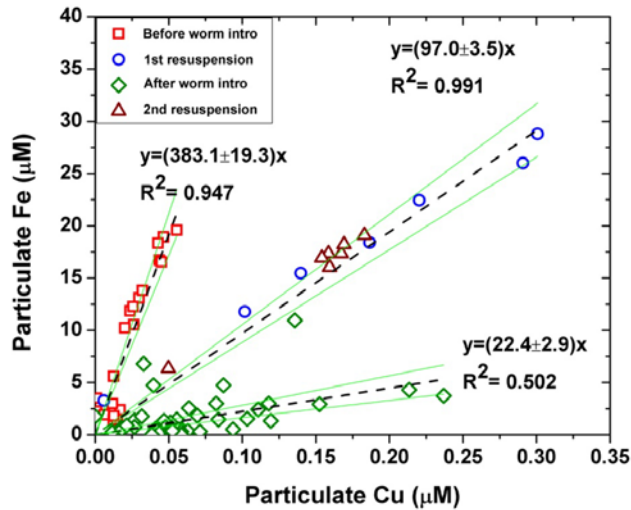
Figure 5-45. Correlation between Fe and Cu concentrations in suspended sediments (particulate fraction of overlying water samples). Red squares represent samples obtained before resuspension and worm introduction (days 10-50). Blue circles represent samples obtained during the first sediment resuspension (day 57). Green diamonds represent samples obtained after the introduction of *N. virens* but before the second sediment resuspension (days 136-173). Brown triangles represent samples obtained during the second resuspension event (day 176).

6. Conclusions and Implications for Future Research/Implementation

The project improves assessment of risks at DOD's contaminated sediment sites by enhancing knowledge of fundamental processes that govern the behavior and effects of metal contaminants in sediments and providing strategies for measuring key effects including metals efflux, bioavailability, and toxicity under complex site conditions. The project results indicate that interactions between overlying flow dynamics and biological structuring of the sediments (e.g., from worm burrowing and other types of bioturbation) can enhance the mobilization of metals from contaminated sediments to the water column. The primary mechanism of metals (Zn and Cu) mobilization from the three different contaminated sediments tested was oxidation of reduced mineral phases near the sediment-water interface (SWI). This process is mediated by hydrodynamic transport of oxygen to reduced sediments, providing a mechanism for overlying flow conditions to enhance metals release. Comparisons of net metals efflux, porewater oxygen profiles, and porewater metals concentrations generally indicated that increased liberation of metals is accompanied by increased porewater transport and deeper oxygen penetration into the sediments. Such enhancement was observed even in sediments with bulk permeability on the order of 10^{-15} m^2, suggesting that hyporheic exchange and porewater transport can play a critical role in mobilizing metals in much finer sediments than previously believed. However, increasing hydrodynamic shear on the SWI did not consistently increase metals efflux in such fine sediments, and instead fluxes varied with sediment size and heterogeneity. Enhanced metals efflux was observed in heterogeneous sediments having a median grain size of ~150 μm and permeability of 10^{-15} m^2, but not in finer sediments with a median grain size of ~60 μm but the same permeability. Despite differences in median grain size, both sediments had similar bulk permeability because of the presence very fine fraction (>20% of particles with d < 45 μm). This suggests that fine-scale sediment structure associated with sediment heterogeneity could control boundary-layer transport and/or flushing of the uppermost sediments, but this scale of transport could not be resolved in the experiments performed here.

To clarify the specific mechanism of enhanced metals efflux under flow, a greater variety of sediments would need to be characterized with high-resolution observations of interfacial flow and contaminant release dynamics. However, this would be challenging as it is notoriously difficult to resolve biogeochemical processes at this scale in dynamic sedimentary environments. Instead of seeking direct measurements of contaminant transport at and near the SWI, advancements in understanding of fundamental hyporheic exchange processes are likely to inform controls on metals efflux from fine sediments. Because this study established the link between hydrodynamic transport, sediment oxidation, and metals release, advancements in understanding basic hydrodynamics of hyporheic exchange can be translated to applications in conceptual models for contaminated sediment dynamics under the assumption that increased porewater transport will yield enhanced oxygen delivery, sediment oxidation, and metals efflux. In addition, direct assessments of oxygen penetration profiles and the distribution of oxidized sedimentary phases can be used diagnostically to assess the likely extent of porewater flushing and therefore the likelihood that metals efflux will vary with overlying flow conditions. This approach is more favorable because it can be assayed through a combination of direct analysis of spatial patterns within sediment cores and laboratory Gust chamber experiments to directly assess the effects of overlying flow conditions on metals efflux from cores. In addition, technologies such as benthic landers with microelectrode-microprofiling suites are becoming increasingly available for direct, *in situ* measurement of porewater geochemical profiles at sites.

Sediment resuspension also substantially mobilized metals from the sediments, but only transitorily. Total metals concentrations in the water column increased immediately and substantially with the onset of sediment resuspension. The mobilized metals were predominately particulate, and little mobilization of dissolved metals was observed during periods of sediment resuspension. As a result, sediment resuspension did not significantly increase metals bioavailability or acute toxicity to *Neanthes arenaceodentata*, *Pyrocystis lunula*, *Daphnia magna*, or *Hyalella azteca*. One important caveat here is that only short-term (typically 4-h) episodic resuspension was investigated, and continuous resuspension was not evaluated. During these short-term resuspension events, some dissolved metals were liberated from the sediments – presumably from near-surface porewaters – but resuspended particles generally did not dissolve in suspension. In particular, the XAS results showed that resuspended particulate ZnS persisted in the water column despite the presence of dissolved oxygen. This indicates a strong kinetic limitation on mobilization of Zn by oxidation of resuspended ZnS, which kept dissolved Zn concentrations relatively low and limited Zn bioavailability and acute toxicity during resuspension. Conversely, oxidation reactions within the surficial sediments dissolved ZnS binding phases, releasing Zn to pore water and water column. The study also showed scavenging of Cu by Fe-rich particles resuspended from the sediment bed and/or produced by oxidation of Fe(II) and subsequent precipitation of Fe oxyhydroxide particles.

These results emphasize that it is important to understand the formation, dissolution, and mobilization of important metals-binding phases. While both oxidized (e.g., oxyhydroxides) and reduced (e.g., sulfidic) particles can be important scavengers of metal contaminants, the processes that lead to the formation and dissolution of these particles occur at very different timescales. In general, both slow sedimentary processes and rapid water column processes can be important, and thermodynamic equilibria should not be assumed under transient conditions such as flow perturbations. These results also emphasize that mobilization and bioavailability/toxicity can be very distinct problems even though they are both generally favored by liberation of metals from the sediments. Because sediment resuspension is a threshold process, particulate metals can be rapidly and substantially mobilized during flow perturbations that mobilize sediments. Further, such mobilized metals can potentially be transported long distances under high-flow conditions. However, because resuspension at contaminated sediment sites is often transitory and some binding phases are relatively refractory (e.g., ZnS here), these events may not directly liberate bioavailable metals. In site assessments, the frequency and magnitude of sediment resuspension should be considered as a risk factor for both off-site migration and ecological effects of contaminated sediments. The potential bioavailability and toxicity of the mobilized metals can then be assessed, where warranted, using the methods developed here: Gust chamber experiments with analysis of dissolved and particulate metals under controlled resuspension conditions, and sediment flux exposure chambers to directly observe bioavailability and toxicity of resuspended particles to test organisms.

Bioturbation produced more complex sediment structure and more complex contaminant release behavior in concert with flow perturbations. Bioturbation by burrowing *Lumbriculus variegatus* (in freshwater sediments) and *Nereis virens* (in estuarine sediments) produced extensive macroporosity in the sediment in the form of u-shaped and branched burrow networks. Direct observations with oxygen optodes showed that bioturbation increased sediment mixing and oxygen penetration depths by an order-of-magnitude (from mm-scale to cm-scale) within burrows. Further, sediment reworking by bioturbation and burrow flushing by bioirrigation greatly increased the

spatial and temporal variability in porewater oxygen concentrations. Bioturbation therefore contributed several related effects that are expected to increase oxidation of sediments and mobilization of metals from sediments: increased sediment mixing, increased surface area of the SWI, increased exposure of buried particles to the SWI, greatly increased sediment heterogeneity through development of macroporosity, and increased porewater flushing through a combination of hyporheic exchange (induced by overlying water column hydrodynamics) and bioirrigation (induced by worm motion and/or biological pumping).

This study observed the effects of these processes on mobilization of Cu from contaminated sediments from Portsmouth Naval Shipyard. Effects of overlying flow, sediment resuspension, and bioturbation/bioirrigation by *Nereis virens* were observed independently and together in long-term flume experiments. As in smaller-scale experiments, bioturbation led to extensive macroporosity in the form of branched burrow galleries with multiple open connections to the overlying water. Oxygen readily penetrated burrows, leading to oxidation of sediments lining burrow walls. Bioturbation liberated Cu into worm burrows at depths up to several cm, and thereby increased the efflux of Cu to the overlying water column. Overlying flow increased flushing of worm burrows. However, particle dynamics associated with bioturbation were more complex. Oxidation of iron liberated from the sediments led to reprecipitation of iron oxy-hydroxide particles that scavenged Cu from the water column. Further, bioturbation destabilized the surficial sediments, leading to greater particle resuspension under episodic high flows than observed without bioturbation. Cu was also co-associated with Fe particles during periods of resuspension, but Cu-Fe associations changed following both bioturbation and resuspension. The combination of bioturbation and resuspension also produced gradual increases in the liberation of dissolved Cu to the overlying water column.

These results further emphasize the need to understand controls on solid phases that bind and sequester metal contaminants. The results presented here show that physical, chemical, and biological processes act in concert to control contaminant mobility and bioavailability in complex ways. In particular, flow perturbations and bioturbation interact to mobilize bioavailable contaminants. However, the underlying dynamics are complex, and specific mechanisms controlling contaminant speciation (and therefore bioavailability) are difficult to discern. Metals binding by suspended particles result from a combination of sedimentary and water-column processes including sediment transport, oxidation/reduction, precipitation/dissolution, and sorption/desorption that all exhibit high degrees of spatial and temporal variability in bioturbated and episodically resuspended sediments. However, it is not possible to isolate individual effects with bulk measurements owing to the high spatial variability in the underlying processes. For example, processes such resuspension of particles from very near the SWI and liberation of dissolved metals by oxidation of burrow walls are extremely difficult to diagnose from bulk measurements in the water column or sediments owing to the fact that the source material can occupy a very small fraction of the bed, and further the distribution can change dramatically over time with variable flow rates and organism activity.

As a practical matter, site assessments should focus on identifying dominant controls on metals mobility and bioavailability that control off-site migration and ecological effects. The experimental results presented here indicate that flow variation and *in situ* biological activity can play important roles in the long-term fate and effects of metals in contaminated sediments. Based on these findings, time-variable flow and sediment resuspension should be considered in

conceptual site models, and assessments of contaminated sediment bioavailability and toxicity should also include measurements of the effects of flow forcing and sediment resuspension in concert with bioturbation and bioirrigation in characterizations of exposure and effects. The experimental approaches developed in this project to measure the effects of flow forcing, sediment resuspension, and bioturbation can be directly employed in site assessments using sediment cores or homogenized sediments obtained from DOD sites. Where warranted, more specific mechanisms of metals mobilization and effects can be determined by detailed high-resolution measurements in combination with advanced analysis of metals speciation to better relate observed contamination to mobilization processes, bioavailability, and ultimately ecological effects.

7. Literature Cited

1.   Apitz, S. E., Conceptualizing the role of sediment in sustaining ecosystem services: Sediment-ecosystem regional assessment (SEcoRA). *Science of the Total Environment* **2012,** *415*, 9-30.

2.   Burton Jr, G. A., Sediment quality criteria in use around the world. *Limnology* **2002,** *3*, (2), 65-76.

3.   USEPA, National sediment quality survey, The Incidence and Severity of Sediment Contamination in Surface Waters of the United States. In Washington, D.C., 1997.

4.   Sorell, T.; McEvoy, K., Incorporating Bioavailability Considerations Into the Evaluation of Contaminated Sediment Sites. *Remediation Journal* **2013,** *23*, (1), 63-72.

5.   Di Toro, D. M.; Zarba, C. S.; Hansen, D. J.; Berry, W. J.; Swartz, R. C.; Cowan, C. E.; Pavlou, S. P.; Allen, H. E.; Thomas, N. A.; Paquin, P. R., Technical basis for establishing sediment quality criteria for nonionic organic chemicals using equilibrium partitioning. *Environmental toxicology and chemistry* **1991,** *10*, (12), 1541-1583.

6.   Stumm, W.; Morgan, J. J., Aquatic chemistry, chemical equilibra and rates in natural waters. *Environmental Science & Technology.* **1996**.

7.   Berner, R. A., *Early diagenesis: A theoretical approach*. Princeton University Press: **1980**.

8.   Gaillard, J.-F.; Pauwels, H.; Michard, G., Chemical diagenesis in coastal marine-sediments. *Oceanologica Acta* **1989,** *12*, (3), 175-187.

9.   Froelich, P. N.; Klinkhammer, G.; Bender, M. a. a.; Luedtke, N.; Heath, G. R.; Cullen, D.; Dauphin, P.; Hammond, D.; Hartman, B.; Maynard, V., Early oxidation of organic matter in pelagic sediments of the eastern equatorial Atlantic: suboxic diagenesis. *Geochimica et Cosmochimica Acta* **1979,** *43*, (7), 1075-1090.

10.   Gaillard, J.-F.; Sarazin, G.; Pauwels, H.; Philippe, L.; Lavergne, D.; Blake, G., Interstitial water and sediment chemistries of Lake Aiguebelette (Savoy, France). *Chemical geology* **1987,** *63*, (1), 73-84.

11.   Webb, S.; Gaillard, J.-F., Zinc Speciation in Contaminated Sediments: Quantitative Determination of Zinc Coordination by X-ray Absorption Spectroscopy. *Aquatic Geochemistry* **2014**, 1-18.

12.   Gaillard, J.-F.; Jeandel, C.; Michard, G.; Nicolas, E.; Renard, D., Interstitial water chemistry of Villefranche Bay sediments: trace metal diagenesis. *Marine Chemistry* **1986,** *18*, (2), 233-247.

13.   Rickard, D.; Morse, J. W., Acid volatile sulfide (AVS). *Marine Chemistry* **2005,** *97*, (3), 141-197.

14.   Eggleton, J.; Thomas, K. V., A review of factors affecting the release and bioavailability of contaminants during sediment disturbance events. *Environment International* **2004,** *30*, (7), 973-980.

15.   Burton, G. A., Metal bioavailability and toxicity in sediments. *Critical Reviews in Environmental Science and Technology* **2010,** *40*, (9-10), 852-907.

16.   Van Cappellen, P.; Gaillard, J.-F., Biogeochemical dynamics in aquatic sediments. *Reviews in mineralogy and geochemistry* **1996,** *34*, (1), 335-376.

17.   Borch, T.; Kretzschmar, R.; Kappler, A.; Cappellen, P. V.; Ginder-Vogel, M.; Voegelin, A.; Campbell, K., Biogeochemical redox processes and their impact on contaminant dynamics. *Environmental science & technology* **2009,** *44*, (1), 15-23.

18.   Aller, R. C., The effects of macrobenthos on chemical properties of marine sediment and overlying water. In *Animal-sediment relations*, Springer, U.S.: 1982; pp 53-102.

19.   Pischedda, L.; Poggiale, J.-C.; Cuny, P.; Gilbert, F., Imaging oxygen distribution in marine sediments. The importance of bioturbation and sediment heterogeneity. *Acta biotheoretica* **2008,** *56*, (1-2), 123-135

20.   Glud, R., NB Ramsing, JK Gundersen, I. Klimant, Planar optodes:a new tool for fine scale measurements of two-dimensional O2 distribution in benthic communities. *Mar. Ecol. Prog. Ser* **1996,** *140*, 217-226.

21.   Zhu, Q.; Aller, R. C.; Fan, Y., High-performance planar pH fluorosensor for two-dimensional pH measurements in marine sediment and water. *Environmental science & technology* **2005,** *39*, (22), 8906-8911.

22.   Boano, F.; Harvey, J.; Marion, A.; Packman, A.; Revelli, R.; Ridolfi, L.; Wörman, A., Hyporheic flow and transport processes: Mechanisms, models, and biogeochemical implications. *Reviews of Geophysics* **2014,** *52*, (4), 603-679.

23.   Elliott, A. H.; Brooks, N. H., Transfer of nonsorbing solutes to a streambed with bed forms: Theory. *Water Resources Research* **1997,** *33*, (1), 123-136.

24.   Elliott, A. H.; Brooks, N. H., Transfer of nonsorbing solutes to a streambed with bed forms: Laboratory experiments. *Water Resources Research* **1997,** *33*, (1), 137-151.

25.   Huettel, M.; Webster, I. T., Porewater flow in permeable sediments. In *The benthic boundary layer: transport processes and biogeochemistry.* , Oxford University Press, New York, 2001.

26.   Thibodeaux, L. J.; Boyle, J. D., Bedform-generated convective transport in bottom sediment. *Nature* **1987,** *325*, 341-343.

27.   Kimball, B. A.; Broshears, R. E.; Bencala, K. E.; McKnight, D. M., Coupling of hydrologic transport and chemical reactions in a stream affected by acid mine drainage. *Environmental Science & Technology* **1994,** *28*, 2065-2073.

28.   Huettel, M.; Ziebis, W.; Forster, S.; Luther Iii, G. W., Advective transport affecting metal and nutrient distributions and interfacial fluxes in permeable sediments. *Geochimica et Cosmochimica Acta* **1998,** *62*, (4), 613-631.

29.   Nagorski, S.; Moore, J., Arsenic mobilization in the hyporheic zone of a contaminated stream. *Water Resources Research* **1999,** *35*, (11), 3441-3450.

30.   Boudreau, B. P.; Jørgensen, B. B., *The benthic boundary layer : transport processes and biogeochemistry*. Oxford University Press: Oxford ; New York, 2001; p xii, 404.

31.   Ren, J.; Packman, A. I., Modeling of simultaneous exchange of colloids and sorbing contaminants between streams and streambeds. *Environmental Science and Technology* **2004,** *38*, (10), 2901-2911.

32.   Ren, J. H.; Packman, A. I., Coupled stream-subsurface exchange of colloidal hematite and dissolved zinc, copper, and phosphate. *Environmental Science & Technology* **2005,** *39*, (17), 6387-6394.

33.   Widdicombe, S.; Needham, H., Impact of CO2-induced seawater acidification on the burrowing activity of Nereis virens and sediment nutrient flux. *MARINE ECOLOGY-PROGRESS SERIES-* **2007,** *341*, 111.

34.   Ziebis, W.; Forster, S.; Huettel, M.; Jørgensen, B. B., Complex burrows of the mud shrimp Callianassa truncata and their geochemical impact in the sea bed. *Nature* **1996,** *382*, (6592), 619-622.

35. Zhu, Q.; Aller, R. C.; Fan, Y., Two-dimensional pH distributions and dynamics in bioturbated marine sediments. *Geochimica et Cosmochimica Acta* **2006,** *70*, (19), 4933-4949

36. Hester, E.; Young, K.; Widdowson, M., Mixing of surface and groundwater induced by riverbed dunes: Implications for hyporheic zone definitions and pollutant reactions. *Water Resources Research* **2013,** *49*, (9), 5221-5237.

37. Aller, R., Sedimentary diagenesis, depositional environments, and benthic fluxes. *Treatise on Geochemistry* **2014,** *8*, 293-334.

38. Smith, M. E.; Lazorchak, J. M.; Herrin, L. E.; Brewer‐Swartz, S.; Thoeny, W. T., A reformulated, reconstituted water for testing the freshwater amphipod, Hyalella azteca. *Environmental Toxicology and Chemistry* **1997,** *16*, (6), 1229-1233

39. Gust, G.; Müller, V., Interfacial hydrodynamics and entrainment functions of currently used erosion devices. In *Cohesive sediments*, 1997; pp 149-174.

40. Law, B. A.; Hill, P. S.; Milligan, T. G.; Curran, K. J.; Wiberg, P. L.; Wheatcroft, R. A., Size sorting of fine-grained sediments during erosion: results from the western Gulf of Lions. *Continental Shelf Research* **2008,** *28*, (15), 1935-1946

41. Allen, H.; Fu, G.; Boothman, W.; Di Toro, D.; Mahony, J. *Determination of acid volatile sulfide and selected simultaneously extractable metals in sediment*; Office of Water Regulations and Standards: US Environmental Protection Agency, Washington, DC, 1991.

42. Ravel, B.; Newville, M., ATHENA, ARTEMIS, HEPHAESTUS: data analysis for X-ray absorption spectroscopy using IFEFFIT. *Journal of Synchrotron Radiation* **2005,** *12*, (4), 537-541.

43. Manceau, A.; Marcus, M. A.; Tamura, N., Quantitative speciation of heavy metals in soils and sediments by synchrotron X-ray techniques. *Reviews in Mineralogy and Geochemistry* **2002,** *49*, (1), 341-428.

44. Van Damme, A.; Degryse, F.; Smolders, E.; Sarret, G.; Dewit, J.; Swennen, R.; Manceau, A., Zinc speciation in mining and smelter contaminated overbank sediments by EXAFS spectroscopy. *Geochimica et cosmochimica acta* **2010,** *74*, (13), 3707-3720.

45. Gaillard, J. F.; Webb, S. M.; Quintana, J. P. G., Quick X-ray absorption spectroscopy for determining metal speciation in environmental samples. *Journal of Synchrotron Radiation* **2001,** *8*, 928-930.

46. Newville, M., Fundamentals of XAFS. *Reviews in Mineralogy and Geochemistry* **2014,** *78*, (1), 33-74.

47. Cahill, R. A.; Bogner, W. C. *Investigation of metal distributions and sedimentation patterns in Lake DePue and Turner Lake*; RR-98; Waste Management and Research Center: Illinois, 2002.

48. *Superfund Record of Decision: Portsmouth Naval Shipyard, OU4, Kittery, ME*; Environmental Protection Agency, Washingtong, DC.: 1999.

49. Hammerschmidt, C. R.; Fitzgerald, W. F., Sediment–water exchange of methylmercury determined from shipboard benthic flux chambers. *Marine Chemistry* **2008,** *109*, (1), 86-97.

50. Wilding, J.; Maltby, L., Relative toxicological importance of aqueous and dietary metal exposure to a freshwater crustacean: implications for risk assessment. *Environmental Toxicology and Chemistry* **2006,** *25*, (7), 1795-1801.

51. Walthert, L.; Graf, U.; Kammer, A.; Luster, J.; Pezzotta, D.; Zimmermann, S.; Hagedorn, F., Determination of organic and inorganic carbon, δ13C, and nitrogen in soils containing carbonates after acid fumigation with HCl. *Journal of Plant Nutrition and Soil Science* **2010,** *173*, (2), 207-216.

52.   Sullivan, L. A.; Bush, R. T.; McConchie, D. M., A modified chromium-reducible sulfur method for reduced inorganic sulfur: optimum reaction time for acid sulfate soil. *Soil Research* **2000,** *38*, (3), 729-734.

53.   Cantwell, M. G.; Burgess, R. M.; Kester, D. R., Release and phase partitioning of metals from anoxic estuarine sediments during periods of simulated resuspension. *Environmental science & technology* **2002,** *36*, (24), 5328-5334.

54.   ASTM., D., Standard test method for particle-size analysis of soils. **2007**.

55.   Standard, A., D2434-68, 2006. *Standard test method for permeability of granular soils (Constant Head). ASTM International, West Conshohocken, PA. doi* **2006,** *10*, D0422.

56.   Norwood, W.; Borgmann, U.; Dixon, D., Saturation models of arsenic, cobalt, chromium and manganese bioaccumulation by Hyalella azteca. *Environmental pollution* **2006,** *143*, (3), 519-528.

57.   Rosen, G.; Rivera-Duarte, I.; Chadwick, D. B.; Ryan, A.; Santore, R. C.; Paquin, P. R., Critical tissue copper residues for marine bivalve (Mytilus galloprovincialis) and echinoderm (Strongylocentrotus purpuratus) embryonic development: conceptual, regulatory and environmental implications. *Marine environmental research* **2008,** *66*, (3), 327-336.

58.   Team, R. C., R: A language and environment for statistical computing. R Foundation for Statistical Computing, Vienna, Austria, 2012. In ISBN 3-900051-07-0: 2014.

59.   Bolker, B. M., *Ecological models and data in R*. Princeton University Press: 2008.

60.   Allen, H. E. e. a., Determination of acid volatile sulfides and simultaneously extractable metals in sediment. In U.S. EPA, 1991.

61.   Canfield, D. E.; Raiswell, R.; Westrich, J. T.; Reaves, C. M.; Berner, R. A., The use of chromium reduction in the analysis of reduced inorganic sulfur in sediments and shales. *Chemical Geology* **1986,** *54*, (1), 149-155.

62.   Element, C. A. S., Method 3051A. Microwave assisted acid digestion of sediments, sludges, soils, and oils. **2007**.

63.   Thomsen, L.; Gust, G., Sediment erosion thresholds and characteristics of resuspended aggregates on the western European continental margin. *Deep Sea Research Part I: Oceanographic Research Papers* **2000,** *47*, (10), 1881-1897.

64.   Seeberg-Elverfeldt, J.; Schlüter, M.; Feseker, T.; Kölling, M., Rhizon sampling of pore waters near the sediment/water interface of aquatic systems. *Limnology and oceanography: Methods* **2005,** *3*, 361-371.

65.   Dickens, G. R.; Koelling, M.; Smith, D. C.; Schnieders, L., Rhizon Sampling of Pore Waters on Scientific Drilling Expeditions: An Example from the IODP Expedition 302, Arctic Coring Expedition (ACEX). *Scientific Drilling* **2007,** *4*, 22-25.

66.   Shotbolt, L., Pore water sampling from lake and estuary sediments using Rhizon samplers. *Journal of Paleolimnology* **2010,** *44*, (2), 695-700.

67.   Taillefert, M. The distribution of trace elements cobalt and lead at the oxic-anoxic transition of a stratified lake : analytical speciation and modeling. Thesis (Ph.D., Civil Engineering)--Northwestern University, 1997.

68.   Stookey, L. L., Ferrozine---a new spectrophotometric reagent for iron. *Analytical chemistry* **1970,** *42*, (7), 779-781.

69.   Viollier, E.; Inglett, P. W.; Hunter, K.; Roychoudhury, A. N.; Van Cappellen, P., The ferrozine method revisited: Fe (II)/Fe (III) determination in natural waters. *Applied geochemistry* **2000,** *15*, (6), 785-790.

70.   Webb, S. M.; Leppard, G. G.; Gaillard, J.-F., Zinc speciation in a contaminated aquatic environment: characterization of environmental particles by analytical electron microscopy. *Environmental science & technology* **2000,** *34*, (10), 1926-1933.

71.   Packman, A. I.; Salehin, M., Relative roles of stream flow and sedimentary conditions in controlling hyporheic exchange. In *The Interactions between Sediments and Water*, Springer: 2003; pp 291-297.

72.   Gough, H. L.; Dahl, A. L.; Nolan, M. A.; Gaillard, J.-F.; Stahl, D. A., Metal impacts on microbial biomass in the anoxic sediments of a contaminated lake. *Journal of Geophysical Research* **2008,** *113*, G02017

73.   Gough, H. L.; Dahl, A. L.; Tribou, E.; Noble, P. A.; Gaillard, J.-F.; Stahl, D. A., Elevated sulfate reduction in metal-contaminated freshwater lake sediments. *Journal of Geophysical Research* **2008,** *113*, G04037

74.   Hong, Y. S.; Kinney, K. A.; Reible, D. D., Effects of cyclic changes in pH and salinity on metals release from sediments. *Environmental Toxicology and Chemistry* **2011,** *30*, (8), 1775-1784

75.   Casas, A. M.; Crecelius, E. A., Relationship between acid volatile sulfide and the toxicity of zinc, lead and copper in marine sediments. *Environmental Toxicology and Chemistry* **2009,** *13*, (3), 529-536.

76.   Scheinost, A. C.; Kretzschmar, R.; Pfister, S.; Roberts, D. R., Combining selective sequential extractions, X-ray absorption spectroscopy, and principal component analysis for quantitative zinc speciation in soil. *Environmental science & technology* **2002,** *36*, (23), 5021-5028.

77.   Malinowski, E. R., Determination of the number of factors and the experimental error in a data matrix. *Analytical Chemistry* **1977,** *49*, (4), 612-617.

78.   Da Silva-Cadoux, C.; Zanella, L.; Gaillard, J.-F., Selecting reference compounds for determining chemical speciation by X-ray absorption spectroscopy. *Journal of Analytical Atomic Spectrometry* **2012,** *27*, (6), 957-965.

79.   Priadi, C.; Le Pape, P.; Morin, G.; Ayrault, S.; Maillot, F.; Juillot, F.; Hochreutener, R.; Llorens, I.; Testemale, D.; Proux, O., X-ray absorption fine structure evidence for amorphous zinc sulfide as a major zinc species in suspended matter from the Seine River downstream of Paris, Ile-de-France, France. *Environmental science & technology* **2012,** *46*, (7), 3712-3720.

80.   Hesterberg, D.; Sayers, D. E.; Zhou, W.; Plummer, G. M.; Robarge, W. P., X-ray absorption spectroscopy of lead and zinc speciation in a contaminated groundwater aquifer. *Environmental science & technology* **1997,** *31*, (10), 2840-2846.

81.   Howard, D. E.; Evans, R. D., Acid‐volatile sulfide (AVS) in a seasonally anoxic mesotrophic lake: Seasonal and spatial changes in sediment AVS. *Environmental Toxicology and Chemistry* **1993,** *12*, (6), 1051-1057

82.   Leonard, E. N.; Ankley, G. T.; Hoke, R. A., Evaluation of metals in marine and freshwater surficial sediments from the Environmental Monitoring and Assessment Program relative to proposed sediment quality criteria for metals. *Environmental Toxicology and Chemistry* **1996,** *15*, (12), 2221-2232.

83.   Huettel, M.; Webster, I. T., Porewater flow in permeable sediments. In *The benthic boundary layer: transport processes and biogeochemistry.* , Oxford University Press, New York, 2001; pp 144-179.

84.   Cappuyns, V.; Swennen, R.; Vandamme, A.; Niclaes, M., Environmental impact of the former Pb–Zn mining and smelting in East Belgium. *Journal of Geochemical Exploration* **2006,** *88*, (1), 6-9.
85.   Concas, A.; Ardau, C.; Cristini, A.; Zuddas, P.; Cao, G., Mobility of heavy metals from tailings to stream waters in a mining activity contaminated site. *Chemosphere* **2006,** *63*, (2), 244-253.
86.   Gorham, E.; Gordon, A. G., The influence of smelter fumes upon the chemical composition of lake waters near Sudbury, Ontario, and upon the surrounding vegetation. *Canadian Journal of Botany* **1960,** *38*, (4), 477-487.
87.   Lindsay, M. B.; Moncur, M. C.; Bain, J. G.; Jambor, J. L.; Ptacek, C. J.; Blowes, D. W., Geochemical and mineralogical aspects of sulfide mine tailings. *Applied Geochemistry* **2015**.
88.   Moore, J. N.; Luoma, S. N., Hazardous wastes from large-scale metal extraction. A case study. *Environmental science & technology* **1990,** *24*, (9), 1278-1285.
89.   Karnachuk, O.; Gerasimchuk, A.; Banks, D.; Frengstad, B.; Stykon, G.; Tikhonova, Z.; Kaksonen, A.; Puhakka, J.; Yanenko, A.; Pimenov, N., Bacteria of the sulfur cycle in the sediments of gold mine tailings, Kuznetsk Basin, Russia. *Microbiology* **2009,** *78*, (4), 483-491.
90.   Byrne, P.; Wood, P.; Reid, I., The impairment of river systems by metal mine contamination: a review including remediation options. *Critical Reviews in Environmental Science and Technology* **2012,** *42*, (19), 2017-2077.
91.   Simpson, S. L.; Apte, S. C.; Batley, G. E., Effect of short-term resuspension events on trace metal speciation in polluted anoxic sediments. *Environmental science & technology* **1998,** *32*, (5), 620-625
92.   Macdonald, D. D.; Carr, R. S.; Calder, F. D.; Long, E. R.; Ingersoll, C. G., Development and evaluation of sediment quality guidelines for Florida coastal waters. *Ecotoxicology* **1996,** *5*, (4), 253-278.
93.   Smith, S. L.; MacDonald, D. D.; Keenleyside, K. A.; Ingersoll, C. G.; Field, L. J., A preliminary evaluation of sediment quality assessment values for freshwater ecosystems. *Journal of Great Lakes Research* **1996,** *22*, (3), 624-638.
94.   Hansen, D. J.; DiToro, D. M.; Berry, W. J.; Boothman, W. S.; Burgess, R. M.; Ankley, G. T.; Mount, D. R.; McGrath, J. A.; DeRosa, L. D.; Bell, H. E., *Procedures for the Derivation of Equilibrium Partitioning Sediment Benchmarks (ESBs) for the Protection of Benthic Organisms: Metal Mixtures (cadmium, Copper, Lead, Nickel, Silver, and Zinc)*. US Environmental Protection Agency: 2005.
95.   Long, E. R.; MacDonald, D. D.; Smith, S. L.; Calder, F. D., Incidence of adverse biological effects within ranges of chemical concentrations in marine and estuarine sediments. *Environmental management* **1995,** *19*, (1), 81-97.
96.   EPA, U., National Recommended Water Quality Criteria EPA-822-R-02-047. *Office of Science and Technology* **2002**.
97.   Hong, Y. S.; Kinney, K. A.; Reible, D. D., Acid volatile sulfides oxidation and metals (Mn, Zn) release upon sediment resuspension: Laboratory experiment and model development. *Environmental toxicology and chemistry* **2011,** *30*, (3), 564-575.
98.   Schlekat, C. E.; Decho, A. W.; Chandler, G. T., Bioavailability of particle‑associated silver, cadmium, and zinc to the estuarine amphipod Leptocheirus plumulosus through dietary ingestion. *Limnology and Oceanography* **2000,** *45*, (1), 11-21.
99.   Zhuang, Y.; Allen, H. E.; Fu, G., Effect of aeration of sediment on cadmium binding. *Environmental toxicology and chemistry* **1994,** *13*, (5), 717-724.

100.	Hwang, K. Y.; Kim, H. S.; Hwang, I., Effect of resuspension on the release of heavy metals and water chemistry in anoxic and oxic sediments. *CLEAN–Soil, Air, Water* **2011,** *39*, (10), 908-915.

101.	Calmano, W.; Hong, J.; Förstner, U., *Binding and mobilization of heavy metals in contaminated sediments affected by pH and redox potential*. 1993.

102.	Atkinson, C. A.; Jolley, D. F.; Simpson, S. L., Effect of overlying water pH, dissolved oxygen, salinity and sediment disturbances on metal release and sequestration from metal contaminated marine sediments. *Chemosphere* **2007,** *69*, (9), 1428-1437.

103.	Caetano, M.; Madureira, M.-J.; Vale, C., Metal remobilisation during resuspension of anoxic contaminated sediment: short-term laboratory study. *Water, air, and soil pollution* **2003,** *143*, (1-4), 23-40.

104.	Simpson, S. L.; Apte, S. C.; Batley, G. E., Effect of short-term resuspension events on trace metal speciation in polluted anoxic sediments. *Environmental Science & Technology* **1998,** *32*, (5), 620-625.

105.	Gough, H. L.; Dahl, A. L.; Tribou, E.; Noble, P. A.; Gaillard, J. F.; Stahl, D. A., Elevated sulfate reduction in metal‐contaminated freshwater lake sediments. *Journal of Geophysical Research: Biogeosciences (2005‐2012)* **2008,** *113*, (G4).

106.	Coquery, M.; Welbourn, P., The relationship between metal concentration and organic matter in sediments and metal concentration in the aquatic macrophyte Eriocaulon septangulare. *Water research* **1995,** *29*, (9), 2094-2102.

107.	Caille, N.; Tiffreau, C.; Leyval, C.; Morel, J. L., Solubility of metals in an anoxic sediment during prolonged aeration. *Science of the Total Environment* **2003,** *301*, (1), 239-250.

108.	Chapman, P. M.; Wang, F.; Janssen, C.; Persoone, G.; Allen, H. E., Ecotoxicology of metals in aquatic sediments: binding and release, bioavailability, risk assessment, and remediation. *Canadian Journal of Fisheries and Aquatic Sciences* **1998,** *55*, (10), 2221-2243.

109.	Huerta-Diaz, M. A.; Morse, J. W., Pyritization of trace metals in anoxic marine sediments. *Geochimica et Cosmochimica Acta* **1992,** *56*, (7), 2681-2702.

110.	Jones‐Lee, A.; Lee, G. F., Role of iron chemistry in controlling the release of pollutants from resuspended sediments. *Remediation Journal* **2005,** *16*, (1), 33-41.

111.	Stauber, J. L.; Benning, R. J.; Hales, L. T.; Eriksen, R.; Nowak, B., Copper bioavailability and amelioration of toxicity in Macquarie Harbour, Tasmania, Australia. *Marine and Freshwater Research* **2000,** *51*, (1), 1-10.

112.	Murray, J. W.; Barber, R. T.; Roman, M. R.; Bacon, M. P.; Feely, R. A., Physical and biological controls on carbon cycling in the equatorial Pacific. *Science* **1994,** *266*, (5182), 58-65.

113.	Nagpal, N., Ambient water quality guidelines for manganese. *Ministry of Environment and Parks, Water Management Branch, Resource Quality Section, Victoria, BC, Canada* **2001**.

114.	Carvalho, R. A.; Benfield, M. C.; Santschi, P. H., Comparative bioaccumulation studies of colloidally complexed and free‐ionic heavy metals in juvenile brown shrimp Penaeus aztecus (Crustacea: Decapoda: Penaeidae). *Limnology and Oceanography* **1999,** *44*, (2), 403-414.

115.	Lee, J.-S.; Lee, B.-G.; Luoma, S. N.; Choi, H. J.; Koh, C.-H.; Brown, C. L., Influence of acid volatile sulfides and metal concentrations on metal partitioning in contaminated sediments. *Environmental science & technology* **2000,** *34*, (21), 4511-4516.

116.	Weltens, R.; Goossens, R.; Van Puymbroeck, S., Ecotoxicity of contaminated suspended solids for filter feeders (Daphnia magna). *Archives of Environmental Contamination and Toxicology* **2000,** *39*, (3), 315-323.

117.   Hill, N. A.; King, C. K.; Perrett, L. A.; Johnston, E. L., Contaminated suspended sediments toxic to an Antarctic filter feeder: Aqueous‐ and particulate‐phase effects. *Environmental Toxicology and Chemistry* **2009,** *28*, (2), 409-417.

118.   Cloran, C. E.; Burton, G. A.; Hammerschmidt, C. R.; Taulbee, W. K.; Custer, K. W.; Bowman, K. L., Effects of suspended solids and dissolved organic carbon on nickel toxicity. *Environmental Toxicology and Chemistry* **2010,** *29*, (8), 1781-1787.

119.   Fichet, D.; Radenac, G.; Miramand, P., Experimental studies of impacts of harbour sediments resuspension to marine invertebrates larvae: bioavailability of Cd, Cu, Pb and Zn and toxicity. *Marine Pollution Bulletin* **1998,** *36*, (7), 509-518.

120.   Bonnet, C.; Babut, M.; Férard, J. F.; Martel, L.; Garric, J., Assessing the potential toxicity of resuspended sediment. *Environmental Toxicology and Chemistry* **2000,** *19*, (5), 1290-1296.

121.   Xie, M.; Jarrett, B. A.; Da Silva-Cadoux, C.; Fetters, K. J.; Burton, G. A.; Gaillard, J.-F.; Packman, A. I., Coupled effects of hydrodynamics and biogeochemistry on Zn mobility and speciation in highly contaminated sediments. *Environmental science & technology* **2015,** *49*, (9), 5346-5353.

122.   Angel, B. M.; Simpson, S. L.; Jolley, D. F., Toxicity to Melita plumulosa from intermittent and continuous exposures to dissolved copper. *Environmental Toxicology and Chemistry* **2010,** *29*, (12), 2823-2830.

123.   Kalnejais, L. H.; Martin, W. R.; Bothner, M. H., The release of dissolved nutrients and metals from coastal sediments due to resuspension. *Marine Chemistry* **2010,** *121*, (1), 224-235.

124.   Roberts, D. A., Causes and ecological effects of resuspended contaminated sediments (RCS) in marine environments. *Environment international* **2012,** *40*, 230-243.

125.   Packman, A. I.; Brooks, N. H.; Morgan, J. J., Kaolinite exchange between a stream and streambed: Laboratory experiments and validation of a colloid transport model. *Water Resources Research* **2000,** *36*, (8), 2363-2372.

126.   Harvey, J.; Drummond, J.; Martin, R.; McPhillips, L.; Packman, A.; Jerolmack, D.; Stonedahl, S.; Aubeneau, A.; Sawyer, A.; Larsen, L., Hydrogeomorphology of the hyporheic zone: Stream solute and fine particle interactions with a dynamic streambed. *Journal of Geophysical Research: Biogeosciences (2005–2012)* **2012,** *117*, (G4).

127.   Carraway, E.; Demas, J.; DeGraff, B., Luminescence quenching mechanism for microheterogeneous systems. *Analytical chemistry* **1991,** *63*, (4), 332-336.

128.   Kristensen, E., Organic matter diagenesis at the oxic/anoxic interface in coastal marine sediments, with emphasis on the role of burrowing animals. *Hydrobiologia* **2000,** *426*, (1), 1-24.

129.   Hines, M. E.; Orem, W. H.; Lyons, W. B.; Jones, G. E., Microbial activity and bioturbation-induced oscillations in pore water chemistry of estuarine sediments in spring. **1982**.

130.   Aller, R. C., Bioturbation and remineralization of sedimentary organic matter: effects of redox oscillation. *Chemical Geology* **1994,** *114*, (3), 331-345.

131.   Simpson, S. L.; Ward, D.; Strom, D.; Jolley, D. F., Oxidation of acid-volatile sulfide in surface sediments increases the release and toxicity of copper to the benthic amphipod Melita plumulosa. *Chemosphere* **2012,** *88*, (8), 953-961.

132.   Packman, A. I.; Salehin, M.; Zaramella, M., Hyporheic exchange with gravel beds: basic hydrodynamic interactions and bedform-induced advective flows. *Journal of Hydraulic Engineering* **2004,** *130*, (7), 647-656.

133.   Bencala, K. E., Simulation of solute transport in a mountain pool‐and‐riffle stream with a kinetic mass transfer model for sorption. *Water Resources Research* **1983,** *19*, (3), 732-738.

134.   Huettel, M.; Røy, H.; Precht, E.; Ehrenhauss, S., Hydrodynamical impact on biogeochemical processes in aquatic sediments. In *The Interactions between Sediments and Water*, Springer: 2003; pp 231-236.

135.   Clark, M. M., *Transport modeling for environmental engineers and scientists*. John Wiley & Sons: 2012.

136.   O'Connor, B. L.; Hondzo, M., Dissolved oxygen transfer to sediments by sweep and eject motions in aquatic environments. *Limnology and Oceanography* **2008,** *53*, (2), 566-578.

137.   Boudreau, B. P., Solute transport above the sediment-water interface. In *The Benthic boundary layer: Transport processes and biogeochemistry*, 2001; pp 104-126.

138.   Dade, W. B.; Hogg, A. J.; Boudreau, B. P., *Physics of flow above the sediment-water interface*. Oxford University Press, New York: 2001.

139.   Jørgensen, B. B.; Des Marais, D. J., The diffusive boundary layer of sediments: Oxygen microgradients over a microbial mat. *Limnology and Oceanography* **1990,** *35*, (6), 1343-1355.

140.   Gundersen, J. K.; Jorgensen, B. B., Microstructure of diffusive boundary layers and the oxygen uptake of the sea floor. *Nature* **1990,** *345*, (6276), 604-607.

141.   Martin, S. T., Precipitation and dissolution of iron and manganese oxides. *Environmental Catalysis* **2005**, 61-81.

142.   Kalnejais, L. H.; Martin, W. R.; Signell, R. P.; Bothner, M. H., Role of sediment resuspension in the remobilization of particulate-phase metals from coastal sediments. *Environmental science & technology* **2007,** *41*, (7), 2282-2288.

143.   Harvey, R. W.; Garabedian, S. P., Use of colloid filtration theory in modeling movement of bacteria through a contaminated sandy aquifer. *Environmental science & technology* **1991,** *25*, (1), 178-185.

144.   Ren, J.; Packman, A. I., Coupled stream-subsurface exchange of colloidal hematite and dissolved zinc, copper, and phosphate. *Environmental science & technology* **2005,** *39*, (17), 6387-6394.

145.   Drummond, J.; Davies-Colley, R.; Stott, R.; Sukias, J.; Nagels, J.; Sharp, A.; Packman, A., Retention and remobilization dynamics of fine particles and microorganisms in pastoral streams. *Water Res* **2014,** *66*, 459-472.

146.   Canavan, R. W.; Van Cappellen, P.; Zwolsman, J. J. G.; Van den Berg, G. A.; Slomp, C. P., Geochemistry of trace metals in a fresh water sediment: field results and diagenetic modeling. *Science of the total environment* **2007,** *381*, (1), 263-279

147.   Zhang, H.; Davison, W.; Miller, S.; Tych, W., In situ high resolution measurements of fluxes of Ni, Cu, Fe, and Mn and concentrations of Zn and Cd in porewaters by DGT. *Geochimica et Cosmochimica Acta* **1995,** *59*, (20), 4181-4192

148.   Cai, W.-J.; Sayles, F. L., Oxygen penetration depths and fluxes in marine sediments. *Marine Chemistry* **1996,** *52*, (2), 123-131.

149.   Berg, P.; Risgaard-Petersen, N.; Rysgaard, S., Interpretation of measured concentration profiles in sediment pore water. *Limnology and Oceanography* **1998,** *43*, (7), 1500-1510.

150.   Packman, A. I.; Brooks, N. H.; Morgan, J. J., A physicochemical model for colloid exchange between a stream and a sand streambed with bed forms. *Water Resources Research* **2000,** *36*, (8), 2351-2361.

8. APPENDICES

8.1 List of Supporting Information:

1. Movie B1_reference sediments

2. Movie B2_contaminated sediments

3. Movie B3_reference sediments

4. Movie B4_contaminated sediments

5. Movie B5_oxygen optode

8.2 List of Technical Publications

Articles or papers in preparation or published in peer-review journals

Xie, M.; Alsina., M.A.; Yuen, J.; Packman, A.I., Gaillard, J.-F., 2016. Effects of long-term resuspension on mobility of metals in contaminated sediments. *In preparation.*

Xie, M.; Wang, N.; Gaillard, J.-F.; Packman, A.I., 2016. Interplay between flow and bioturbation enhances metal efflux from low-permeability sediments. *In preparation.*

Roche, K.R., Aubeneau, A.F., Xie, M., Aquino, T., Bolster, D., Packman, A.I., 2016, Bioturbation causes anomalous mixing in freshwater sediments., *Environ. Sci. Technol.*, *In review*.

Xie, M.; Wang, N.; Gaillard, J.-F.; Packman, A.I., 2016. Hydrodynamic forcing mobilizes Cu in Low-permeability estuarine sediments. *Environ. Sci. Technol.* 50 (9):4615-4623.

Fetters, K.J.; Costello, D.M.; Hammerschmidt C.R.; Burton G.A., 2016. Toxicological effects of short-term resuspension of metal-contaminated freshwater and marine sediments. *Environ. Toxicol. Chem.*, 35: 676-686, DOI: 10.1002/etc.3225.

Xie, M., Jarrett, B.A., Silva-Cadoux, C.D., Fetters, K.J., Burton, G.A., Gaillard, J-F and Packman, A.I. 2015. Coupled effects of hydrodynamics and biogeochemistry on Zn mobility and speciation in highly contaminated sediments. *Environ Sci. Technol.* 49 (9):5346–5353.

Siva-Cadoux, C.D., Zanella, L., and Gaillard, J.-F.; 2012. Selecting reference compounds for determining chemical speciation by X-ray absorption spectroscopy. *J. Analytical Atomic Spectrometry.* 27 (6): 957-965.

Conference/symposium proceedings

Xie, M; Jarrett, B.A.; Silva-Cadoux, C.D; Gaillard, J-F and Packman, A.I., 2015, Effects of resuspension on metal dynamics and speciation in contaminated lake sediments. Society for Freshwater Science Annual Meeting. Milwaukee, WI, May 17-21, 2015.

Hernandez, L.M., Roche, K.R., Xie, M., and Packman, A.I, 2015, Quantification of the bioturbation activity of *Lumbriculus variegatus* worms using fluorescent particulate tracers. Society for Freshwater Science Annual Meeting. Milwaukee, WI, May 17-21, 2015.

Burton GA, Daley, J.,Harrison, A., Sano, L. , 2015, Simulating resuspension and bioturbation in aquatic sediments: Differentiating the effects on metal bioavailability. Battelle Conference on

Remediation and Management of Contaminated Sediments. New Orleans, LA, January 12-15, 2015.

Hernandez, L.M., Roche, K.R., Xie, M., and Packman, A.I., 2014, Quantification of the bioturbation activity of *Lumbriculus variegatus* worms using fluorescent particulate tracers. American Geophysical Union Fall Meeting. 2014, San Francisco, CA, December 15-19, 2014.

Burton GA. 2014. Improving spatial and temporal characterizations of metal bioavailability in sediments and overlying waters. SETAC Asia Pacific Biannual Conference. Adelaide, Australia, September, 14-17, 2014.

Xie, M; Jarrett, B.A.; Silva-Cadoux, C.D; Keane, D.T.; Ma, Q; Gaillard, J-F and Packman, A.I., 2014, Effects of resuspension on speciation and mobilization of zinc in sediments. Synchrotron Environmental Science VI, Argonne, IL, September 11-12, 2014.

Roche, K.R., Xie, M., Aubeneau, A., and Packman, A.I. , 2014, Anomalous sediment mixing by bioturbation. American Geophysical Union Fall Meeting, San Francisco, CA, December 9-13, 2013.

Fetters, K.J., Costello, D.M., Hammerschmidt, C.R., and Burton, G.A., 2013, Toxicological effects of short-term resuspension of metal-contaminated freshwater and marine sediments. SETAC North America. 2013, Nashville, TN, November 17-21, 2013.

Xie, M.; Fetters, K.J.; Jarrett, B.A.; Yuen, J; Silva-Cadoux, C.D.; Burton, G.A., Gaillard, J-F and Packman, A.I., 2012, Coupling between pore water fluxes, structural heterogeneity, and biogeochemical processes controls contaminant mobility, bioavailability, and toxicity in sediments. American Geophysical Union Fall Meeting. 2012, San Francisco, CA, December 3-7, 2012.

Fetters, K.J., Costello, D.M., Eggleston, M. and Burton, G.A., 2012, Sediment resuspension affects metal bioavailability. SETAC North America. 2012, Long Beach, CA, November 11-15, 2012.